

CHALMERS



Data Fusion
- For Vehicle Positioning in Intersection
Active Safety Applications

TOHID ARDESHIRI
SOGOL KHARRAZI

Department of Applied Mechanics
Division of Vehicle Safety
CHALMERS UNIVERSITY OF TECHNOLOGY
Göteborg 2005, Sweden

Master's Thesis 2005:23

Data Fusion
- For Vehicle Positioning in Intersection
Active Safety Applications

by

TOHID ARDESHIRI

and

SOGOL KHARRAZI

Department of Applied Mechanics
Division of Vehicle Safety
CHALMERS UNIVERSITY OF TECHNOLOGY
Göteborg, Sweden, 2005

Data Fusion
- For Vehicle Positioning in Intersection Active Safety
Applications

TOHID ARDESHIRI, SOGOL KHARRAZI

© TOHID ARDESHIRI, SOGOL KHARRAZI, 2005

Master's Thesis 2005:23
ISSN 1652-8557

Department of Applied Mechanics
Division of Vehicle Safety
Chalmers University of Technology
SE-412 96 Göteborg
Sweden
Telephone +46 (0)31 772 1000

Performed in co-operation with
Autoliv Development AB
Wallentinsvägen 22
SE-447 83 Vårgårda
Sweden
Contact Person: Jonas Bårgman
Jonas.Bargman@autoliv.com

Abstract

The use of position and map information as a part of algorithms in active safety applications is coming more and more in focus. One field of active safety in which navigation information can be used is intersection active safety applications which require a precise and continuous position of vehicle on the road to help the driver to avoid intersection accidents or mitigate their effects.

Today most of land navigation systems are based primarily on the GPS; However in an intersection active safety application, positioning requirements can not be satisfied by GPS alone due to possible occlusions by high buildings or heavy foliage. Thus complementary onboard sensors should be implemented in the navigation system. Furthermore a digital road map should be used to utilize the restriction of land vehicles to the road network and provide information about the vehicle's position relative to road.

In this thesis work a Kalman filter and a map matching algorithm are presented. The Kalman filter fuses data from GPS receiver and other complementary onboard sensors such as differential odometer, yaw rate sensor and longitudinal accelerometer to achieve the required performance for intersection active safety applications. The map matching algorithm uses heading, position and vehicle trajectory given by Kalman filter to calculate vehicle position on the road network.

To verify the performance of the fusion algorithm a test was conducted in downtown Alingsås, Sweden which showed encouraging results. The project goals: filling the gaps of GPS coverage, giving a smooth and continuous position and matching the vehicle position to the digital road map were achieved.

Abbreviations

GPS: Global Positioning System
DGPS: Differential GPS
INS: Inertial Navigation System
DR: Dead Reckoning
ICAS: Intersection Collision Avoidance System
ICA: Intersection Collision Avoidance
IASA: Intersection Active Safety Application
WGS84: World Geodetic System 84
ITS: Intelligent Transportation system
CPS: Continuous Positioning System

Glossary

GPS Occlusion: blockage of GPS signal.

GPS outage Error: increase in error due to lack of GPS coverage and relying on INS/DR.

Latency: The time between initiating a request for data and the beginning of the actual data transfer

MLE: Maximum Likelihood Estimation. A statistical estimation method based on likelihood functions (as opposed to probability functions) and on maximizing the likelihood of the estimate, rather than minimizing some expected loss functions (e.g., minimum mean square).

Position Fix: The given position by positioning system before map matching is performed.

WGS84: The world geodetic System (WGS) is an international standard for navigation coordinates. WGS84 is a reference model released in 1984. It approximates mean sea level by an ellipsoid of revolution with its rotation axis coincident with the rotation axis of the earth, its center at the centre of mass of the earth, and its prime meridian through Greenwich. Its semimajor axis (equatorial radius) is defined to be 6,378,137 m, and its semiminor axis (polar radius) is defined to be 6,356,752.3142 m.

White Noise: White noise is a signal (or process) with a flat frequency spectrum. In other words, the signal has equal power in any band, at any centre frequency, having a given bandwidth. A white noise has zero autocorrelation with itself over time, except at zero time shift.

Acknowledgements

This master's thesis was accomplished at Autoliv Research, Vårgårda, Sweden. The work was supported by Chalmers University of Technology, Gothenburg, Sweden.

We thank all the people who helped us with our work and supplied us with information, specially:

M.Sc. Jonas Bårgman, Autoliv Research, Vårgårda, Sweden, our supervisor for his support, clear guidance, valuable discussions and advises throughout this thesis.

Associate Professor Robert Thomson, Department of Applied Mechanics, Division of Vehicle safety, Chalmers University of Technology, Gothenburg, Sweden, our supervisor and examiner for his support.

Professor Jonas Sjöberg, Department of Signals and Systems, Mechatronics, Chalmers University of Technology, Gothenburg, Sweden, for his advises.

PhD, Mathias Lidberg, Chalmers University of Technology, Gothenburg, Sweden, for his support.

Table of Contents

1. Introduction	1
1.1. Background	1
1.2. Aim of the study	3
1.3. Intersection Active Safety	3
1.3.1. Active Safety Systems	3
1.3.2. Intersection Collision Avoidance System	5
1.3.3. Vehicle Positioning in Automotive Applications.....	5
1.4. Global Positioning System	7
1.4.1. GPS Data Stream	7
1.4.2. Differential GPS	8
1.4.3. GPS Data Errors	8
1.4.4. Dilution of Precision	9
1.5. Inertial Navigation System	9
1.5.1. Advantages and Disadvantages of INS	9
1.5.2. INS Error Sources	10
1.6. Dead Reckoning	10
1.7. Requirements on Digital Map and Positioning Accuracy in IASA.....	10
1.7.1. Requirements for Intersection Collision Avoidance System.....	13
1.7.2. Analysis of positioning requirements	15
1.8. References.....	19
2. Method.....	20
2.1. Test Vehicle	20
2.2. Data Fusion.....	22
2.3. Kalman Filter.....	24
2.3.1. Extended Kalman Filter.....	25
2.3.2. Vehicle Dynamic Model	26
2.4. Stop and Turn Detection	29
2.5. Map Matching	29
2.5.1. Literature Review on Map Matching Algorithms.....	30
2.5.2. Proposed Map Matching Algorithm	32
2.5.3. Searching Mode.....	36
2.5.4. Tracking Mode	37
2.5.5. Intersection Mode	40
2.6. Summary of the Fusion Algorithm.....	42
2.7. References.....	42
3. Results.....	43
3.1. Test Trajectory	43
3.2. Estimated Position	43
3.3. Estimated Heading.....	47
3.4. Estimated Speed.....	48
3.5. Uncertainty in Estimations	48
3.5.1. Estimated Uncertainty in Position	49
3.5.2. Estimated Uncertainty in Heading.....	52
3.5.3. Estimated Uncertainty in Speed.....	52

3.6. Map Matching Results	53
4. Analysis	60
4.1. Sources of error in Fusion.....	60
4.1.1. Modeling errors.....	60
4.1.2. Measurement errors.....	64
4.2. Analysis of effect of clock errors on fusion.....	65
4.2.1. Effect of delay in Fiber Optic Gyro	65
4.2.2. Effect of delay in Cronos Unit	68
4.2.3. Summary of effect of sensors' clock error on fusion	71
5. Conclusion.....	72
Appendix A	73
Appendix B	78
Appendix C	80

1. Introduction

1.1. Background

The use of position and map information as a part of algorithms in active safety applications is becoming more and more in focus. Many in-vehicle navigation and safety applications are under development that provide warnings to the vehicle driver or modify operation of the vehicle (or component thereof) based upon the position of the vehicle on the road network and conditions around the vehicle or other factors. Such applications require the measured position to be relatively well defined and the digital map information to be fairly accurate in order for the algorithms not to misinterpret the information.

Today, most of land navigation systems are based primarily on the Global Positioning System (GPS) readings together with a relatively crude digital map. Although GPS has been widely used for land navigation, GPS alone cannot satisfy most land vehicle navigation requirements due to signal occlusions by high buildings or heavy foliage and multipath in urban environments. Therefore implementation of complementary onboard sensors such as Inertial Navigation System (INS) or Dead Reckoning (DR) sensors (gyros, accelerometers, odometers, etc) is essential to maintain a precise and continuous position.

Both GPS and INS/DR devices fail to utilize the restriction of land vehicles to the road network and a valuable source of information is lost. Thus digital map are used in land navigation systems to provide information about the vehicle's relationship to the roadway infrastructure that is not feasible to obtain with other sensors.

In land navigation systems which use two or much more different navigation sensors a fusion method should be used to continuously fuse the noisy measurements from different sensors in an optimal manner. There are different methods for data fusion such as Kalman Filter, Artificial Neural Network [6], Particle Filters [7], etc. The most common method is the Kalman filter. The Kalman filter is a predictor-corrector type estimator that is optimal in the sense that it minimizes the estimated error covariance when some presumed conditions are met.

One field of active safety in which land navigation systems can be used is to aid the driver in avoiding an intersection accident. Statistical data from the U.S. shows that roughly 43 percent of vehicle crashes occur at intersections or are intersection-related. A significant part of them takes place at intersections with traffic signals or stop signs. Their causes are often due to drivers' misjudgment of the situation, failure to correctly observe the situation, or inability to accurately perceive the degree of danger. These findings suggest that interventions such as warning systems and driver assistance could be particularly effective in reducing intersection crashes. Different intersection collision scenarios are shown in Figure 1-1. [8]

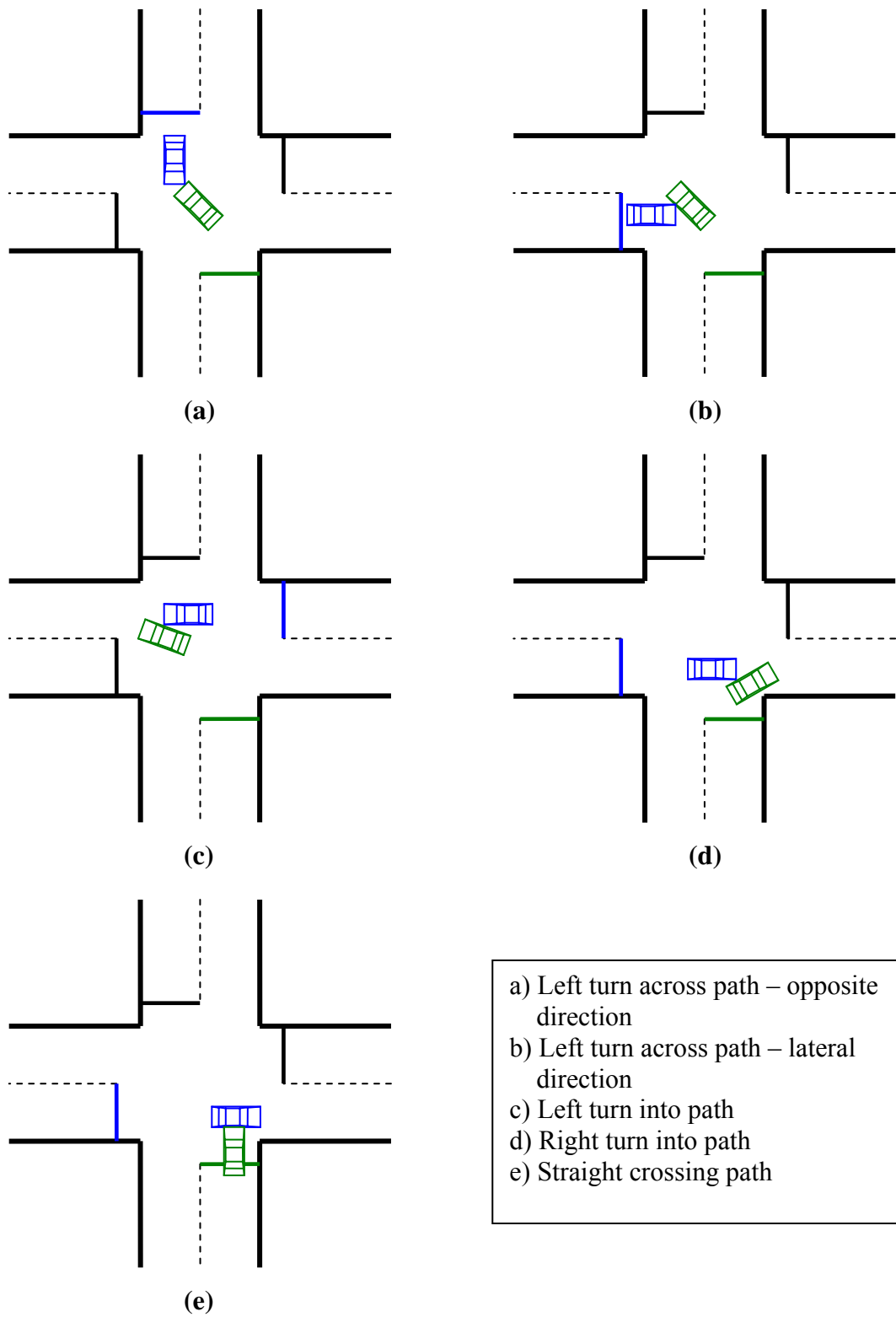


Figure 1-1 Intersection Collision scenarios [8]

1.2. Aim of the study

One of the fields in which Autoliv Research is working is intersection safety. A method for a precise and continuous positioning of the vehicle on the road network may be part of a future intersection active safety application.. However this task can not be done just based on GPS data and implementation of complementary onboard sensors such as INS/DR sensors is essential.

The objective of this thesis work is to create a data fusion algorithm which integrates all the noisy data from a GPS receiver and INS/DR sensors with information obtained from a digital map to achieve the required performance in vehicle positioning for intersection applications. The result of the algorithm will be analyzed and evaluated.

Since the content of this report will not cover automotive-grade implementation of the algorithm, all the data will be treated in non real-time, that is, that they will not be treated at the same time they are collected. The algorithm will use stored output data collected by the sensors on a test vehicle driven in the field.

1.3. Intersection Active Safety

The requirements for positioning and map data fusion were investigated to identify priorities for the fusion and error estimation algorithms, specifically for intersection active safety applications.

In this section, first active safety systems, especially Intersection Collision Avoidance Systems (ICAS) are introduced. Then vehicle positioning in automotive applications is discussed which will be followed by requirements for digital map and positioning accuracy in ICAS and criteria for evaluation of a positioning system.

1.3.1. Active Safety Systems

There are many different safety models. In this section two of them; the Mercedes Benz safety model [10] and Autoliv safety phase chart are presented.

Mercedes Benz Safety Model: In the Mercedes Benz safety model an active safety system is a system that can be applied to any of the blocks F1, F2 and F3 shown in Figure 1-2.

During the warning phase, block F1, sensors detect a safety deficit or a running state which deviates from the desired state and therefore the driver or the passenger are informed by warning alerts. During Assistance phase if sensors detect a critical operating condition the driver is assisted by automatic safety system. If sensors detect a high probability of an accident, pre-crash phase is activated and along with further action designed to avoid accident, in this phase protective measures can be activated.

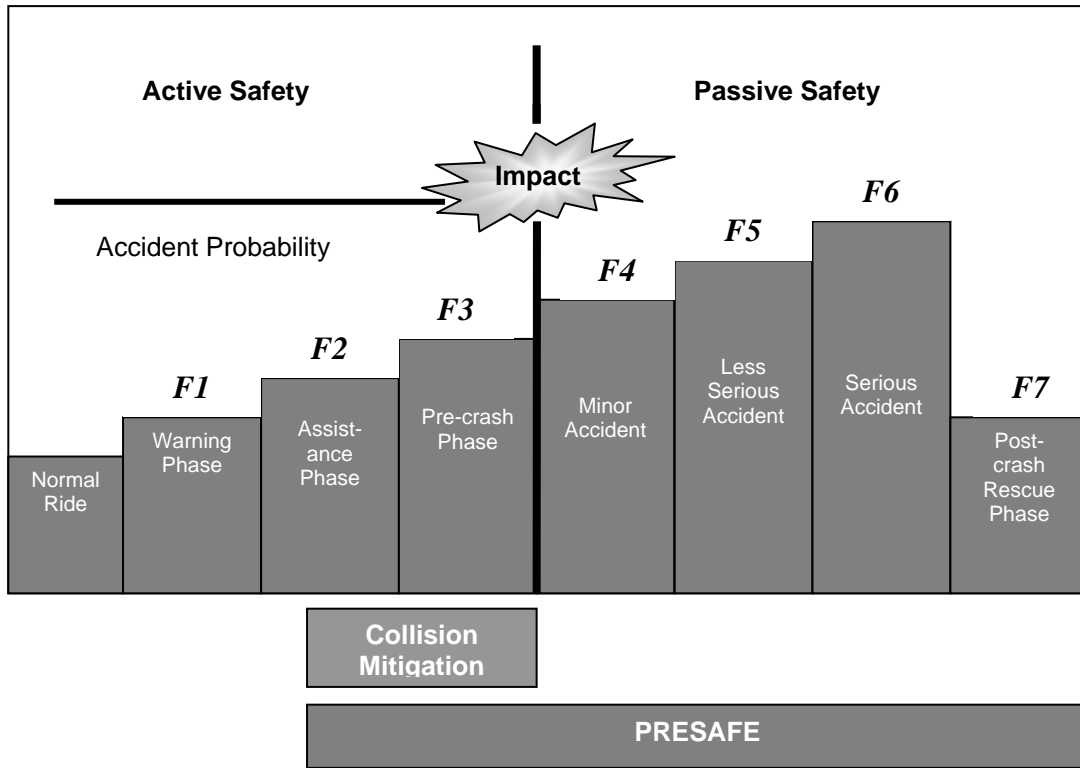


Figure 1-2 Mercedes Benz Safety Model [10]

Autoliv Safety Model: The Autoliv safety phase chart (Figure 1-3) agrees with the Mercedes model. In Autoliv safety phase chart active safety systems are the systems that are utilized before the “point of no return”.

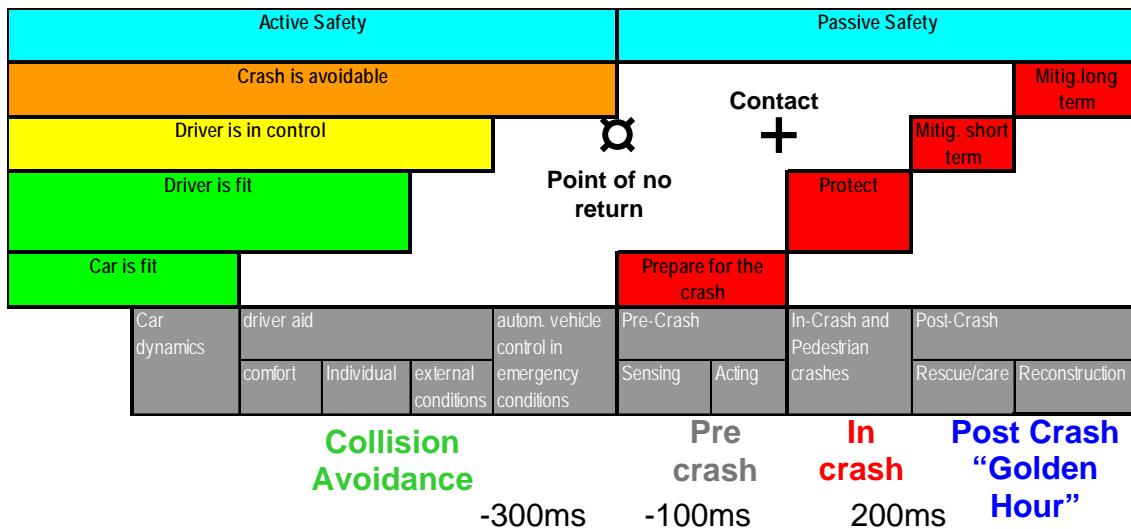


Figure 1-3 Autoliv Safety Phase Chart

1.3.2. Intersection Collision Avoidance System

An Intersection Collision Avoidance System is an active safety system that is designed to provide a driver with warnings of an impending crash or potential hazards at intersections or intervene to prevent the collision or mitigate the consequences. Intersection Collision Avoidance Systems use sensors to gather information about vehicle movements near an intersection, process that information to determine if a collision is at risk of occurring, and take the necessary actions. [8]

There are three types of ICAS systems:

- Vehicle-based autonomous systems, which have been developed mainly by private sector manufacturers;
- Infrastructure-based systems, where the warnings and sensors are located in roadside arrays;
- Systems that link vehicles to other vehicles or vehicles to infrastructure, so-called "cooperative" systems.

The latter two are more often the purview of state department of transportations and government-supported research institutions because they would demand public investments. Vehicle-based systems can be divided into systems that:

- Advise or warn the driver (collision warning)
- Partially control the vehicle, either for steady-state or as an emergency intervention to avoid a collision (driver assistance)
- Fully control the vehicle (vehicle automation). [8]

1.3.3. Vehicle Positioning in Automotive Applications

The implementation of the ICAS requires that vehicle position be known, and that this position data be related to upcoming intersections. An onboard Continuous Positioning System (CPS) and a digital map database should be used to provide this information. This application utilizes position data derived from the CPS to locate the vehicle on a specific roadway segment.

The required accuracy in the positioning of a road vehicle depends on its application. In general as Tomas J. Nagel has pointed out in [1], there are three rough levels of accuracy that are relevant, road level, lane level, and control level. Road level is adequate to identify the road that a vehicle is on; this is the current status of GPS (10m). The next level of accuracy, lane level, allows a vehicle to identify a specific lane on a road, this accuracy is about 1 meter. Finally, a vehicle may be located to a level sufficient for collision avoidance and control applications, on 0.1 meters. These three levels are described briefly in Table 1-1. [1]

Table 1-1 Vehicle interaction possibilities vs. position accuracy

Position Accuracy	Application Information Capabilities
Road Level	General situation-needs to be confirmed or interpreted by driver
Lane Level	Warning capable- Applications have enough information to appeal to instinctive responses of drivers- still need driver in loop.
Within Lane Level	Control capability- accurate enough to take control of car if situation is well defined.

Furthermore active safety applications are not based on position alone- they require knowledge of relative position to either other vehicles or infrastructure (traffic controls, road edge, etc.). While a vehicle application may know the vehicle position quite accurately, often the reliability is limited by the certainty of the information regarding the location of the other object. This information can be either highly variable (as in the position of another vehicle), or static (the location of a bridge abutment). Every type of information has an associated ‘time constant’ over which you can expect the data to be accurate, and after which an application would require an update or validation [1]. Figure 1-4 and 1-5 shows some required update rates and positioning accuracy for automotive applications.

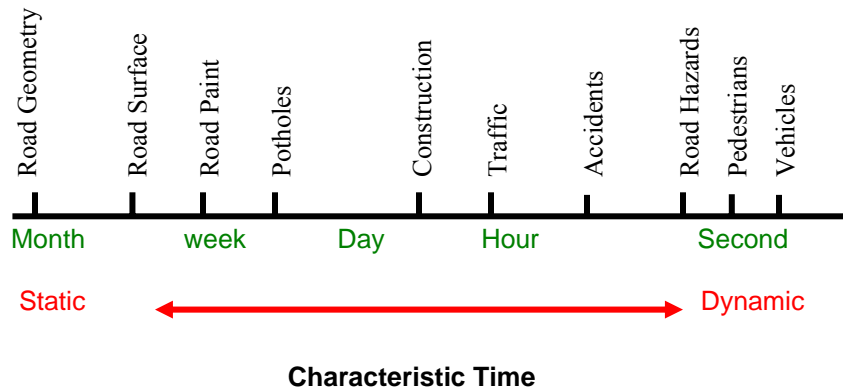


Figure 1-4 Required update rates for automotive applications [1]

Once the position of other objects in the driving environment is determined, many new applications become possible. These systems provide the vehicle a preview of the road ahead based on a digital map in the vehicle.

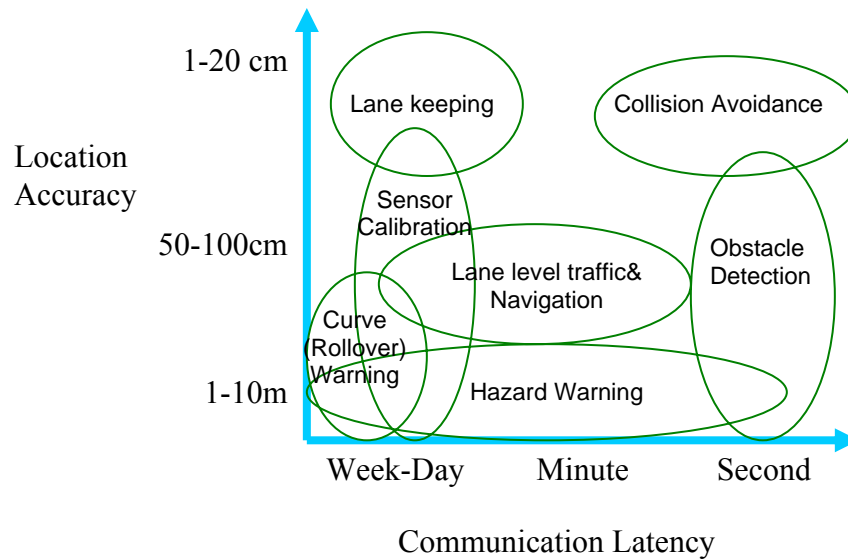


Figure 1-5 Communication latency and required positioning accuracy for different automotive applications [1]

Map information can also be integrated into other intelligent systems such as Automatic Cruise Control (ACC). In this case the map information is used to determine if the target seen in the radar directly ahead is in fact in the same lane, or an adjacent lane (e.g. in a curve). Similar techniques can also be used with intelligent sensor systems to provide the sensor with information on the driving environment. For example a map database might identify guardrails, overpasses, and other potential sources for false returns in a radar system or other attributes such as lane markings and paint patterns in the map database could improve a vision system reliability and allow advanced warning at locations where the infrastructure may not support the operation of the vision system. [1]

1.4. Global Positioning System

The Global Positioning System (GPS) is a satellite-based navigation system. The fully operational GPS includes 28 active satellites approximately uniformly dispersed around six circular orbits with four or more satellite each. The orbits are inclined at an angle of 55° relative to the equator and are separated from each other by multiples of 60° right ascension. Theoretically three or more GPS satellites will always be visible from most points on the earth's surface. [5]

1.4.1. GPS Data Stream

Each GPS satellite conveys the navigation message which includes, but is not limited to, the following information: [5]

1. *Satellite Almanac Data.* Orbital data which can be used to calculate the approximate location of every GPS satellite at any given time and is valid for many months. It is preliminary used to determine which satellites are visible at a

- given location so that the receiver can search for those satellites when it is first turned on.
2. *Satellite Ephemeris data*. Orbital data which enables much more accurate determination of satellite position needed for ranging. Ephemeris data for a particular satellite is only broadcasting by that satellite, and is valid for only several hours.
 3. *Signal Timing Data*: Time tagging included in GPS data stream which is needed to determine the satellite-to-user propagation delay used for ranging.
 4. *Ionospheric Delay Data*: estimates of ionospheric delay (described in 1.5.3).
 5. *Satellite Health Message*: Information regarding the current health of the satellite.

1.4.2. Differential GPS

Differential GPS (DGPS) is a technique for reducing the error in GPS-derived positions by using additional data from a reference GPS receiver at a known position. The most common form of DGPS involves determining the combined effects of navigation message ephemeris and satellite clock errors (including propagation delays) at a reference station and transmitting pseudorange corrections, in real time, to a user's receiver, which applies the corrections in the process of determining its position. [5]

1.4.3. GPS Data Errors

Errors associated with the GPS data can be divided into the following categories:

Ionospheric Propagation Errors: The ionosphere¹ changes GPS signals propagation velocity and consequently causes errors in the pseudorange measurements. This error in the pseudorange for a satellite at zenith varies from about 1 m at night to 5-15 m during late afternoon due to daily variation of the ionosphere's characteristics. At low elevation angles the corresponding error can increase to several meters at night and as much as 50 m during the day. This error can be reduced to about 50% by using a model of the ionosphere and can be nearly eliminated by the use of DGPS. [5]

Tropospheric Propagation Errors: The troposphere² lengthens the GPS signal propagation path and consequently causes errors in the pseudorange measurements. This error in the pseudorange varies from about 2.5 m in the zenith direction to 10-15 m at low satellite elevation angles. This error can be reduced to within about 0.5 m by using a model of the standard atmosphere at the antenna location and can also be nearly eliminated by the use of DGPS. [5]

The Multipath Problem: Multipath propagation of the GPS signal is a dominant source of error in differential positioning. Objects in the vicinity of a receiver antenna (notably the ground) can easily reflect GPS signals and significantly distort the amplitude and phase of the direct-path signal. Errors due to multipath can not be reduced by the use of

¹ A region of the earth's atmosphere where ionization caused by incoming solar radiation affects the transmission of radio waves

² The lower region of atmosphere which is composed of dry gases and water vapor

DGPS, since they depend on local reflection geometry near each receiver antenna. Multipath errors can increase in urban areas due to more severe reflection geometry. [5]

Ephemeris Data Errors: Small errors in the ephemeris data transmitted by each satellite cause corresponding errors in the computed position of the satellite which result in range errors less than 1 m. This error can also be nearly eliminated by use of DGPS. [5]

Onboard Clock Errors: The satellite's clock error can cause error about 1 m in range. This error can also be nearly eliminated by use of DGPS. [5]

Receiver Clock Errors: Because the navigation solution includes a solution for receiver clock error, the requirements for accuracy of receiver clocks is far less severe than for the GPS satellite clocks. [5]

For more detailed information about GPS data errors refer to Appendix B.

1.4.4. Dilution of Precision

GPS positioning is based on range measurements and a better accuracy is obtained by using reference points (satellites) well separated in space. For example, the range measurements made to four reference points clustered together will yield nearly equal values. Position calculation involves range differences, and where the ranges are nearly equal, small relative errors are greatly magnified in the difference. This effect, brought about as a result of satellite geometry is known as Dilution of Precision (DOP). This means that range errors that occur from other causes such as clock errors are also magnified by the geometric effect, in other words, when ranges are nearly equal due to geometry of satellites, errors from other sources are also magnified in the difference. [5]

1.5. Inertial Navigation System

Inertial Navigation System (INS) relies on knowing the initial position, velocity and altitude and thereafter measuring attitude rates and accelerations and integration of them to maintain an estimate of the host vehicle. An inertial measurement unit contains a cluster of sensors (accelerometers and gyroscopes) which are rigidly mounted to a common base to maintain the same relative orientations.

1.5.1. Advantages and Disadvantages of INS

The advantages of INS over other forms of navigation for active safety applications are as follows:

1. It is autonomous and does not rely on external aids or on visibility conditions. It can operate anywhere on the globe.
2. It is inherently well suited for integrated navigation, guidance and control of host vehicle.

The main disadvantage of INS is that the mean-squared navigation errors increase with time due to integration of sensing errors.

1.5.2. INS Error Sources

Initialization Errors: Inertial navigation can only integrate sensed accelerations to propagate initial estimates of position and velocity. Initialization errors are the errors in these initial values.

Alignment Errors: Errors between sensors input axes and the navigation axes are the alignment errors.

Sensors Compensation Errors: Sensor Calibration is a procedure for estimating the parameters of models used in sensor error compensation. It is not uncommon for these modeled parameters to change over time and between turn-ons which causes sensor compensation errors.

1.6. Dead Reckoning

Dead Reckoning methods can be of many kinds. The one widely used in vehicles is odometry which measures vehicle speed. Odometry means integration of incremental motion information over time, which leads to accumulation of errors. These errors increase proportionally with the traveled distance. The main errors are caused by wheel slippage, variations in tire pressure or radius and travel over nonsmooth surfaces or unexpected objects. [11]

1.7. Requirements on Digital Map and Positioning Accuracy in IASA

Digital road maps may be able to act as an additional sensor for various driver assistance systems, providing information about the vehicle's relationship to the roadway infrastructure that is not feasible to obtain with other sensors such as radar or computer vision. It will not preclude the need for these other sensors, but may add a necessary component for successful implementation of future systems. [2]

However there are also imprecisions associated with digital road maps due to model error or data error. These errors can be either geometrical or topological and a summary follows below.

- Digital road maps are mostly based on a single line model; however, real world roads are multi lane.
- Roads are usually described by piece-wise linear links which approximate road curvature, while real world roads are smooth.
- Current road network models can not describe road intersections perfectly. In current road network models intersections are shown by their center point and there is no information about intersection geometry, e.g. whether there are traffic

islands or traffic circle (see Figure 1-6). Another attribute that is not available in current road maps is intersection corner curvature which is specified either by road side marking line or asphalt edge and which determines space available for turning maneuver. (see Figure 1-7)

- There are deficiencies due to the road network topological¹ model. For example a road network model which is based on the connection of nodes, can describe vehicle motion along one road segment, however it can not describe the turn restrictions in an intersection. [3]

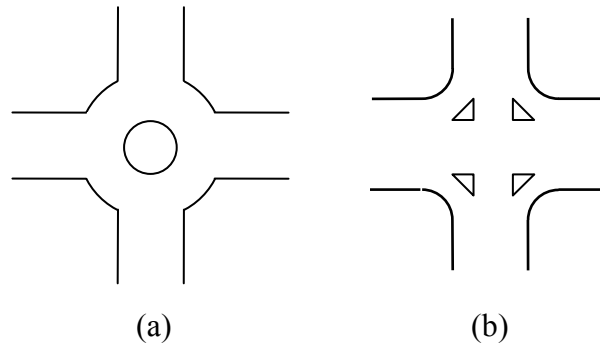


Figure 1-6 (a) Traffic Circle, (b) Traffic islands

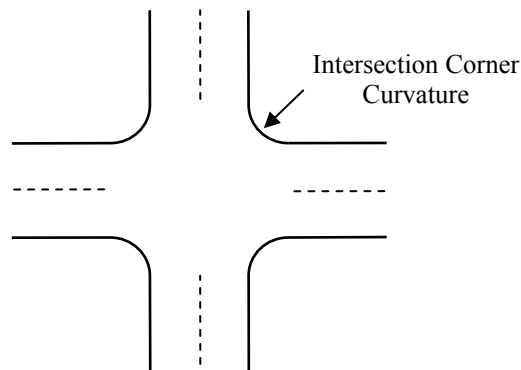


Figure 1-7 Intersection Corner Curvature

There is a need for further information in road databases for active safety applications such as width of each lane, lane marking, shoulder information, etc.

Much effort has been put into the enhancement and specification of digital road maps. For example the Enhanced Digital Maps Project, carried out by DaimlerChrysler Research and Technology North America (DCRTNA), Ford, GM, Navigation Technologies (NavTech) and the Toyota Technical Center (Toyota). The Enhanced Digital Map Project is a three-year effort launched in April, 2001 to develop a range of

¹ Relationship between spatial entities, such as connecting, separating, etc.

digital map database enhancements that enable or improve the performance of driver assistance systems currently under development or consideration by U.S. automakers. This effort is examining the feasibility of expanding the content and / or enhancing the resolution of current digital maps as an enabling technology for various collision avoidance systems. [2]

An activity was included in the Enhanced Digital Map Project to investigate the required accuracy for three different active safety applications; Stop Sign Assist, vision based Traffic Signal Assist and Intersection Collision Avoidance System (ICAS). A summary of its suggested requirements for Stop Sign Assist and Traffic Signal Assist applications are presented in Table 1-2. Suggested requirements for ICAS are presented in section 1.7.1.

Table 1-2 Positioning requirements for Stop Sign Assist application [2]

Assumptions	Driving speed: - Maximum speed at non-posted section	55MPH, 88km/h, 24.4m/s
	Maximum Deceleration	0.3G (2.94m/s ²)
	Stop line width	0.3m
	Stop line offset	3m
	Brake actuator response delay	100ms, 2.5meter at 24.4 m/s
Positioning Requirements for Stop Sign Assist (Warning)	Absolute map position error in longitudinal direction	1m
	Vehicle positioning error in longitudinal direction	5m
	Data update rate	10Hz
Positioning Requirements for Stop Sign Assist (Control)	Absolute Map position error in longitudinal direction	0.3m
	Vehicle positioning error in longitudinal direction	0.5m
	GPS outage error: (in last 10s prior to reaching the stopping point)	0.1m
	Data update rate will directly relate to the response delay	At least 50Hz is expected
Positioning Requirements for Traffic Signal Assistant	Vehicle positioning error	1m to 2m
	Traffic signal longitudinal position error in map	2m
	Traffic signal lateral position error in map	3m

1.7.1. Requirements for Intersection Collision Avoidance System

The infrastructure is stationary but vehicles are not, therefore, positioning requirements should be a concern mainly for vehicles. ICAS assists in avoiding “inattentive” or “aggressive¹” driving. To do so, the ICAS should transmit warnings/control commands to vehicles to stop/reduce speed and/or control the drive path when the vehicle is likely to run past defined stopping locations or likely to get into a collision. [2]

The functionality of the ICAS is quite similar to the “Stop Sign Assistant (Control)” in terms of making a stop. Therefore, positioning requirements for ICAS application are similar to requirements for Stop Sign Assist. Regarding communication capability, shorter communication latency would be required due to the fact that both vehicles are moving and their relative speed is vector addition of their speeds. (e.g. the distance traveled in 20ms corresponds to 0.2m when driven at 40km/h). [2]

Summary of vehicle positioning requirements for ICAS is covered in Table 1-3.

Table 1-3 Summary of vehicle positioning requirements for ICAS [2]

Positioning Requirements for ICAS	Longitudinal absolute positioning error	Less than 0.5m for control
	Lateral absolute positioning error	Less than 0.2m for control
	GPS outage error in 10 seconds	Less than 0.1m for control
	Data update rate	At least 50Hz
	Communication latency	Less than 20ms, at least 50H
	Expected absolute accuracy of road/lane geometry ²	0.3m

In another report published by NHTSA [4] performance guideline for an ICAS system using GPS and ITS countermeasures (laser radar) is investigated. Some important parameters, the source of the parameters, the current and desired values of the parameter and a comment on how the parameter affects system performance are listed in table 1-4.

ICAS vehicle speed should be accurate within 0.15 m/sec. The ICAS vehicle’s speed is estimated by the Continuous Positioning System (CPS) which uses the vehicle speed sensor and GPS. In addition to causing errors in positioning, the error in the CPS’s speed estimate can result in tracking targets which have zero velocity. These stationary targets would appear to have a velocity equal to the error in vehicle speed. This would cause the

¹ Aggressive driving has been said generally to include excessive horn-honking, running red lights, traffic weaving, tailgating, headlight flashing, braking excessively, excessive speeding, profanity/obscene gestures, blocking the passing lane, etc. [7]

² The travel distance to the stopping point or road signs could be obtained from this attribute. The ICAS should be capable of providing precise lane guidance. Lane-by-lane representations of each map element would be required because restrictions are lane dependent. The centerline represents the lane. [2]

tracker to establish a track and the warning algorithm to be applied causing possible false alarms.

Position and roadway information update rate of 10 Hz adequate for ICAS. The ICAS system performed adequately when operating at a system update rate of 10Hz. Investigation of vehicle position update rate of 1 Hz, which is the update rate for standard GPS systems, was found to be inadequate to support the countermeasure function. The inadequate update rate caused false alarms and inconsistency of the warnings provided by the GIS/GPS un-signalized intersection warning system.

The latency of data is important in the ICAS, and needs careful attention to detail. The latency of data being provided by the various sensors in the ICAS is a critical area that must be addressed. Common to many applications where vehicle position and dynamics are being measured, the synchronization of data streams is important.

Time delays in the accessing of map data should not be sufficient to cause problems with data flow and processing of countermeasure functions.

Table 1-4 Performance Guidelines of Threat Detection System (ICAS capable of issue warnings) [4]

Parameter	Source	Desired Value	Affects
Target and ICAS vehicle position accuracy	DGPS /GIS	<3 m	Countermeasure logic, warning times
ICAS vehicle speed	CPS	<0.15m/s	Target and ICAS speed estimate
Intersection location accuracy	GIS	1 m	consistency of alarms, tracker accuracy
Vehicle position update rate	DGPS	10 Hz	consistency of alarms
Data latency	GIS/ GPS	0.3 sec	Provision of warnings
Accuracy of roadway data elements	GIS	Highly Accurate	ability of system to function
Accuracy of roadway shape characteristics	GIS	Highly Accurate	ability to point radar, vehicle position
Accuracy of Traffic Control Device Inventory	GIS	Highly Accurate	Provision of warning, system actions at intersection

1.7.2. Analysis of positioning requirements

In conclusion positioning requirements for an ICAS can be categorized into two levels; warning level requirements and control level requirements. A summary of these requirements found in the literature are presented in Table 1-5.

Table 1-5 positioning requirements stated in literature for Intersection active safety applications

No.	Item	Warning level	Control level
1	Longitudinal absolute positioning error	5m	0.5m
2	Lateral absolute positioning error	2m	0.2m
3	Expected absolute accuracy of road/lane geometry	1m Road level	0.3
4	Speed Accuracy	0.15m/s	----
5	GPS outage error in 10 seconds	1m	0.1m
6	Position update rate	10Hz	50Hz
7	Communication latency	100ms	20ms

There are some other specifications of the positioning system that should be identified regarding these requirements. To have an estimate of these requirements, effect of these variables on positioning system performance was analyzed.

According to Table 1-5, GPS outage error should be less than 0.1m during last 10 seconds of GPS blockage for control level and less than 1 m for warning level. To achieve this requirement, needed heading accuracy, speed accuracy and acceleration accuracy can be calculated as follows:

Assume that the vehicle shown in Figure 1-8 is driving on a straight road in x direction at time t_0 and after Δt seconds of GPS blockage, $\delta x, \delta y, \delta \psi$ are errors in x and y position and heading respectively.

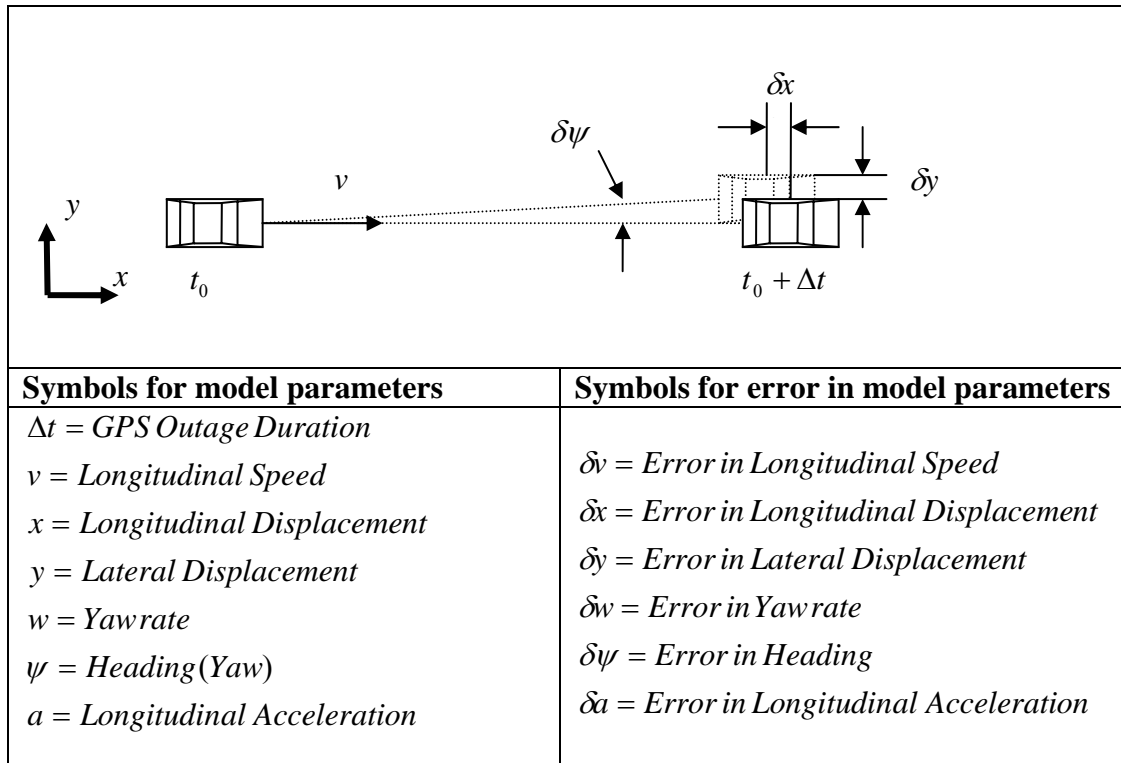


Figure 1-8 A model and symbols used for analysis of positioning requirements

Based on vehicle's equations of motion:

$$x = v \cdot \cos \psi \cdot \Delta t$$

$$y = v \sin \psi \cdot \Delta t$$

$$\psi = w \cdot \Delta t + \theta_0$$

$$v = a \cdot \Delta t + v_0$$

$$\psi_0 = 0$$

$$v_0 = 20 \text{ m/s}$$

$$\Delta t = 10 \text{ s}$$

Required speed accuracy to achieve longitudinal position requirement, is:

$$x = v \cos \psi \cdot \Delta t$$

$$\delta x = \underbrace{\delta v \cos \psi \cdot \Delta t}_{\approx 1} - \underbrace{v \sin \psi \cdot \delta \psi \cdot \Delta t}_{\approx 0} = \delta v \cdot \Delta t$$

$$\delta v = \frac{\delta x}{\Delta t}$$

$$\text{Warning Level : } \delta v = \frac{1m}{10s} = 0.1m/s$$

$$\text{Control Level : } \delta v = \frac{0.1m}{10s} = 0.01m/s$$

So required acceleration accuracy is:

$$v = a.\Delta t + v_0$$

$$\delta v = \delta a.\Delta t + \delta v_0$$

$$\delta a = \frac{\delta v - \delta v_0}{\Delta t}$$

$$\text{Warning Level : } \delta w = \frac{0.1m/s - 0}{10s} = 0.01m/s^2$$

$$\text{Control Level : } \delta w = \frac{0.01m/s - 0}{10s} = 0.001m/s^2$$

Required heading accuracy to achieve lateral position requirement, is:

$$y = v \sin \psi . \Delta t$$

$$\delta y = \underbrace{\delta v \sin \psi . \Delta t}_{\approx 0} + v \underbrace{\cos \psi}_{\approx 1} . \delta \psi . \Delta t = v . \delta \psi . \Delta t$$

$$\delta \psi = \frac{\delta y}{v . \Delta t}$$

$$\text{Warning Level : } \delta \psi = \frac{0.4m}{20m/s . 10s} = 0.002 \text{ rad} \approx 0.1 \text{ deg}$$

$$\text{Control Level : } \delta \psi = \frac{0.04m}{20m/s . 10s} = 0.0002 \text{ rad} \approx 0.01 \text{ deg}$$

So required yaw rate accuracy is:

$$\psi = w . \Delta t$$

$$\delta \psi = \delta w . \Delta t$$

$$\delta w = \frac{\delta \psi}{\Delta t}$$

$$\text{Warning Level : } \delta w = \frac{0.002 \text{ rad}}{10s} = 0.0002 \text{ rad/s} = 0.01 \text{ deg/s}$$

$$\text{Control Level : } \delta w = \frac{0.0002 \text{ rad}}{10s} = 0.00002 \text{ rad/s} = 0.001 \text{ deg/s}$$

In the calculation of heading accuracy, maximum acceptable GPS outage error in lateral direction is estimated from absolute longitudinal and lateral positioning requirement and GPS outage error stated in table 1-5.

The required heading accuracy in both levels of application are very high. Achieving such level of accuracy even by using a highly accurate gyro is not feasible due to lack of an accurate absolute heading measurement for initiation. Therefore heading data should be corrected by other sources of data such as digital map or data from local positioning systems like vision system or active cruise control system.

A summary of requirements on positioning system parameters suggested by the authors is presented in Table 1-6.

Table 1-6 Positioning Requirements suggested by Author

No.	Item	Warning level	Control level
1	Longitudinal absolute positioning error	5m	0.5m
2	Lateral absolute positioning error	2m	0.2m
3	Expected absolute accuracy of road/lane geometry	1m Road level	0.3
4	Speed Accuracy	0.1m/s	0.01m/s
5	GPS outage error	1m	0.1m
6	Position update rate	10Hz	50Hz
7	Communication latency	100ms	20ms
8	Heading Accuracy	0.1 <i>deg</i>	0.01 <i>deg</i>
9	Yaw rate Accuracy	0.01 <i>deg/s</i>	0.001 <i>deg/s</i>
10	Acceleration accuracy	0.01 m/s^2	0.001 m/s^2

1.8. References

1. Tomas J. Nagel, James A. Arnold, Christopher K.H. Wilson, Paul M. Novak, "Automotive Concepts for use of the Modernized Global Positioning System (GPS)", SAE Technical Paper, No. 2003-01-0538
2. Mike Shulman, Richard K Deering, "Second Annual Report of the Crash Avoidance Metrics Partnership", NHTSA office of Advanced Safety Research, Report No. DOT HS 809 663, January 2003
3. Zhang Xiaoguo, Wang Qing, Wan Dejun, "The Relationship Among Vehicle Positioning Performance, Map Quality, And Sensitivities And Feasibilities Of Map-Matching Algorithms", IEEE Paper, 2003
4. J. Pierowicz, E Jocoy, "Intersection Collision Avoidance Using ITS countermeasures-Intersection Collision Avoidance System Performance Guidelines", NHTSA office of advanced safety research, Report No. DOT HS 809 171, September 2000
5. Mohinder S. Grewal, Lawrence R. Weill, Angus P. Andrews, "Global Positioning Systems, Inertial Navigation, and Integration", Wiley, New York, 2001
6. Mathieu St-Pierre, Denis Gingras, "Neural Network Based Data Fusion for Vehicle Positioning in Land Navigation System", SAE Technical Paper, 2004-01-0752
7. F. Gustafsson, F. Gunnarsson, N. Bergman, U. Forssell, J. Jansson, R. Karlsson, P. Nordlund, "Particle Filters for Positioning, Navigation and Tracking", IEEE Transactions on Signal Processing
8. http://www.calccit.org/itsdecision/serv_and_tech/Collision_avoidance/intersection.html#CHALLENGES, California Center for Innovative Transportation (CCIT)
9. Sheila Sarkar, "Spatial and Temporal Analyses of the Variations in Aggressive Driving and Road Rage Behaviors Observed and Reported on San Diego Freeways".
10. European Enhanced Vehicle-Safety Committee, Working Group 19, Primary and secondary safety Interactions.
11. Ferenc Vajda, Miklós Vogel, László Vajta, "Position Estimation and Optimal Landmark Arrangement in the Field of Landmark Based Navigation", Budapest University of Technology and Economics Department of Control Engineering and Information Technology

2. Method

In this chapter an overview of the test vehicle and sensors used for navigation will be presented, followed by an explanation of fusion method which integrates the data from GPS receiver and other sensors. Finally the map fusion algorithm will be explained.

2.1. Test Vehicle

The test vehicle is a standard Volvo V70, which is equipped with a GPS receiver (G12), a Cronos unit - which collects CAN bus data and analogue sensor measurements - and a fiber optic gyro (FOG) which are explained below.

G12 GPS Receiver: According to its manual, G12 GPS receiver features 12-channel/ 12-satellite operation; each of up to 12 visible satellites can be assigned to a discrete channel for continuous tracking. Each satellite broadcasts almanac and ephemeris data every 30 seconds which will be recorded by G12. Obviously G12 does not use data from satellites which are marked unhealthy in ephemeris. The G12 is designed for both stand alone and DGPS operation; when it is in DGPS operation, it will use SWEPOS¹ reference GPS stations.

The G12 uses instantaneous Doppler values from four satellites to compute velocity which make it independent of the last position fix. (For information about Doppler measurements refer to Appendix C.)

The major sources of error affecting the accuracy of GPS range measurements (stated in section 1.5.3) are ephemeris data error, satellite clock error, ionosphere, troposphere, multipath and receiver noise in measuring range). In stand alone operation, the G12 uses ionospheric and tropospheric models to compensate for errors caused by ionospheric and tropospheric delay. However when it is operating in differential mode, these errors as well as ephemeris data error and satellite clock error are nearly removed, the residual error due to these sources is in the order of one millimeter for every kilometer of separation between base and remote receivers.

Multipath error and receiver noise are not correlated between the base and remote receiver and is not canceled by differential GPS; however in the G12, integrated doppler measurements are used to smooth the range measurements and reduce the errors resulting from receiver noise. Multipath errors are also reduced by means of a digital signal processing technique implemented in the hardware and software of the G12 receiver. This technique removes multipath errors for reflected signals with delays of 37 meters or more, almost entirely. [7]

¹ <http://swepos.lmv.lm.se/english/index.htm>

On the whole stand alone position accuracy is 3 meters in case of PDOP¹ less than 4, but when the G12 is operating in differential mode, position accuracy improves to better than 1 m.

The GPS parameters which were used in this thesis work are presented in Table 2-1 and Figure 2-1.

Cronos unit: The Cronos unit is a measurement device which offers direct connection of different components like the Controller Area Network (CAN) bus and analog/digital sensors in the vehicle. The cronos out parameters which were used in this thesis work are presented in Table 2-1 and Figure 2-1.

Fiber Optic Gyro (FOG): FOG is an optical fiber gyro in the test vehicle which measures the yaw rate.

Table 2-1 Measurements used in this thesis work

Measurements	Symbol	Source	Sampling Frequency
Longitude ^a	θ_{GPS}	GPS	10Hz
Latitude ^a	ϕ_{GPS}		10Hz
Altitude ^a	h_{GPS}		10Hz
Ground Speed	V_{GPS}		10Hz
Heading ^b	ψ_{GPS}		10Hz
HDOP ^c	$HDOP$		10Hz
ABS Speed	V_{CAN}	Cronos	50Hz
Longitudinal Acceleration	a_{CAN}		50Hz
Yaw Rate	\dot{Y}_{CAN}		50Hz
Yaw Rate	\dot{Y}_{FOG}	FOG	50Hz

^a Referenced to an earth fixed global reference frame called World Geodetic System 1984 (WGS84)

^b Measured clockwise from north axis

^c Horizontal Delusion of Precision

¹ Position Dilution of Precision

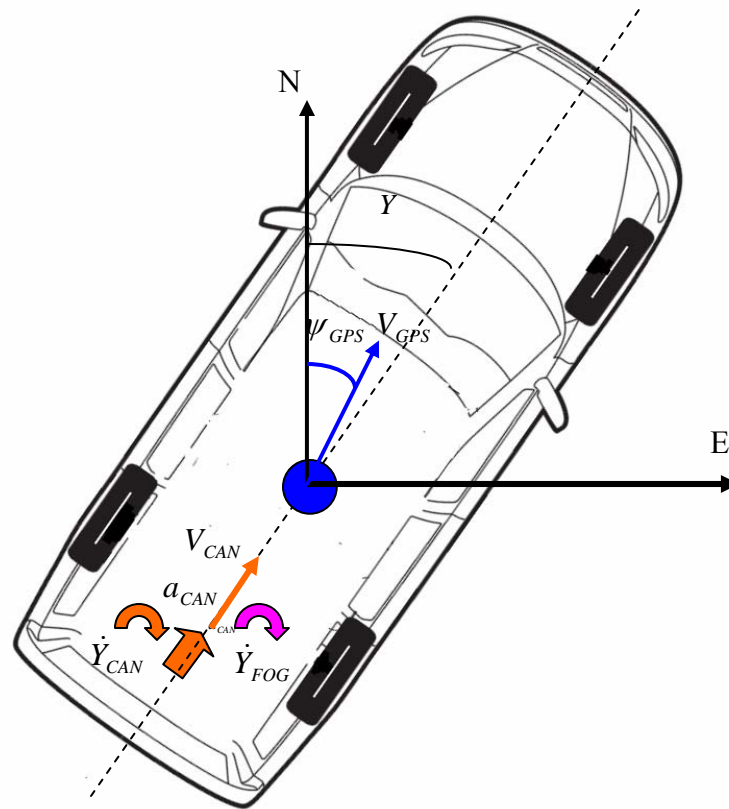


Figure 2-1 Measurements used in this thesis work with position of relative sensor

2.2. Data Fusion

GPS has been playing a major role in land navigation systems; however due to signal blockage by high buildings or heavy foliage and severe multipath in urban environments, GPS alone cannot satisfy requirements for an intersection active safety application. Thus, in this thesis work, data from GPS was integrated with data from complementary onboard sensors (presented in Table 2-1) to maintain a continuous and more accurate position. A schema of fusion system is presented in Figure 2-2.

A Kalman filter, which is the most common data fusion method, was used to integrate all the noisy measurements from different sensors in an optimal manner. In the following section a short description of Kalman filter along with Kalman filter formulation of vehicle positioning system established in this project is presented.

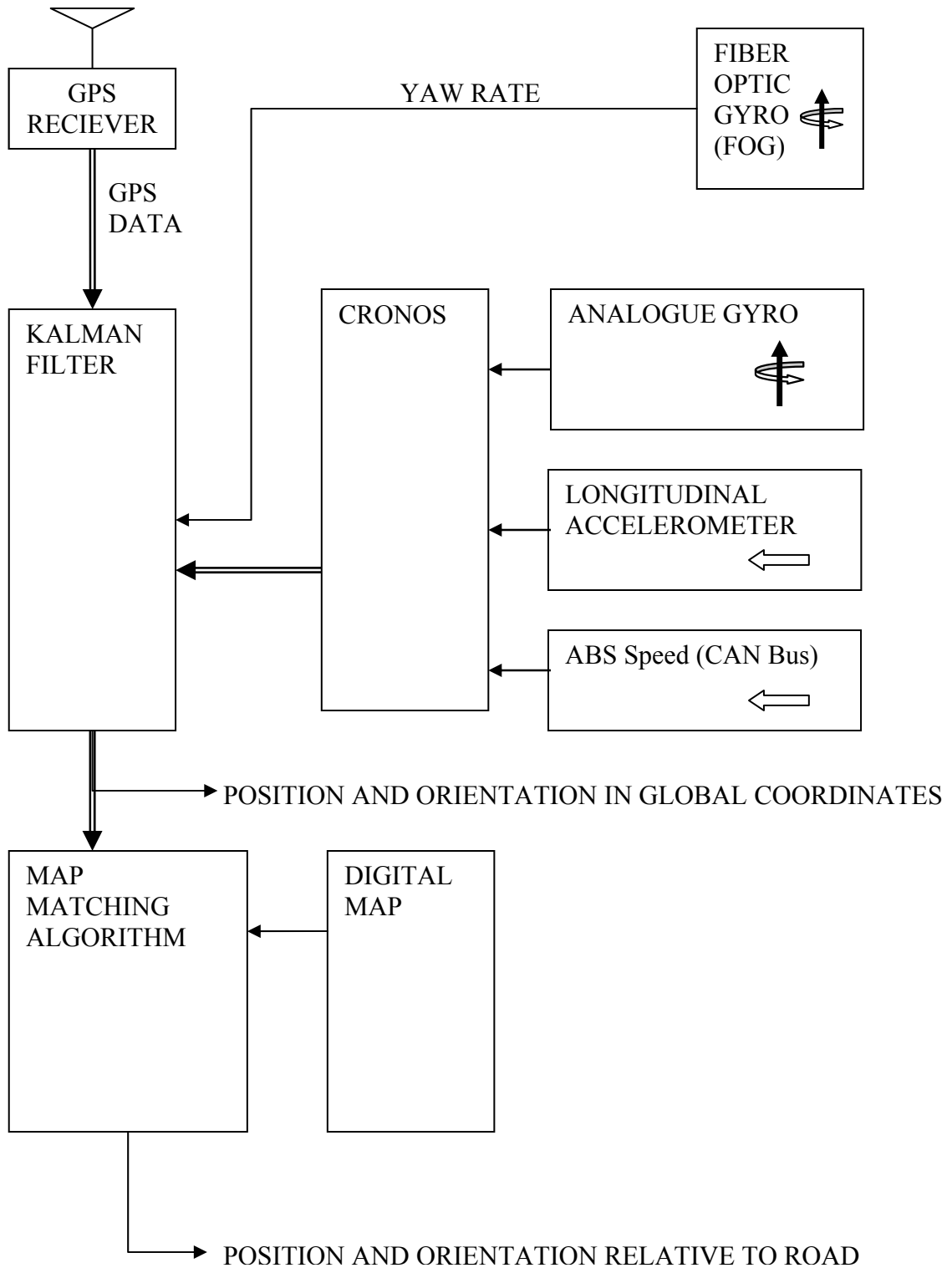


Figure 2-2 Schema of the fusion system

2.3. Kalman Filter

Theoretically the Kalman Filter is an estimator for what is called the linear-quadratic problem which is the problem of estimating the instantaneous “state” of a linear dynamic system perturbed by a white noise:

$$\frac{d}{dt}x = \Phi(t)x + w(t)$$

by using measurements linearly related to the state but corrupted by white noise:

$$z = Hx + v(t)$$

The random variables $w(t)$ and $v(t)$ represent the process and measurement noise, respectively. They are assumed to be independent of each other, white, and with normal probability distributions.

The Kalman filter is an optimal recursive data processing algorithm. It is optimal in the sense that it minimizes the estimated error covariance. Another aspect of its optimality is that the Kalman filter incorporates all information that can be provided to it. It processes all available measurements, regardless of their precision, to estimate the current value of the variables of interest, with use of (1) knowledge of the system and measurement device dynamics, (2) the statistical description of the system noises, measurement errors, and uncertainty in the dynamics models, and (3) any available information about initial conditions of the variables of interest.

The word recursive in the previous description means that the Kalman filter does not require all previous data to be kept in storage and reprocessed every time a new measurement is taken. This will be of vital importance to the practicality of filter implementation. [9]

The Kalman Filter is a two-step process, “prediction” and “correction”. In the prediction step, the estimate of state variables \hat{x} and its associated covariance matrix of uncertainty, P , are propagated from one time step to another. This is the part where the dynamics of underlying physical processes come into play. The correction step makes corrections to the estimate of state variables and covariance matrix P , based on new information obtained from sensor measurements.

The equations used to propagate the covariance matrix, model and manage uncertainty; taking into account how sensor noise and dynamic uncertainty contribute to uncertainty about the estimated system state. By maintaining an estimation of its own estimation uncertainty and the relative uncertainty in the various sensor outputs, the Kalman filter is able to combine all sensor information optimally.

The main focus in the Kalman filter is on computation of the optimal value of the Kalman gain matrix \bar{K} used for correcting estimate of \hat{x} and its associate covariance matrix $P(-)$, based on a measurement:

$$\begin{aligned}\hat{x}(+) &= \hat{x}(-) + \bar{K}[z - H\hat{x}(-)] \\ P(+) &= P(-) - \bar{K}HP(-)\end{aligned}$$

The Kalman gain matrix \bar{K} is derived based on Gaussian Maximum-Likelihood Estimate (MLE) which results in:

$$\bar{K} = P(-)H^T (HP(-)H^T + R)^{-1}$$

Where $P(-)$ is the predicted value of estimation covariance, H is the measurement sensitivity matrix and R is the covariance of sensor noise or measurement uncertainty. [1, 2]

2.3.1. Extended Kalman Filter

Kalman filter is defined for linear dynamic systems with linear sensors, However it has been applied more often to real world applications without truly linear dynamics or sensors, which is also the case in this thesis work. It is due to these nonlinearities that Extended Kalman Filter, which is an approach to Kalman filtering for nonlinear systems using linearization of the system model about the estimated state, was used in this thesis work.

The essential Extended Kalman Filter equations are summarized in Table2-2. The following are some names commonly used for the symbols in Table 2-2. [1]

H is the *measurement sensitivity matrix*.

$H\hat{x}_k(-)$ is the *predicted measurement*.

$z - H\hat{x}_k(-)$, the difference between the measurement vector and the predicted measurement is the *innovations vector*.

\bar{K} is the *Kalman gain*.

$P_k(-)$ is the *predicted or a priori value* of estimation covariance.

$P_k(+)$ is the *corrected or a posteriori value* of estimation covariance.

Q_k is the covariance of *dynamic disturbance noise*.

R is the covariance of *sensor noise or measurement uncertainty*.

$\hat{x}_k(-)$ is the *predicted or a priori value* of the estimated state vector.

$\hat{x}_k(+)$ is the *corrected or a posteriori value* of the estimated state vector.

z is the *measurement vector*.

Table 2-2 Extended Kalman Filter equations [1]

System dynamic model $w(t)$ is white noise	$\frac{d}{dt} x = f(x, t) + w(t)$	(2.1)
Measurement model $v(t)$ is white noise	$z = h(x) + v(t)$	(2.2)
Initial conditions	$\hat{x}_0 = E\langle x_0 \rangle$	(2.3)
	$P_0 = E\langle \tilde{x}_0 \tilde{x}_0 \rangle$	(2.4)
<hr/> <i>Predictor (Time Updates)</i> <hr/>		
Predicted state	$\hat{x}_k(-) = \hat{x}_{k-1}(+) + \int_{t_{k-1}}^{t_k} f \cdot dt$	(2.5)
Predicted covariance matrix	$P_k(-) = \Phi_k P_{k-1}(+) \Phi_k^T + Q_{k-1}$	(2.6)
Where	$\hat{x}_k = \Phi_k \hat{x}_{k-1}$	(2.7)
	$\dot{\Phi} = F\Phi$	(2.8)
	$\Phi(t_{k-1}) = I$	(2.9)
	$F = \left. \frac{\partial f}{\partial x} \right _{x=\hat{x}_k}$	(2.10)
<hr/> <i>Corrector (Measurement Updates)</i> <hr/>		
Kalman gain	$\bar{K}_k = P_k(-) H_k^T (H_k P_k(-) H_k^T + R_k)^{-1}$	(2.11)
Where	$H_k = \left. \frac{\partial h}{\partial x} \right _{x=\hat{x}_k}$	(2.12)
Corrected state prediction	$\hat{x}_k(+) = \hat{x}_k(-) + \bar{K}_k [z_k - h(\hat{x}_k(-))]$	(2.13)
Corrected covariance matrix	$P_k(+) = P_k(-) - \bar{K}_k H_k P_k(-)$	(2.14)

2.3.2. Vehicle Dynamic Model

As stated in previous section, the Kalman filter is an extremely effective and versatile procedure for combining *noisy sensor outputs* to estimate the *state of a system* with *uncertain dynamics* optimally. For the purpose of this thesis:

- The *noisy sensors* include GPS receiver, inertial sensors (accelerometer and gyroscope) and ABS wheel speed sensor. (see Table 2-1)
- The *system state* includes position, velocity, acceleration, heading (yaw) and heading rate. (see Table 2-3)
- *Uncertain dynamics* includes unpredictable disturbance of the vehicle, whether caused by a human operator or by medium (e.g., wind or turn in the road).

Table 2-3 State variables used in Kalman filter

State Variables	Description
Longitude (θ)	Longitude coordinate of vehicle reference point position in WGS84
Latitude (ϕ)	Latitude coordinate of vehicle reference point position in WGS84
Altitude (h)	Altitude coordinate of vehicle reference point position in WGS84
Heading (ψ)	Direction of vehicle reference point velocity measured clockwise from north axis of local tangent plane coordinate
Speed (V)	Magnitude of vehicle reference point velocity
Acceleration (A)	acceleration of vehicle reference point along roll axis in RPY coordinate (see Figure 2-3)
Yaw Rate (\dot{Y})	Rate of change of vehicle angle about yaw axis in RPY coordinate (see Figure 2-3)

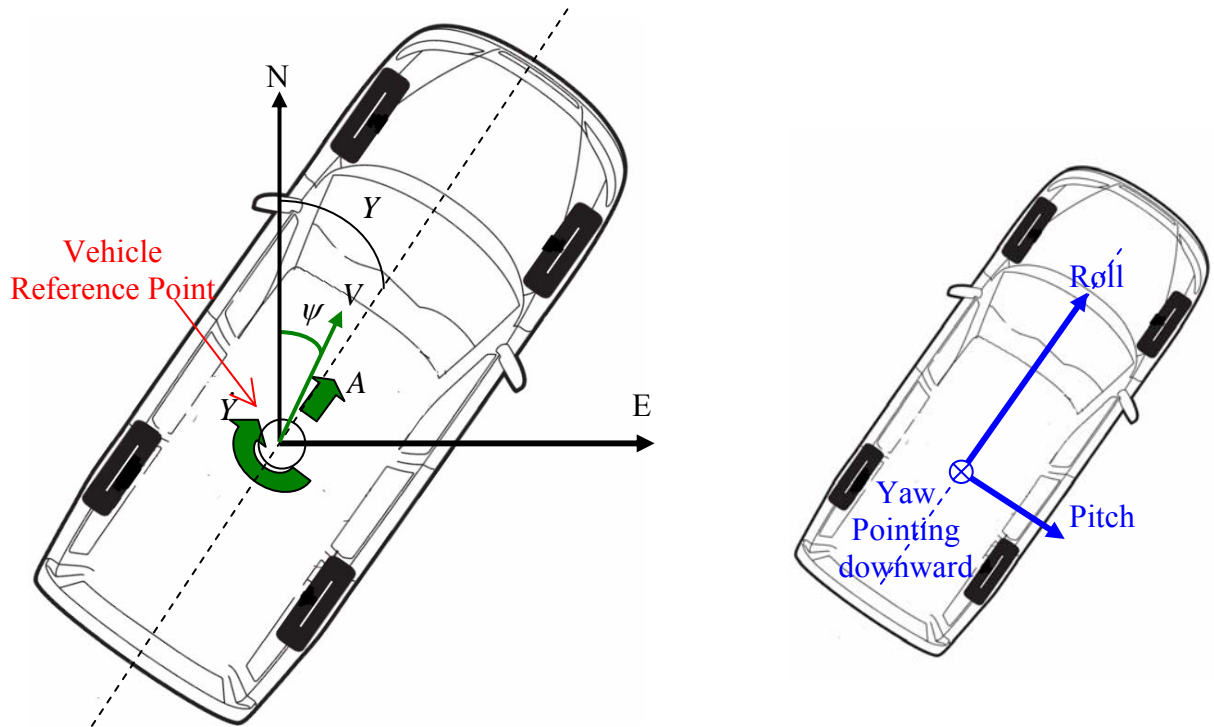


Figure 2-3 Test vehicle and state variables

The vehicle dynamic model on which Kalman filter equations were written is fairly a standard model, with: (For established extended Kalman filter equations refer to Appendix A.)

$$\frac{d}{dt} \theta = \frac{V_E}{\cos(\phi)(r_T + h)}$$

$$\frac{d}{dt} \phi = \frac{V_N}{r_M + h}$$

$$\frac{d}{dt} h = V_U$$

where V_E, V_N, V_U are east, north and up coordinates of velocity in local tangent plane coordinate, respectively. r_T, r_M are transverse radius of curvature and meridional radius of curvature of WGS84 reference ellipsoid at altitude ϕ , respectively, with following equations:

$$r_T = \frac{a}{\sqrt{1 - e^2 \sin^2 \phi}}$$

$$r_M = \frac{a(1 - e^2)}{(1 - e^2 \sin^2 \phi)^{3/2}}$$

a is the semi major axis of reference ellipse and e is the eccentricity.

For simplicity, it was assumed in this model that vehicle speed is in local tangent plane or in other words, the up coordinate of vehicle velocity, V_U is zero. It was also assumed that the state variable; heading, is equal to yaw and consequently its rate of change is equal to yaw rate. This is only true at non-slip conditions where direction of vehicle reference point velocity is along the vehicle centerline (Roll axis) and lateral speed is zero. To reduce the error caused by this assumption vehicle reference point (GPS antenna location) should be close to vehicle center of rotation¹. Vehicle center of rotation moves back and forth as vehicle yaw rate, speed and slip condition changes. Therefore the best solution is to put GPS antenna somewhere on vehicle centerline close to vehicle center of rotation in normal driving condition (see section 4.X). These assumptions lead to following equations:

$$V_E = V \sin(\psi)$$

$$V_N = V \cos(\psi)$$

$$\frac{dV_E}{dt} = A \sin(\psi) - V\dot{\psi} \cos(\psi)$$

¹ Vehicle center of rotation is somewhere on vehicle centerline in which vehicle speed in lateral direction is zero

$$\begin{aligned}\frac{dV_N}{dt} &= A \cos(\psi) + V\dot{\psi} \sin(\psi) \\ \frac{d}{dt}A &= w_{\dot{a}} \\ \frac{d}{dt}\psi &= \dot{\psi} \\ \frac{d}{dt}\dot{\psi} &= w_{\dot{\psi}}\end{aligned}$$

Where $w_{\dot{a}}, w_{\dot{\psi}}$ are white noises.

2.4. Stop and Turn Detection

In the fusion algorithm, there are sub modules which detect vehicle stop and turning. Stop detection is important due to the fact that the position given by GPS receiver can varies up to 10 meters during a stop, although vehicle position does not change¹. Therefore the fusion algorithm maintains the last estimated vehicle position until vehicle movement is resumed; vehicle stop can easily be detected by checking ABS speed which returns a zero value during the stop.

A turning module processes vehicle heading and yaw rate to detect a turning maneuver which will be used in Map Matching algorithm explained in the following section. The turning module will be triggered whenever the yaw rate value exceeds 2.3deg/s- this value was determined by observing yaw rate values during field tests- and if there be an increase or decrease more than 20 degree in heading afterwards, the vehicle would be assumed to be in a turning maneuver. The value of 20 degree is the maximum heading change in an overtaking maneuver in a straight road according to Ocheing [3] which is also approved by field test results conducted during this thesis work.

2.5. Map Matching

As stated in chapter 1, digital road maps are used in land navigation systems as an additional sensor which utilize the restriction of land vehicles to the road network and provide information about the vehicle's position relative to road network. However, there are also imprecision with digital road maps as described in section 1-4. Moreover, even with very good sensor calibration and sensor fusion algorithms, inaccuracies are often inevitable in positioning results. Hence, positioning results do not always match onto the digital road map. This phenomenon is even more severe at intersections which is topic of this thesis work. Therefore, map matching algorithms are usually used to match the positioning results with digital road map. Generally Map Matching refers to the procedure of determining the location of a vehicle with respect to a digital road map.

¹ This may be due to use of GPS heading and velocity for calculation of position in GPS receiver and the fact that the GPS heading and velocity measurement is really poor in low velocities and during stops.

2.5.1. Literature Review on Map Matching Algorithms

A literature survey on different map matching algorithm already developed was done as a part of this thesis work, a summary of which follows:

Point-to-Point matching: In this approach, each positioning point is matched to the closest 'node' in the network. This approach is easy to implement, however, it is very sensitive to the way in which road network is digitized, like number of nodes per meter of a road, etc. In this approach the best achievable precision is the map resolution or in other words the least distance between map nodes. [3]

Point-to-Curve matching: In this approach, the positioning point is matched with the closest curve in the network. Each curve is described by piece-wise linear segments. The line segment which gives the smallest distance is selected as the one on which the vehicle is assumed to be traveling. Although this approach gives better results than point-to-point matching, it also has some deficiencies such as generating very unstable results in dense urban networks with too many intersections and roads which are too close to each other. [3]

On the whole a matching algorithm which just relies on instant position of the vehicle rather than its historical trajectory can lead to unstable results and unreasonable jump from one road to another one especially in dense urban networks and at intersections where distance from all intersecting roads is almost equal.

Curve-to-Curve Matching: In this approach, the historical vehicle path is compared to the possible candidate paths on the map. These candidate paths are paths on the map which lie within general vicinity of the vehicle at any instant time. The candidate map path which best matches the vehicle path is selected as the path on which the vehicle is traveling. Many different pattern recognition techniques can be applied to this approach, the most common of which is cross-correlation. This approach is computationally rather intensive and is quite sensitive to outliers. [5]

Fuzzy Logic Based Matching: Syed (2004) propose a fuzzy logic based map matching algorithm, the basic steps of which are: 1) Identifying the first road link and determining the position of vehicle on it. 2) Tracking the correct link subsequently. 3) Determining the position on the road link tracked in step2. In each steps, algorithm uses fuzzy inputs such as: proximity of positioning solution, small heading differences, average distance traveled on the current link and time. [6]

Ochieng Method: Ochieng (2003) propose a method of map matching which has two distinct processes for identification of the correct link, namely the Initial Matching Process (IMP) and Subsequent Matching Process (SMP). IMP identifies an initial correct link for an initial position fix (position obtained from positioning unit). It uses a confidence region around a position fix based on variance-covariance information associated with GPS or GPS/DR. Then the segments in the confidence region are filtered based on the heading difference between vehicle and each segment. If there remains more

than one candidate, the most appropriate segment will be selected considering the link connectivity and historical information of vehicle location. SMP identifies the consequent road links using turning information.

When the actual road link is identified whether by IMP or SMP, the location of vehicle on it is calculated in two ways. In one way the position fix is projected perpendicularly on the actual road to obtain the easting and northing coordinates of vehicle location on the road. In the other way, bearing of actual road link, vehicle speed and the previous matched point are used to calculate the location of vehicle on the road as below:

$$E_{i+1} = E_i + v \cdot \sin \theta$$

$$N_{i+1} = N_i + v \cdot \cos \theta$$

Where E_i , E_{i+1} are the easting coordinates of vehicle location on road link at time t and $t+1$ respectively and N_i , N_{i+1} are northing coordinates. θ is bearing of actual road link and v is vehicle speed. Finally the optimal estimate of the easting and northing coordinates of vehicle location on the road is obtained by a linear function of two methods:

$$E = k_1 \cdot E_1 + k_2 \cdot E_2$$

$$N = k_1 \cdot N_1 + k_2 \cdot N_2$$

Where E , N are easting and northing coordinates of vehicle location on the road and k_1 , k_2 are weight factors which are calculated based on error variances associated with each method. [3]

Scott Method: Another method for calculating vehicle location on an identified road link is proposed by Scott (1994). This method utilizes the spatial correlation of the measurements errors in a coordinate with one axis collinear with the identified road link. The spatial correlation arises from the angle between the road link and the measurement coordinate in which vehicle position is measured and can be shown by using standard coordinate transformation techniques:

$$\sigma_x^2 = \sigma_a^2 \cdot \cos^2 \theta + \sigma_b^2 \cdot \sin^2 \theta$$

$$\sigma_y^2 = \sigma_a^2 \cdot \sin^2 \theta + \sigma_b^2 \cdot \cos^2 \theta$$

$$\sigma_{xy}^2 = \sin \theta \cos \theta (\sigma_b^2 - \sigma_a^2)$$

$$r = \frac{\sigma_{xy}}{\sigma_x \sigma_y}$$

Where σ_a, σ_b are the error variances in the measurement coordinate and $\sigma_x, \sigma_y, \sigma_{xy}$ are error variances and covariance in the coordinate with one axis collinear with the road link (see Figure 2-4); r is the resulted spatial correlation. [4]

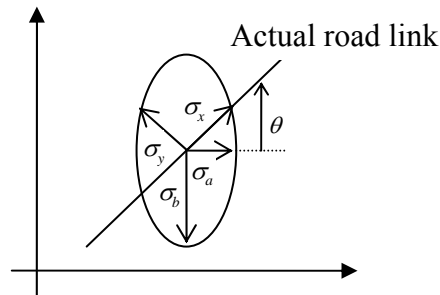


Figure 2-4 Error variances in the measurement coordinate and transferred coordinate

2.5.2. Proposed Map Matching Algorithm

As explained in previous section, in current map matching algorithms, the vehicle position fix is matched on the centerline of roads. This means that the given vehicle trajectory by these map matching methods follows a road's centerline pattern and vehicle maneuvers on the road such as lane changing and turning in an intersection can not be presented (For example vehicle turning in an intersection will be presented by an in place turning on the node where centerlines of intersected roads meet). However in an intersection active safety application the vehicle trajectory is most likely of great importance, therefore in proposed map matching algorithm in this thesis it has been tried to keep the given vehicle trajectory by Kalman and not to match the given vehicle position only to a point on the road centerline, but to match it to a point within the road width. This has been done by calculating and updating the general offset (explained further in following paragraphs) between vehicle position fixes and their respective vehicle location on the road map, which is referred to as "common offset" in this report.

In general the offset between a given vehicle position and its respective location on a given road is calculated as below:

The given vehicle position will be projected on the centerline of given road, which is the only available data about road geometry. Next, the road width will be estimated based on the speed limit on the road (Table 2-4), since road width is not available in the map data but speed limit is.

Table 2-4 Assumed road widths based on the speed limit [8]

Speed Limit (km/h)	Road Width (m)
0-70	7
71-90	9
91-100	13
>100	Highway *

* Since there is no intersections at highways, there are not covered in this thesis and while on a highway, the position fix is considered as vehicle location on the map as well.

Then the offset between the given vehicle position and its respective location on the given road is calculated based on the situation of the given vehicle position relative to its projection on the centerline of given road which can be categorized as follows:

On two way roads (see Figure 2-5):

- a. The given vehicle position is on the right side of the centerline and it is within the road width. In this case the vehicle position is also considered as the vehicle location on the road and the offset is equal to zero.
- b. The given vehicle position is on the right side of the centerline but it is outside the road width. In this case the offset between the vehicle position and the vehicle location on the given road is assumed to be: $d1-d2$, referenced in WGS84, where $d1$ is the distance between vehicle position and projection of it on the centerline of the road and $d2$ is the largest possible distance between centerline and center of a vehicle which is within the road width.
- c. The given vehicle position is on the left side of the centerline. In this case, the offset between the vehicle position and the vehicle location on the road is assumed to be: $d1+d2$, referenced in WGS84, where $d1$ is the distance between vehicle position fix and projection of it on the centerline of the road and $d2$ is half of the vehicle width.

On one way roads (see Figure 2-6):

- a. The given vehicle position is within the road width on either side of the centerline. In this case the vehicle position is also considered as the vehicle location on the road and the offset is equal to zero.
- b. The given vehicle position is on either side of the centerline and is outside the road width. In this case the offset between the vehicle position and the vehicle location on the given road is assumed to be: $d1-d2$, referenced in WGS84, where $d1$ is the distance between vehicle position and projection of it on the centerline of the road and $d2$ is the largest possible distance between centerline and center of a vehicle which is within the road width.

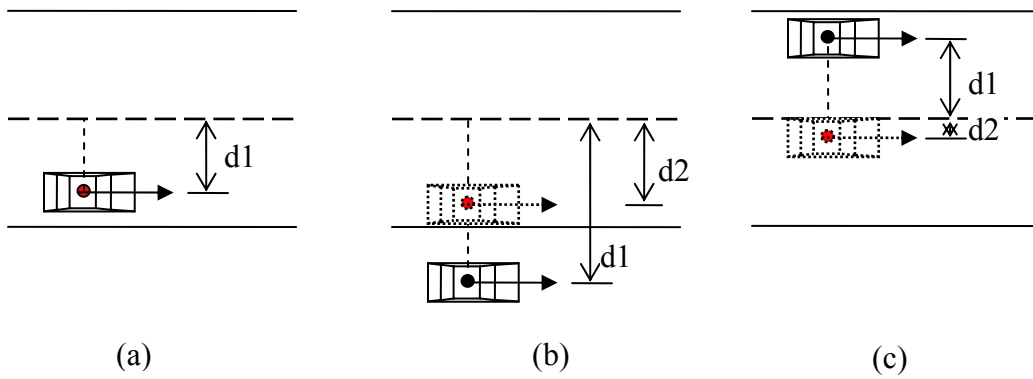


Figure 2-5 given vehicle position and its respective calculated location on a two way road (shown by dashed line if different from given vehicle position)

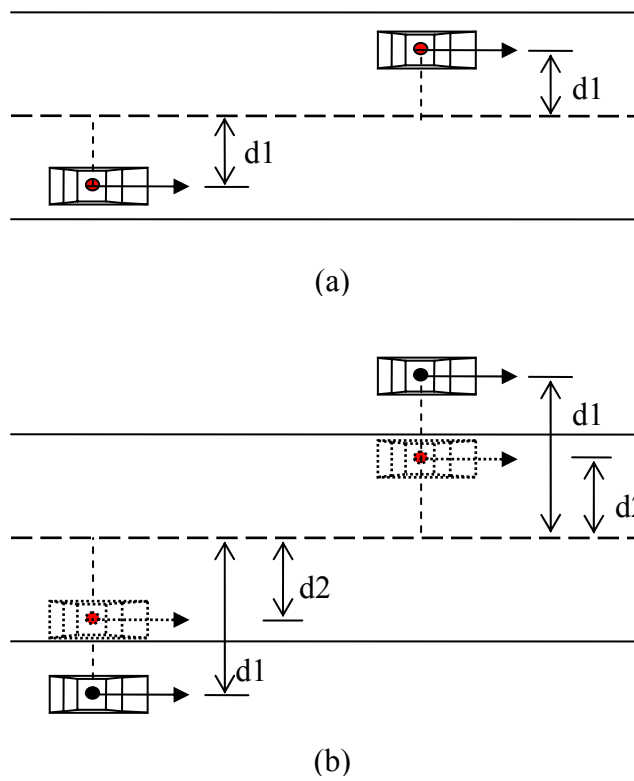


Figure 2-6 given vehicle position and its respective calculated location on a one way road (shown by dashed line if different from given vehicle position)

Clearly, by the above described method only the offset perpendicular to the road can be obtained but not the offset along the road. Even the perpendicular offset is the minimum of that offset which if be added to given vehicle position will give a location within the road width and on the correct side of the road. Here is where the common offset comes to play. By keeping and updating a common offset based on local calculated offsets, which are referenced to a global coordinate: WGS84, and adding it to each vehicle position fix before projection, the position fix will also be corrected for offsets which are along the road. For example in Figure 2-7, when the vehicle is at point 1 and point 2, the local offsets are $d1$ and $d2$ respectively. However by keeping $d1$ as a common offset and adding it to vehicle position fix at point 2 and then calculating the residual local offset, the vehicle location on the road respective to vehicle position fix 2 would be point 4 rather than point 3 which is a better estimation of vehicle location along the road regarding the vehicle trajectory.

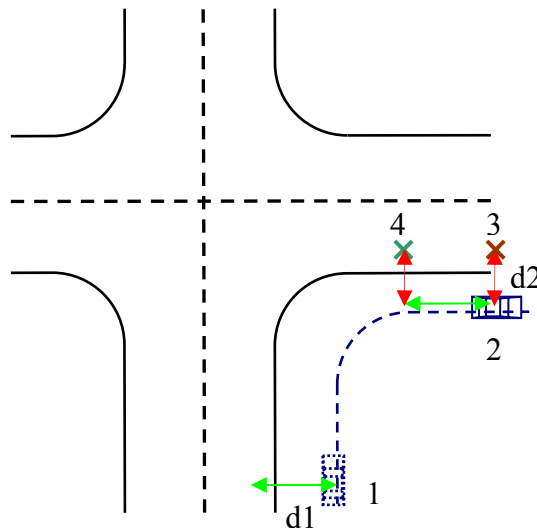


Figure 2-7 Effect of common offset on calculation of respective vehicle location to a vehicle position fix

When the algorithm starts the common offset will be equal to zero and will be updated by each projection and calculation of the residual local offset. However the residual local offset will not be directly added to common offset and a filtering will be applied on it by a Kalman filter based on uncertainty of respective position fix.

Considering the fact that projection does not give reasonable results at intersections due to vehicle turning and lack of information about intersection in the map data and the fact that it is just presented by a node, knowing common offset will improve calculation of vehicle location on the road network at intersections noticeably. This process will be explained in the following sections where different modes of algorithm, namely:

1. Searching Mode
2. Tracking Mode
3. Intersection Mode

are presented.

2.5.3. Searching Mode

In this mode, algorithm searches for the road link on which the vehicle is traveling. Algorithm will be in this mode when it starts or if the tracking fails unexpectedly.

The road link will be determined based on the vehicle position and heading in a sequence of time steps. In each time step a rectangular search region based on the positioning uncertainty will be used (see Figure 2-8). Road links which were in search region in all time steps will be considered for further analysis. If there is only one candidate road link, it will be given as the actual road link, however, in the case of more than one candidate, the most appropriate road link will be the one with the least average total error which is calculated as follows:

In each time step, a total error is obtained for each road link in the search region by summing up normalized distance error and normalized heading error. Normalized distance error is the distance between the vehicle position (calculated by Kalman filter) and the nearest point on the road link, divided by a nominal distance error based on positioning uncertainty. In a similar way, normalized heading error is the heading difference between vehicle and road link, divided by a nominal heading error based on heading uncertainty. Obviously average total error for each road link will be the average of its total error in considered time steps. This mode is summarized in the flow chart in Figure 2-9.

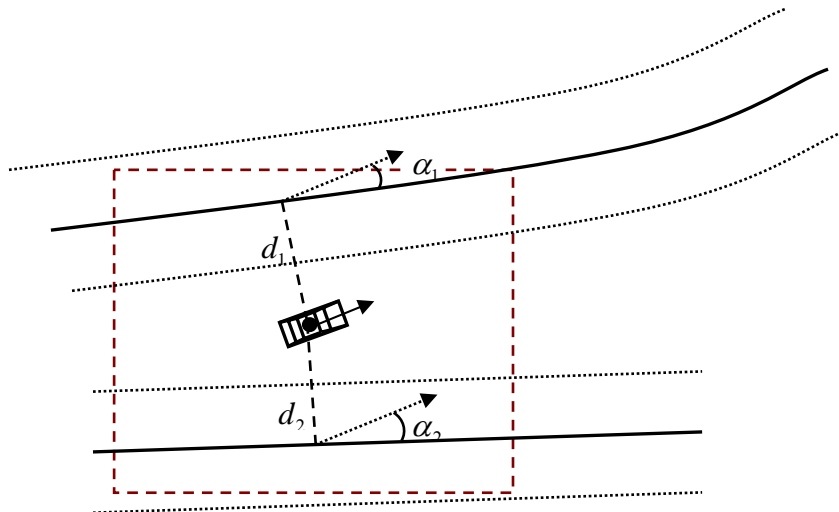


Figure 2-8 A search region around vehicle position with two roads in it and projected point of vehicle position on each road with associated distance and heading errors are shown.

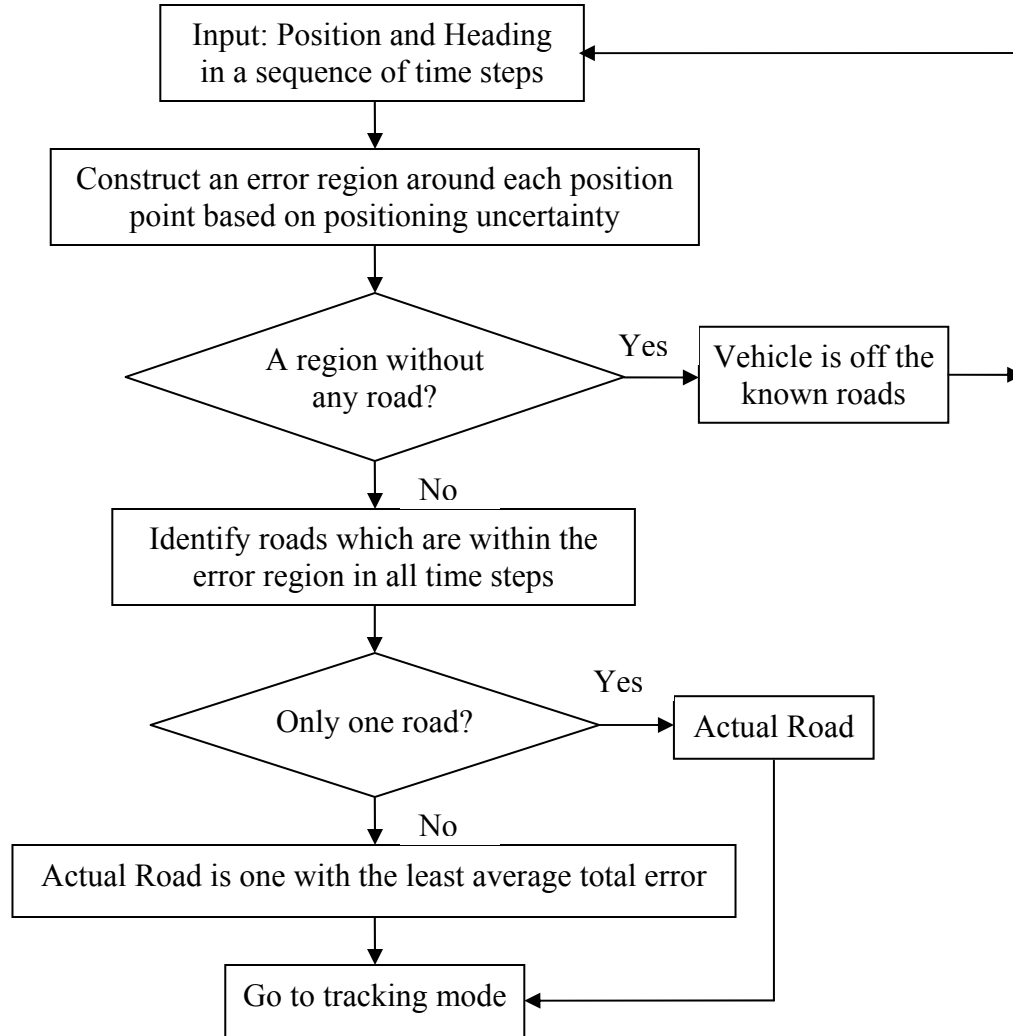


Figure 2-9 Flowchart of searching mode algorithm

2.5.4. Tracking Mode

In this mode, the vehicle will be tracked on the previously selected road in either of searching mode or intersection mode and the distance to the coming intersection will be calculated. The algorithm will stay in this mode until vehicle is in the proximity of a coming intersection (e.g. 30 m). Since the focus of this thesis work is on intersection safety and the vehicle is far from an intersection in this mode, the process of calculating the vehicle location on the road map from respective position fix will be done once in a while (e.g. every 20 m) instead of every time step. In time steps which this process is not performed, the distance to coming intersection will be updated by simple integration of velocity.

To calculate the vehicle location on the road map, common offset (described in section 2.5.2) would be added to the vehicle position fix, then the resulted vehicle position will be projected on the road centerline and distance to next intersection(see Figure 2-10) and

residual local offset (as described in 2.5.2) will be calculated. Other factors which has been used in the existed map matching algorithms such as velocity (in Ochieng method) and positioning variances (in Ochieng and Scott method), have been already considered in the Kalman filter which determines the vehicle position fix. This mode is summarized in the flow chart of Figure 2-11.

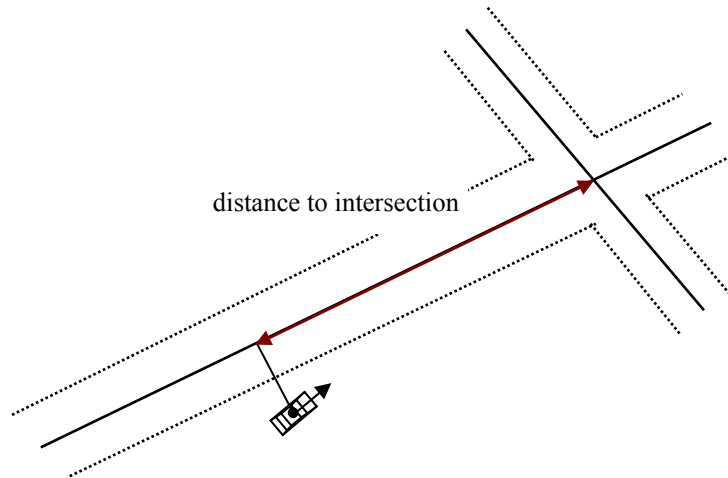


Figure 2-10 Projection of the vehicle position on the actual road and associated distance to intersection

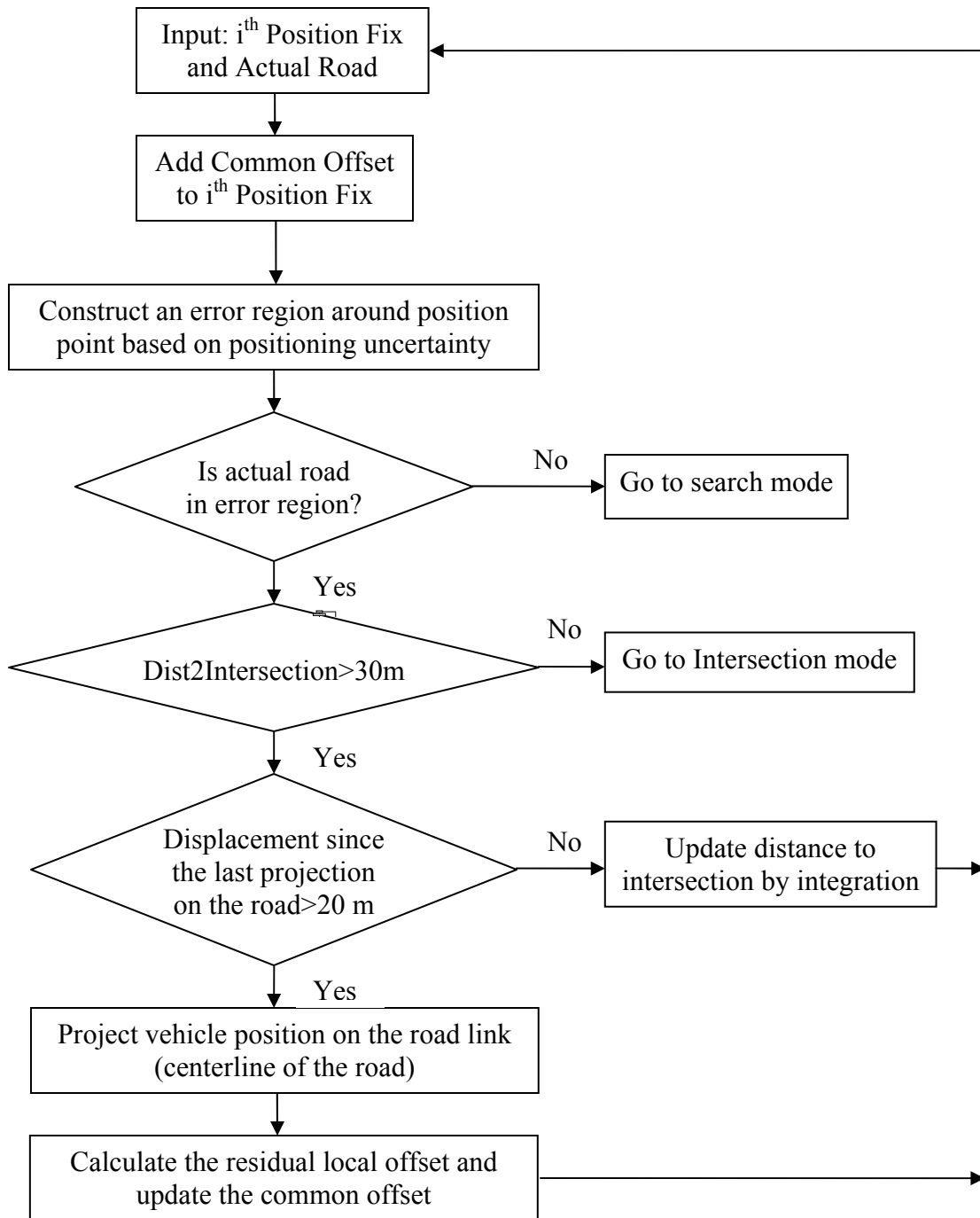


Figure 2-11 Flowchart of tracking mode algorithm

2.5.5. Intersection Mode

In this mode, the vehicle location on the road it is traveling on will be calculated more frequent (e.g. each 2m) but with the same method as explained in tracking mode, until it starts turning or reaches a certain distance to intersection point (e.g. 10 m). From this point on, as stated before, the projection method will not give reasonable results due to vehicle turning and lack of information about intersection in the map data and the fact that it is just presented by a node. Thus, from this point on the vehicle location on the map will be calculated by adding the last obtained offset between vehicle positioning fix and map data to each position fix (See Figure 2.12). Last offset is equal to common offset plus last residual local offset. This mode will end when the turning ends or vehicle gets far enough from the intersection node (e.g. 10 m). At the end of Intersection mode the road on which the vehicle is, will be determined by using turning magnitude and vehicle heading and comparison of it by intersected roads bearing.

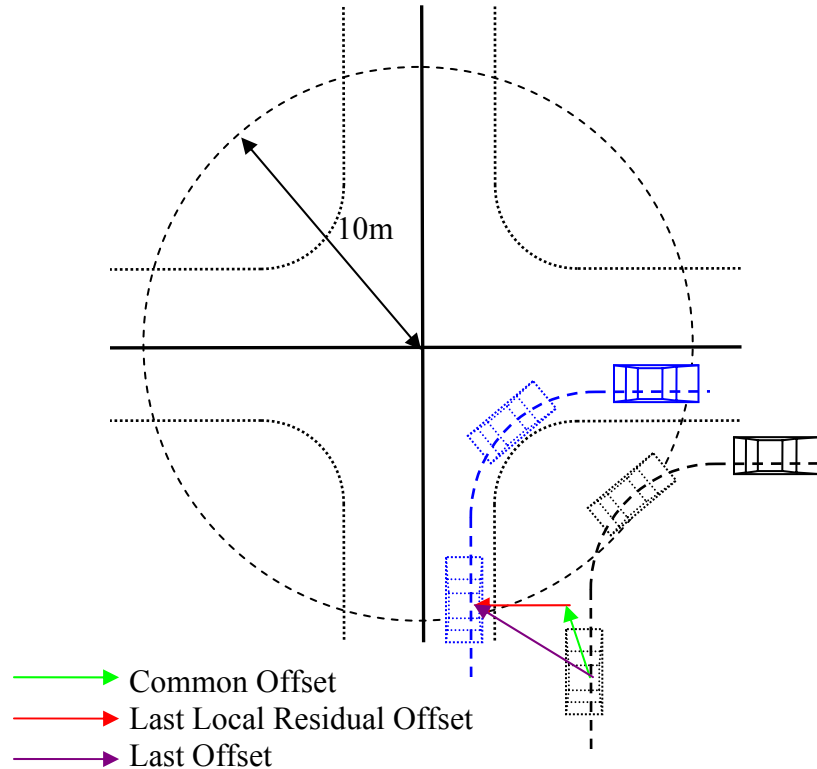


Figure 2-12 vehicle trajectory based on position fix (black) and after matching on the road (blue)

The road map data present each intersection by a “node”, so there can appear two close intersections nodes in the map data which in reality is one intersection with roads that have an offset to each other. In such cases the algorithm will merge these two intersections to one. This mode is summarized in the flow chart in Figure 2-13.

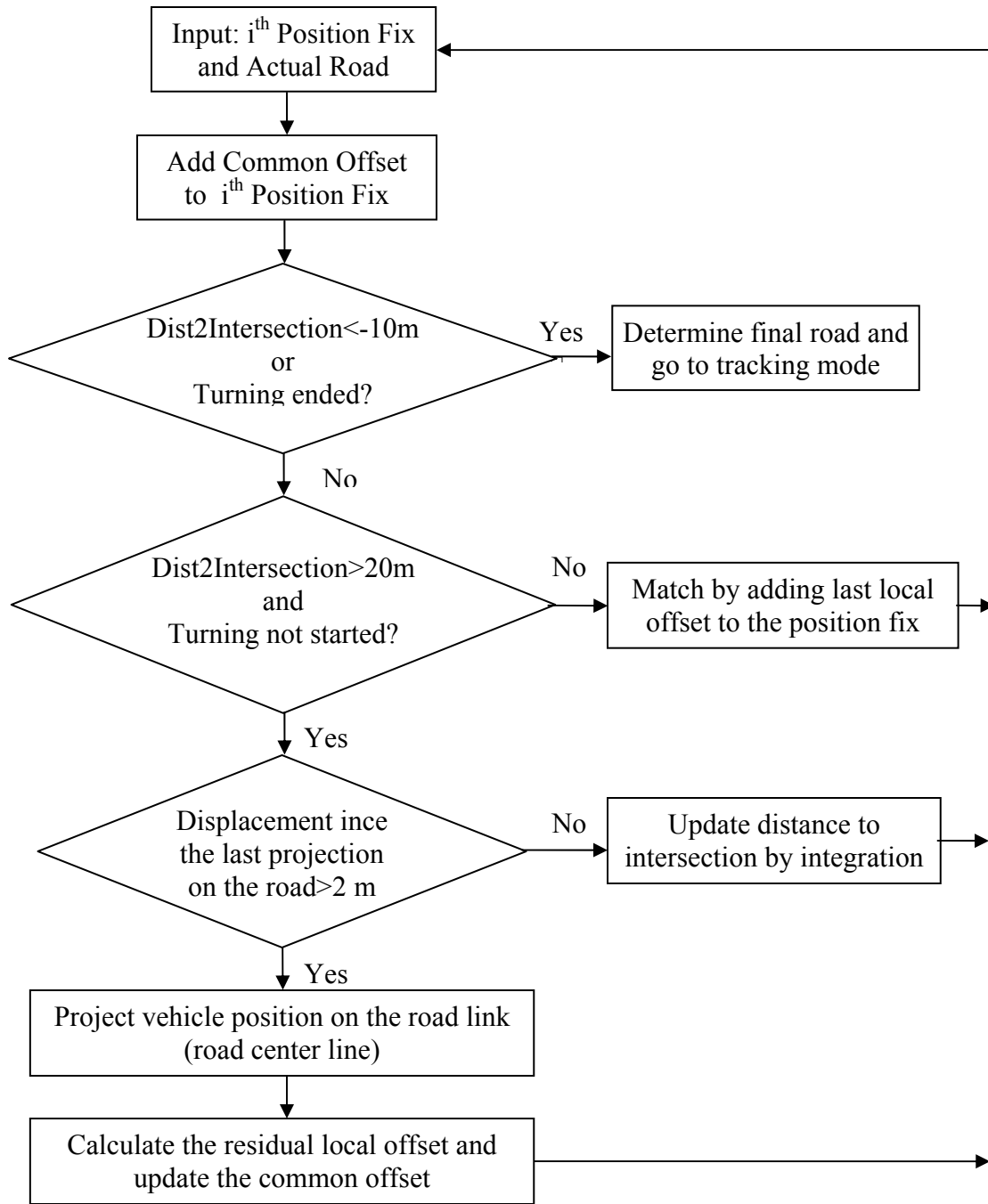


Figure 2-13 Flowchart of intersection mode algorithm

2.6. Summary of the Fusion Algorithm

A data fusion algorithm based on Kalman filtering and a map matching algorithm for vehicle positioning in intersection active safety applications are presented. The Kalman filter integrates complementary sensors and GPS data to achieve a continuous and precise positioning and map matching algorithm determines location of vehicle on the digital road map with respect to a position fix given by Kalman filter. Both Kalman filter and map matching algorithm are implemented in Matlab. The map matching algorithm uses the NAVTech digital map and a program developed by Carmenta Company, Sweden, which works as an interface between digital map and Matlab. The fusion algorithm is intended to be run off-line on high end workstations.

2.7. References

1. Mohinder S. Grewal, Lawrence R. Weill, Angus P. Andrews, "Global Positioning Systems, Inertial Navigation, and Integration", Wiley, New York, 2001
2. Mohinder S. Grewal, Angus P. Andrews, "Kalman Filtering: Theory and Practice, Using Matlab", Wiley, New York, 2001
3. W. Y. Ochieng, M. Quddus, R.B. Noland, "Map-Matching in Complex Urban Road Networks", Brazilian Journal OF Cartography, No 55/02, December 2003
4. Craig A. Scott, C. R. Drane, "Increased Accuracy of Motor Vehicle Position Estimated by Utilizing Map Data, Vehicle Dynamics, and Other Information Sources", Proceedings of IEEE Vehicle, Navigation & Information Systems Conference, 1994
5. Rajashri R. Joshi, A new Approach to Map Matching for In-Vehicle Navigation Systems: The Rotational Variation Metric", Proceedings of IEEE Intelligent Transportation Systems Conference, Oakland, USA, August 25-29, 2001
6. S. Syed, M. E. Cannon, "Fuzzy Logic Based-Map Matching Algorithm for Vehicle Navigation System in Urban Canyons", Presented at ION National Technical Meeting, San Diego, CA, January 26-28, 2004
7. G12 OEM Board & Sensor Manual
8. Andreas Larsson, Henrik Linger, "Adaptive Image Pan Methods for Curve Negotiations", Master Thesis at Autoliv-Chalmers, 2004
9. Peter S. Maybeck, "Stochastics Models, Estimation and Control", Vol. 1, Academic Press, Inc, 1979

3. Results

In order to evaluate created Kalman filter and map matching algorithm, the system was tested on a complex urban roadway. The test trajectory is introduced in section 3.1 which will be followed by Kalman filter and map matching results.

3.1. Test Trajectory

A test was conducted in downtown Alingsås located in Västra Götalands län, Sweden. Figure 3-1 shows the full test trajectory which was close to 2 km long and which included driving in narrow streets (7 meters width) where triple floor buildings restricted view of the sky creating urban canyon conditions.

The GPS receiver was in stand alone operation and DGPS data was not available during the test.

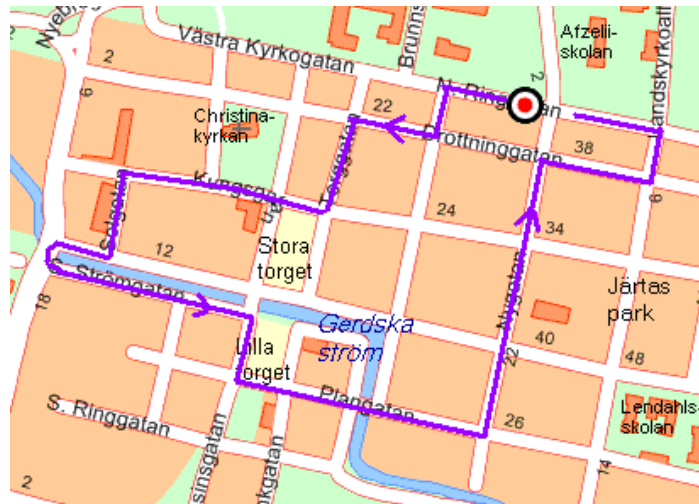


Figure 3-1 Test Trajectory

3.2. Estimated Position

In Figure 3-2 performance of unaided GPS receiver is presented. As it can be seen GPS derived position is not available in some segments of trajectory due to signal blockage by high buildings, and even in segments with GPS coverage, data is faulty where HDOP (described in 1.5.3) is rather high.

The estimated trajectory by Kalman filter is presented in Figures 3-3. As it can be seen goals of filling the gaps of GPS coverage and giving a smooth and continuous position were achieved. Three zoomed view of estimated trajectory with respective explanation follow.

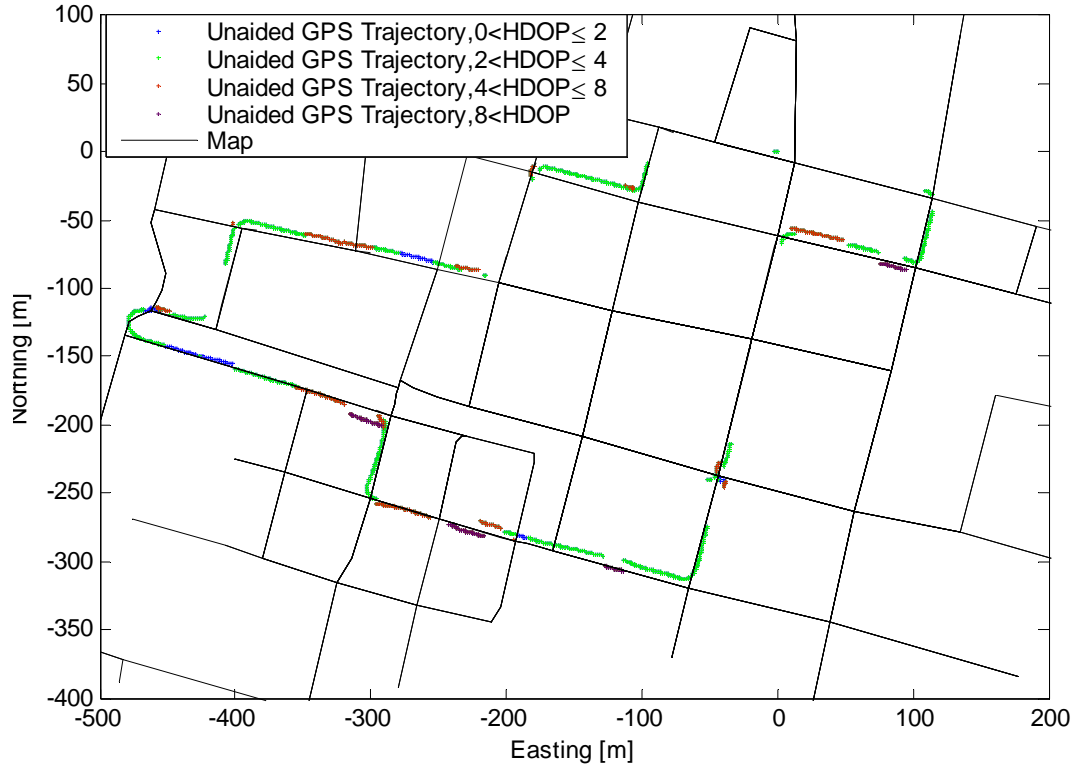


Figure 3-2 Unaided GPS trajectory

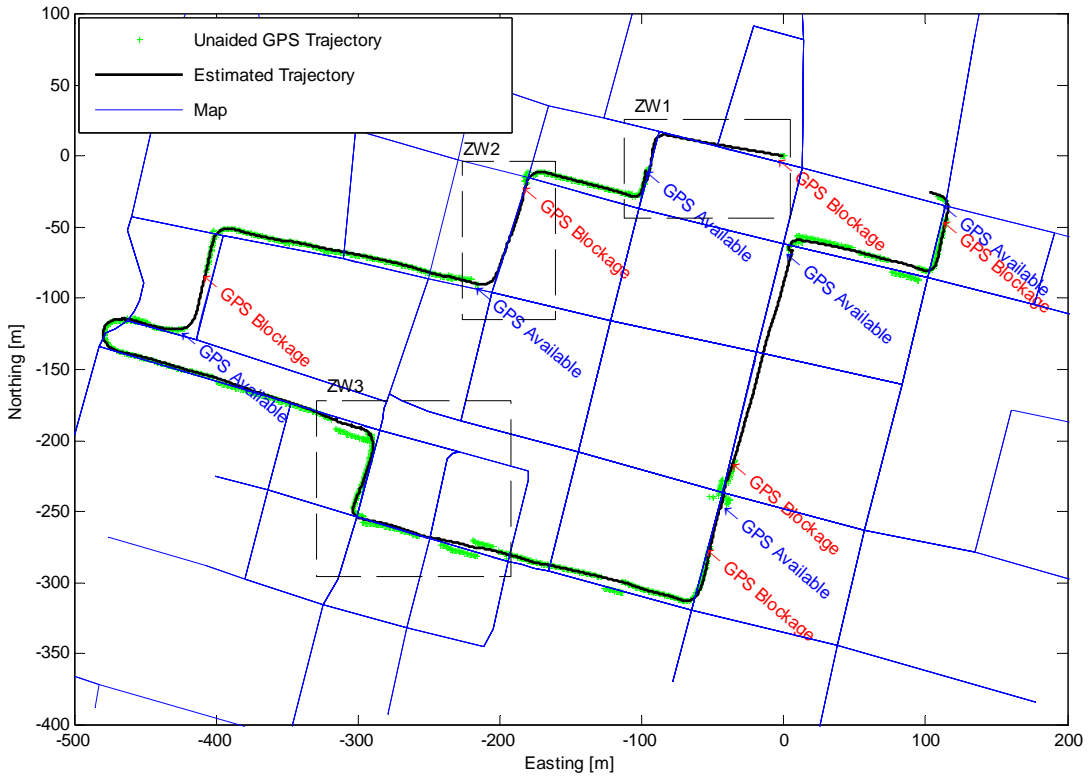


Figure 3-3 Kalman estimated trajectory

Figure 3-4 shows a zoomed view of first turn of test trajectory. The trajectory starts with a few GPS measurements (five measurement in half a second) which as can be seen in Figure 3-5 do not give a precise measurement of heading and shows almost 20 degrees variation. In addition half a second of data gathering is not enough for the Kalman filter to converge to a more precise estimation of heading. Thus this poor initiation of heading leads to a lateral position error which consequently causes longitudinal error after turning. This error is corrected as soon as GPS measurement becomes available again. It should be noted that estimated uncertainty of position (explained in section 3.6) also has a large value in this section of trajectory and shows the unreliability of estimated position.

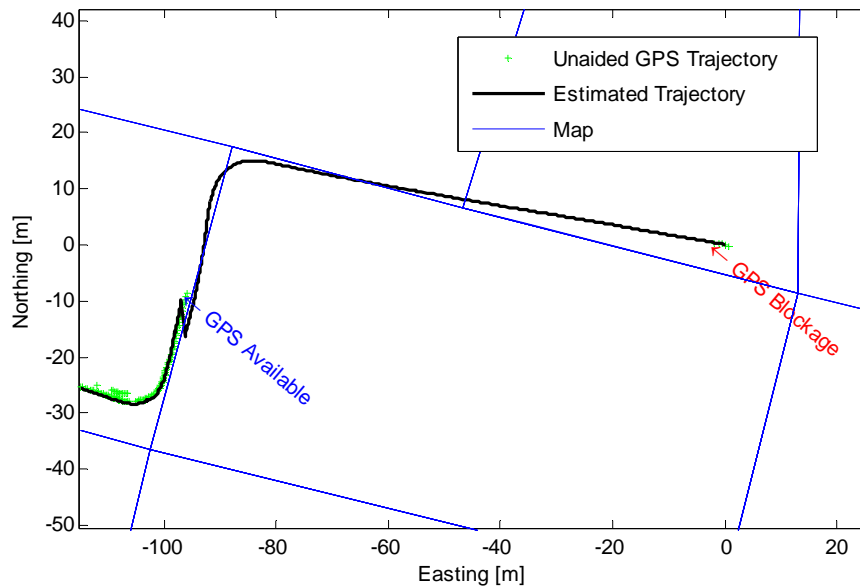


Figure 3-4 Estimated trajectory-zoom window 1

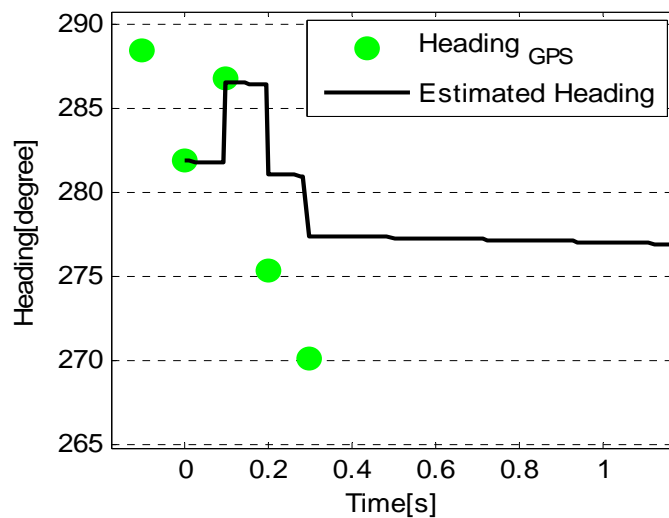


Figure 3-5 GPS heading and estimated heading in first second of trip

A zoomed view of another turn in the trajectory where GPS blockage has occurred is presented in Figure 3-6. This figure shows that the Kalman filter succeeded in estimating the trajectory of vehicle in two close turns with GPS blockage and rejecting faulty GPS data at the end of first turn.

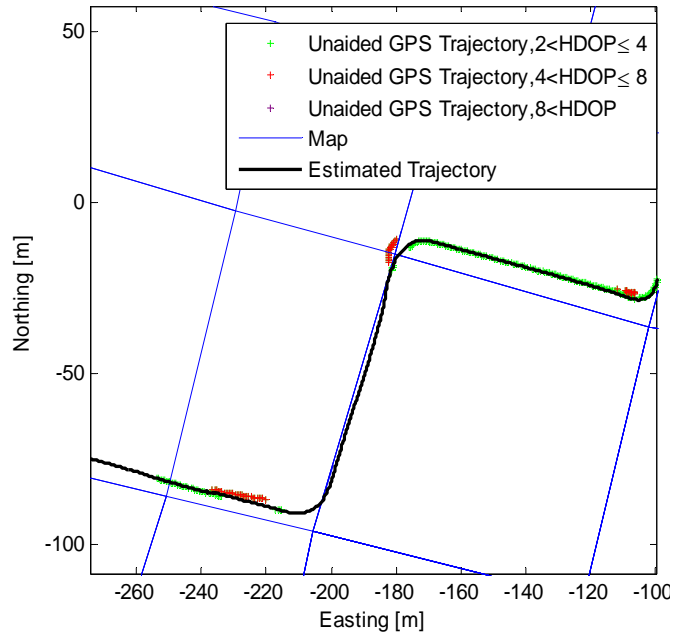


Figure 3-6 Estimated trajectory-zoom window 2

Performance of Kalman filter in fusion of GPS data and other sensors measurements can also be seen in Figure 3-7. This figure highlights how the Kalman filter rejects faulty GPS measurements and keeps a smooth trajectory.

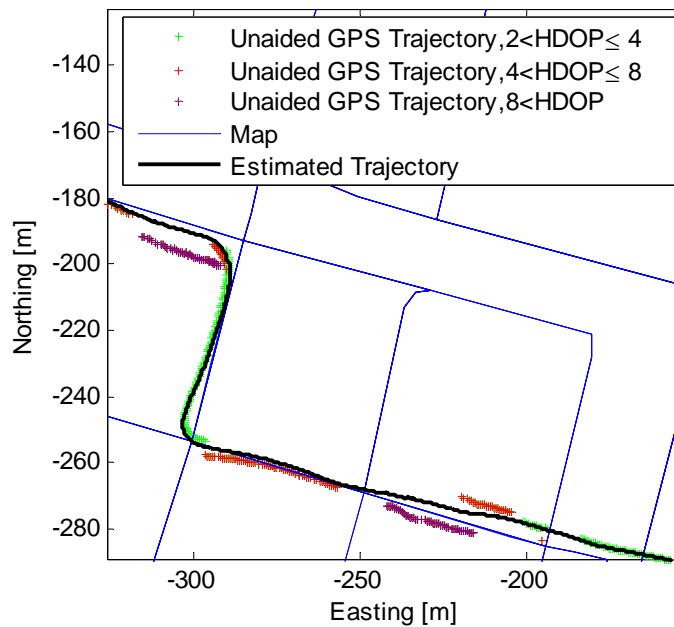


Figure 3-7 Estimated trajectory-zoom window 3

3.3. Estimated Heading

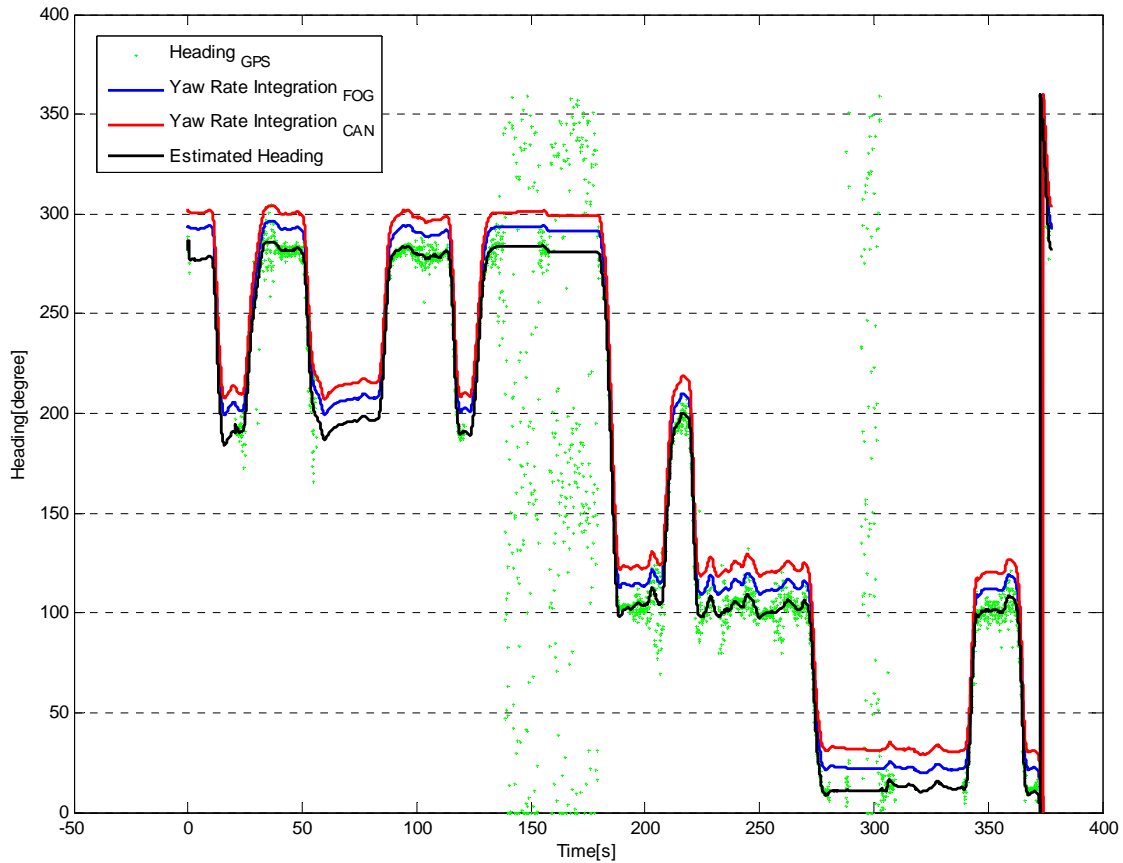


Figure 3-8 Heading improvement by fusion of Doppler derived heading, yaw rate from fiber optic gyro and yaw rate from analogue yaw rate sensor

The Kalman filter estimates vehicle reference point heading by fusing GPS Doppler derived heading (see Appendix C), yaw rate from FOG and analogue yaw rate sensor. The resulted heading is presented in Figure 3-8. Heading is tracking the GPS derived heading while heading rate is following the same pattern as measured yaw rate by FOG/analogue sensor. The offset between the estimated heading and the heading derived by integration of yaw rate sensors is just due to deliberate difference in initial values for better visualization.

The Kalman filter has enhanced the estimate of heading noticeably compared to noisy GPS Doppler derived heading which has even magnified error in low velocities (less than 2 m/s^2). This magnified error can be seen in time intervals 150-170s and 300-310s in Figure 3-8.

3.4. Estimated Speed

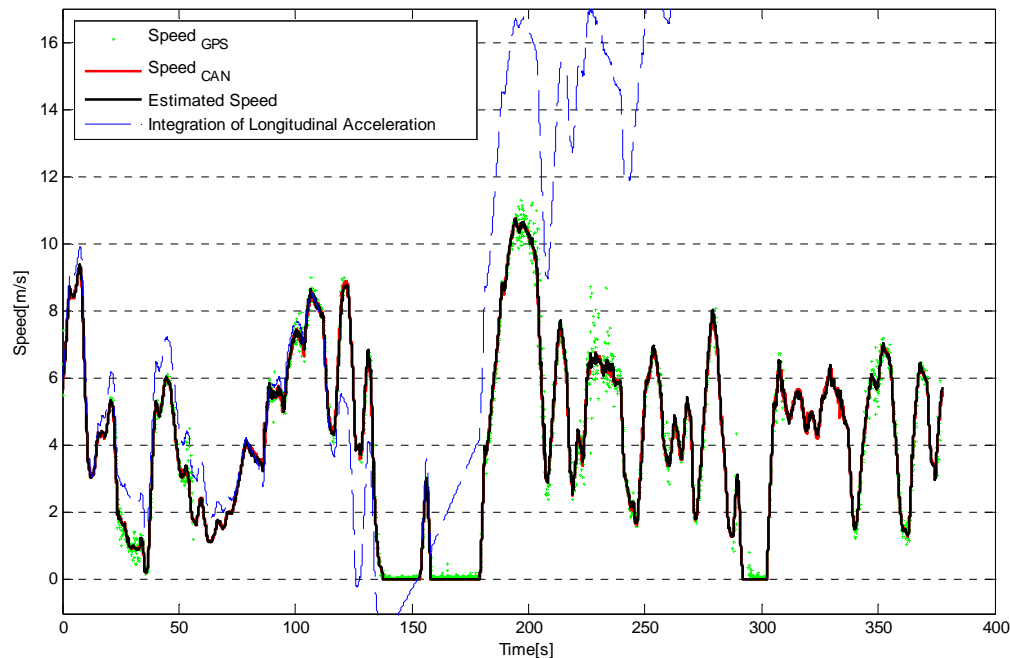


Figure 3-9 Vehicle speed obtained by fusion of ABS speed, Doppler derived GPS speed and longitudinal acceleration

The Kalman filter estimate of vehicle speed is plotted in Figure 3-9. Vehicle speed estimate which is obtained by fusion of ABS speed (from CAN bus), Doppler derived GPS speed and longitudinal acceleration follows both GPS speed and ABS speed, but is more inclined to ABS speed due to its higher precision.

As it can be seen the accelerometer measurement is really poor due to its non linearity and variable offset, therefore its contribution to speed estimation was reduced in Kalman filter by applying higher measurement noise covariance.

3.5. Uncertainty in Estimations

As stated in section 2.3, the Kalman filter maintains two types of variables: estimated state vector and covariance matrix. Covariance matrix is a measure of estimation uncertainty. The equations used to propagate the covariance matrix model and manage uncertainty, taking into account how sensor noise and dynamic uncertainty contribute to uncertainty about the estimated system state.

Covariance matrix is defined as

$$P(t) = E\left\{[x(t) - E\langle x(t)\rangle][x(t) - E\langle x(t)\rangle]^T\right\}$$

If $E\langle x(t)\rangle$ is replaced with the estimate of $x(t)$ defined by $\hat{x}(t)$ then the $P(t)$ will be called the *error covariance matrix*.

In the following uncertainty in estimation of position, speed and heading, which are diagonal elements of matrix P , are presented.

3.5.1. Estimated Uncertainty in Position

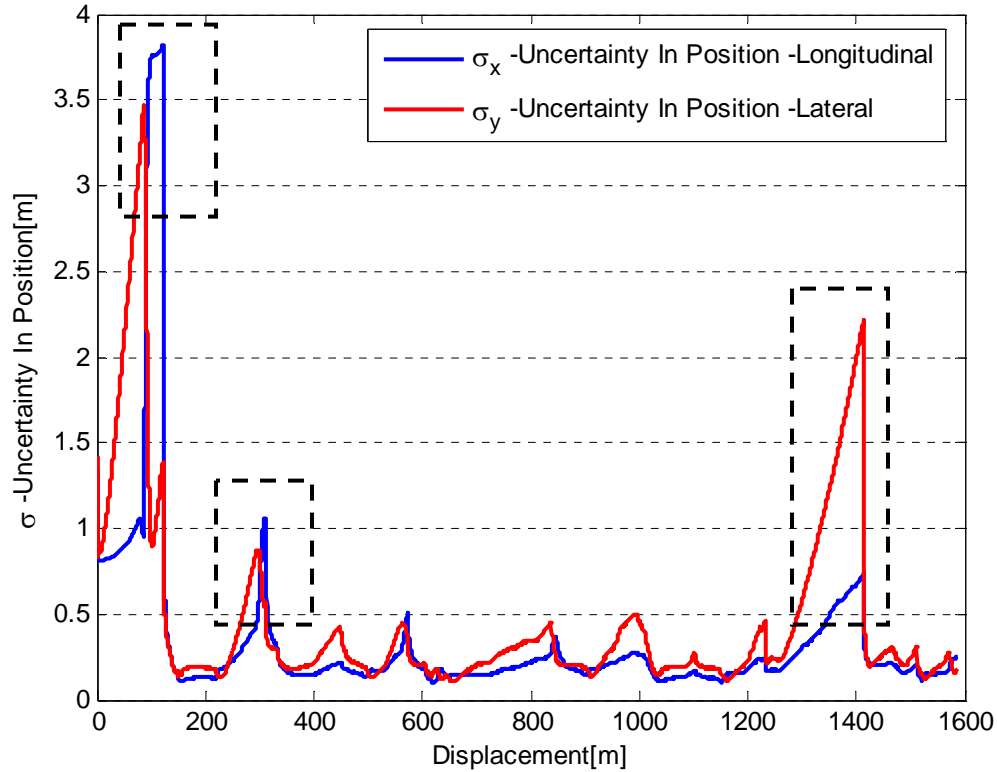


Figure 3-10 Position uncertainty in lateral and longitudinal direction

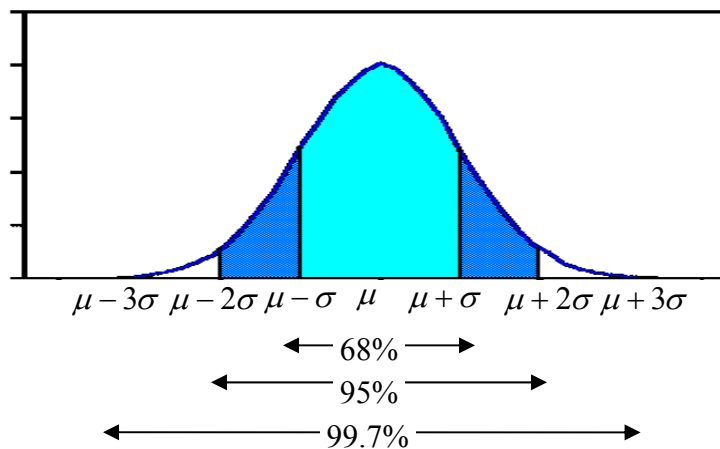
Estimated uncertainty in position both in longitudinal (tangent to vehicle trajectory) and lateral direction (perpendicular to vehicle trajectory) is presented in Figure 3-10. During GPS blockage periods uncertainty in both directions increases. Uncertainty increase in longitudinal direction is mostly due to integration of speed uncertainty during this time, while lateral uncertainty increase is primarily due to uncertainty in heading which can cause large lateral uncertainty in long distances. It can be concluded that accurate estimation of speed and heading is crucial for fusion to function properly.

The large peak value in the beginning of the test is due to lack of enough GPS data and initiation error as described in section 3.3. On average the increase in longitudinal uncertainty is about 0.5m for each 100m of GPS blockage, and this value for lateral uncertainty is about 1.5m for each 100m of GPS blockage. The mean uncertainty either in longitudinal direction or lateral direction is about 0.3m.(Table 3-1)

Table 3-1 Position Uncertainty

	Mean Uncertainty (m)	Uncertainty Increase / Displacement during GPS blockage (m/m)
Longitudinal	0.3	0.5 / 100
Lateral	0.3	1.5 / 100

Figure 3-12 shows the estimation of position uncertainty in lateral direction on the vehicle trajectory. Width of shadowed area is equal to 3 times of respective uncertainty. As stated in section 2.3, in a Kalman filter all the noises are assumed to have a normal distribution, and 3 times of uncertainty represents 99.7% probability in a normal distribution as shown in Figure 3-11.

**Figure 3-11 Probabilities associated with a normal distribution**

The lateral uncertainty increases during GPS blockage due to uncertainty in heading, lateral uncertainty will change into longitudinal uncertainty after turnings, which are almost 90 degree in the entire trajectory.

Figure 3-13 shows the estimated position uncertainty in longitudinal direction on the vehicle trajectory, which has been plotted laterally for easier interpretation. The width of the shadowed area is equal to 3 times of respective uncertainty.

The longitudinal uncertainty increases during GPS blockage due to integration of speed uncertainty during this time, however this increase is less than lateral uncertainty increase during GPS blockage. Therefore the largest longitudinal uncertainty has occurred after turnings in a GPS blockage period where lateral uncertainty before turning has changed into longitudinal uncertainty after it.

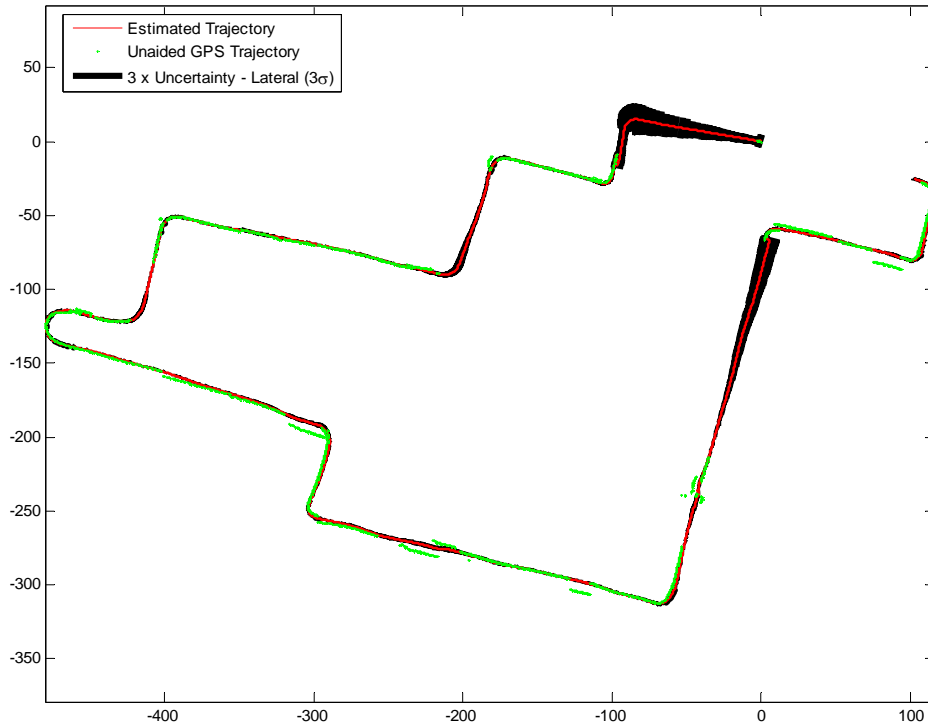


Figure 3-12 Uncertainty in lateral direction

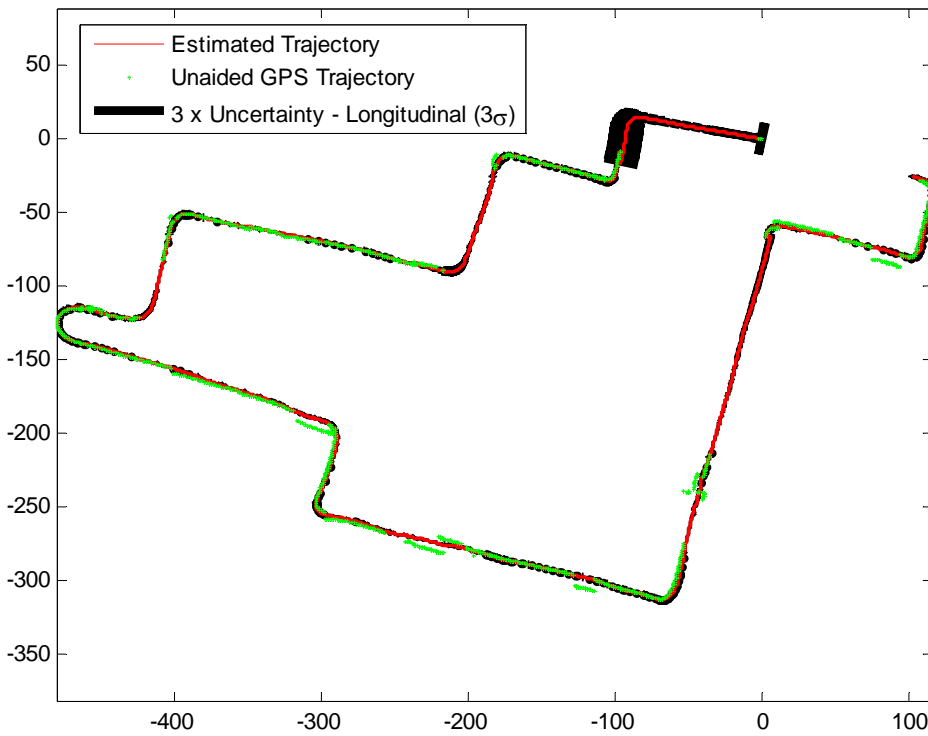


Figure 3-13 Uncertainty in longitudinal direction

3.5.2. Estimated Uncertainty in Heading

Kalman estimation of heading uncertainty is presented in Figure 3-14. As it can be seen it is not affected by GPS blockage, since heading estimation relies more on FOG measurements rather than on noisy Doppler derived heading except in initiation. Estimated uncertainty of heading is between 0.5-1.0 degrees. The large peak value in the beginning of the test is due to lack of enough GPS data and initiation error as described in section 3.3.

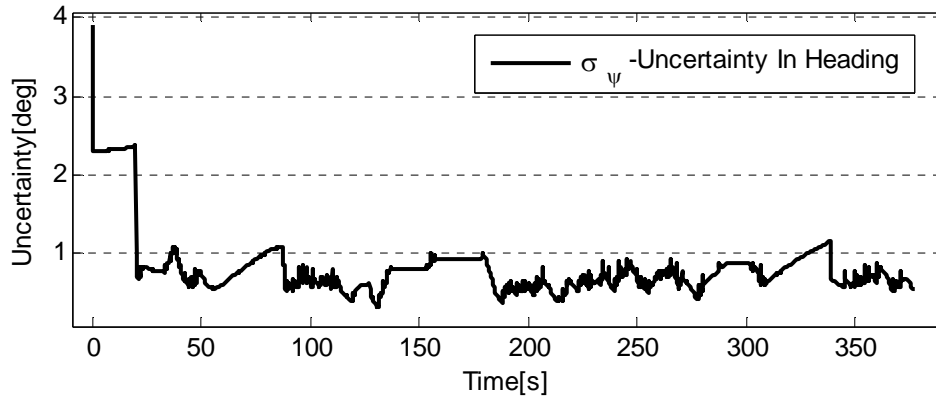


Figure 3-14 Uncertainty in Heading

3.5.3. Estimated Uncertainty in Speed

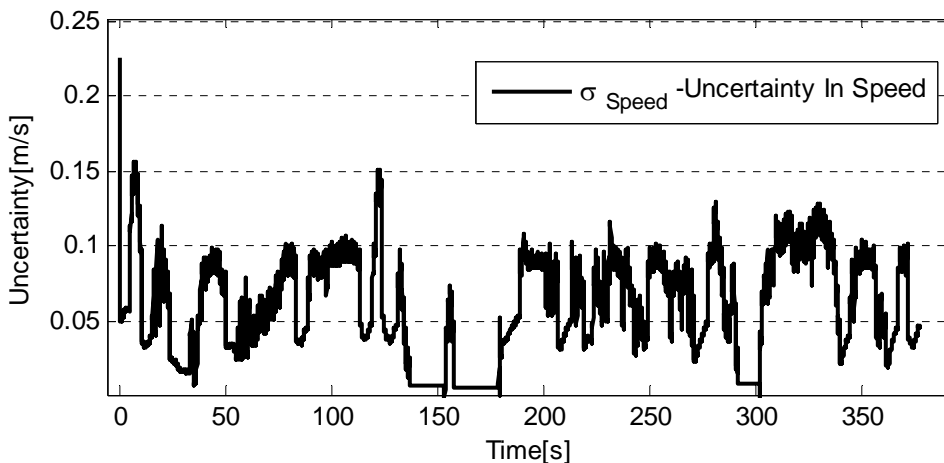


Figure 3-15 Uncertainty in vehicle speed

Figure 3-15 shows the estimated uncertainty of speed and the fact that it is not affected by GPS blockage, since speed estimation relies more on ABS speed rather than on noisy Doppler derived speed. Estimated uncertainty of speed is between 0.05-0.15 m/s.

3.6. Map Matching Results

The performance of the developed map matching method is analyzed and presented in this section. For this purpose, the vehicle position fixes (Kalman estimate of vehicle position) and respective estimated vehicle locations on the road by map matching method are overlaid on the digital road network map. In addition, in order to present the effect of common offset (described in 2.5.2), the vehicle location was also calculated just based on local offsets (see Figure 3-16). This method which is a comparison base is referred to as “MM-without Common Offset”- MM stands for Map Matching- while the main map matching method is referred to as “MM-with Common Offset” in the following figures.

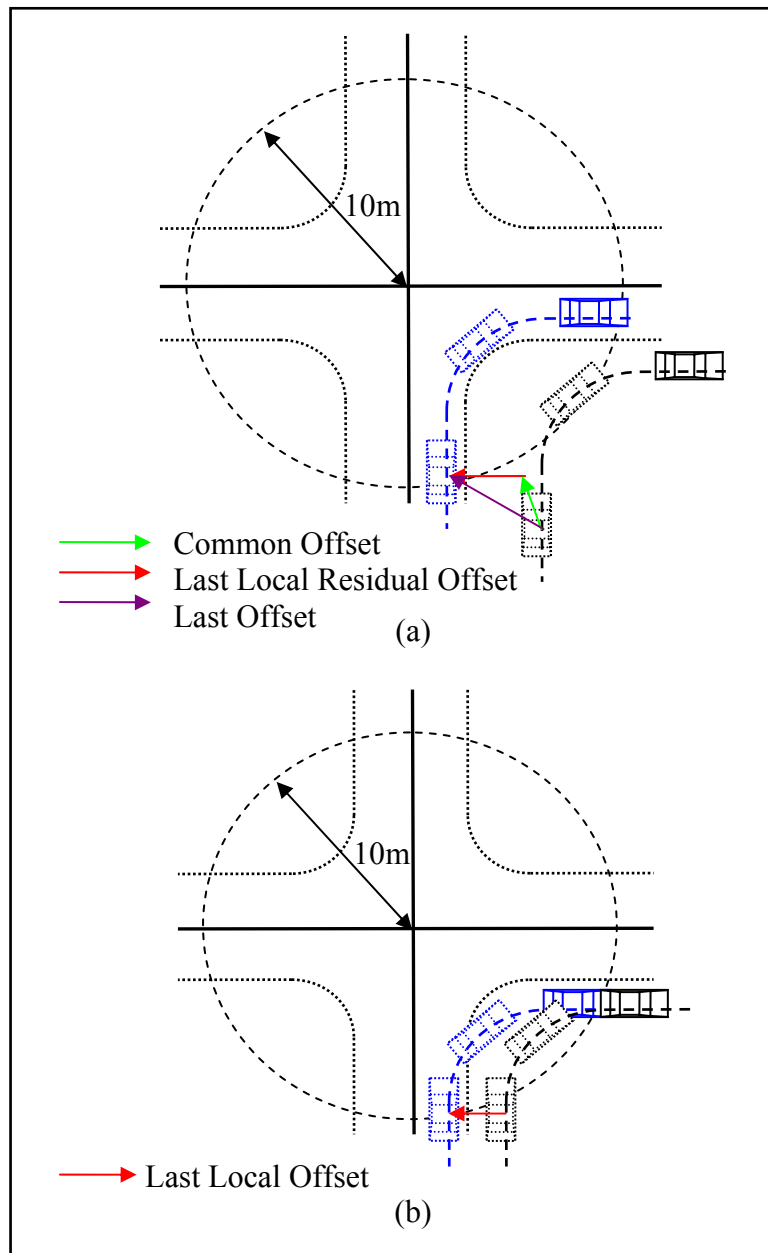


Figure 3-16 a) MM method with common offset b) MM method without common offset

In Figure 3-17 the estimated vehicle trajectory by Kalman filter and resulted trajectories in an intersections area after each map matching method are overlaid on the digital road network map. In order to examine intersections in more detail, each zoom window in Figure 3-17 is presented in a separate figure in the following pages.

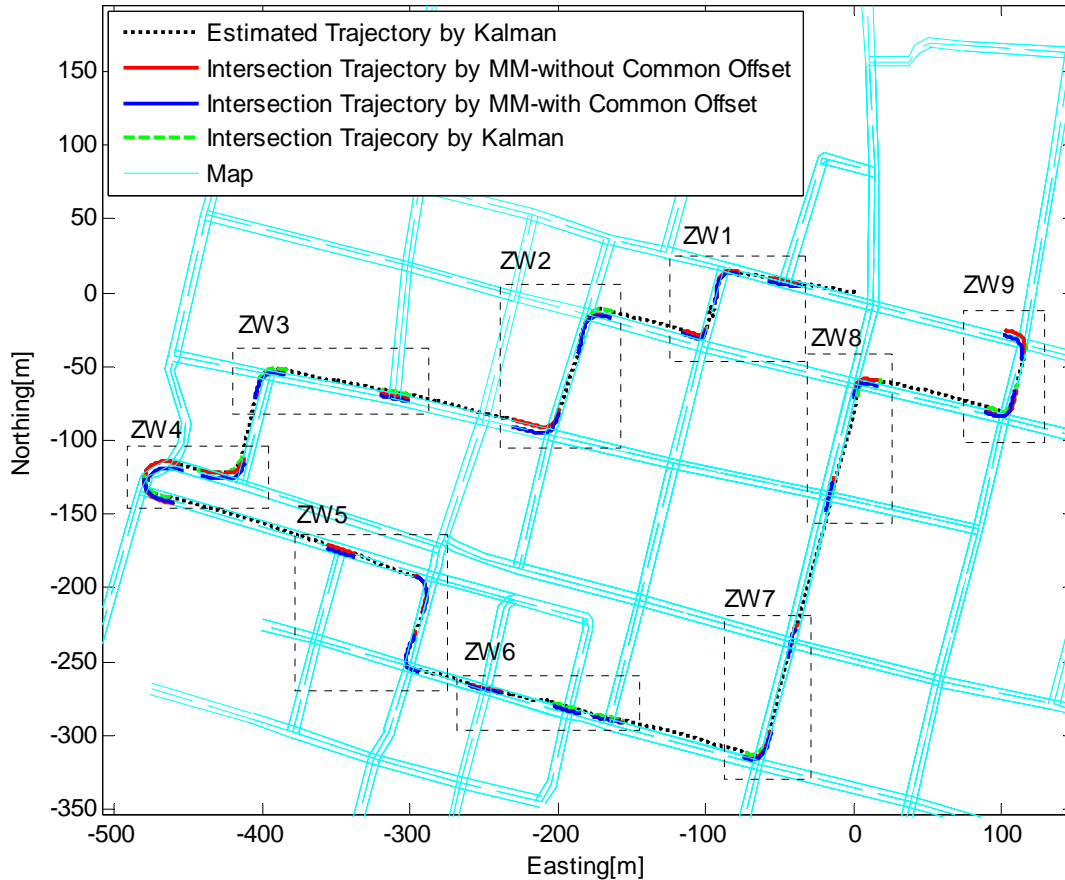


Figure 3-17 Estimated Trajectory by Kalman and after map matching on the road map

As it can be seen the estimated trajectory by Kalman has been matched onto the road map fairly good. It should be noted that aim of common offset calculation is to improve the estimation of vehicle location along the road which can not be done just based on local offset, which is across the road. Second, the target in across positioning of the vehicle is to position it on the correct side of the centerline and within the road width which is the maximum achievable accuracy with the available information. Thus comparing results of map matching method 1 and 2, it can be concluded that estimation of vehicle location along the road and consequently estimation of distance to coming intersection has enhanced.

Most of the roads in the test trajectory were one way road except those which are shown with two brown arrows in the figures¹. The algorithm never lost track of roads on which the vehicle was traveling.

As explained in section 2.5.2 the road parameters which were used in the proposed map matching algorithm are road centerline, road width and whether the road is a two way or one way road, but since road width is not available in the digital map, it was estimated based on speed limit on the road, available in the digital map data. Knowing the exact road width will improve the map matching results significantly due to its important role in the map matching algorithm.

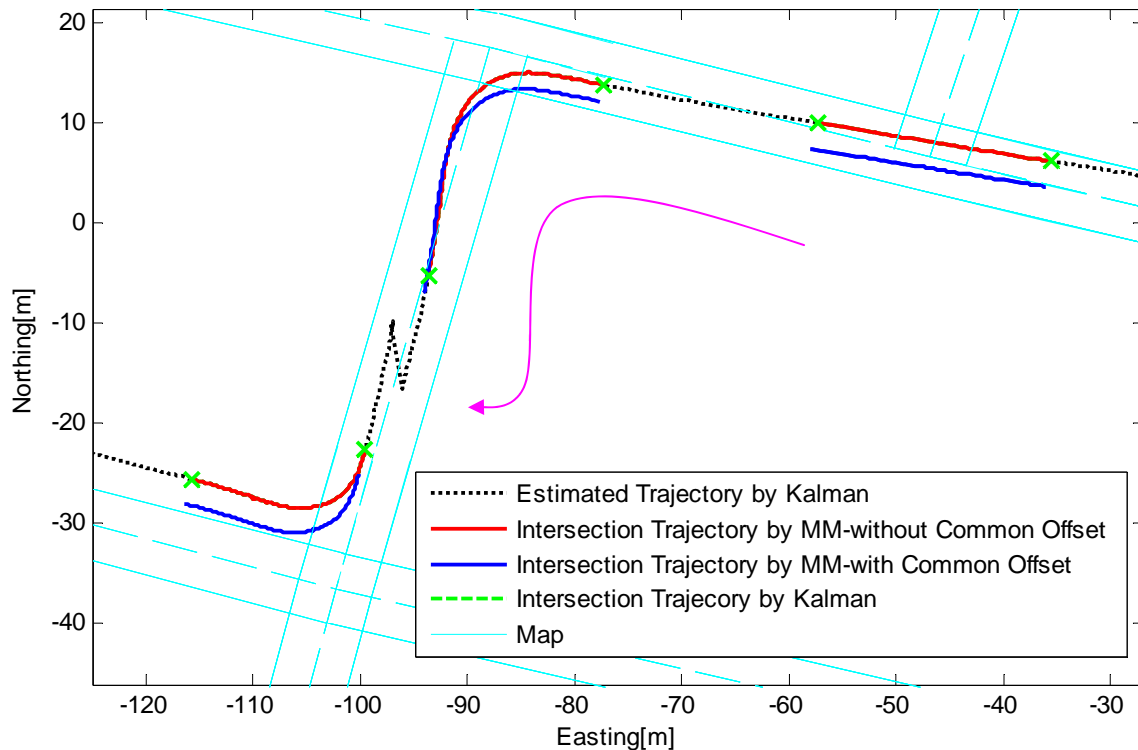


Figure 3-18 Zoom Window 1

¹ The information about whether a road is one way or two way is available in the digital road map data, however in the version of “RoadAnalyzer”, which is an interface between road map data and written algorithm in matlab and which is developed by Carmenta company, used in this thesis, it is not given as a road attribute; Therefore it was checked by the name of the road.

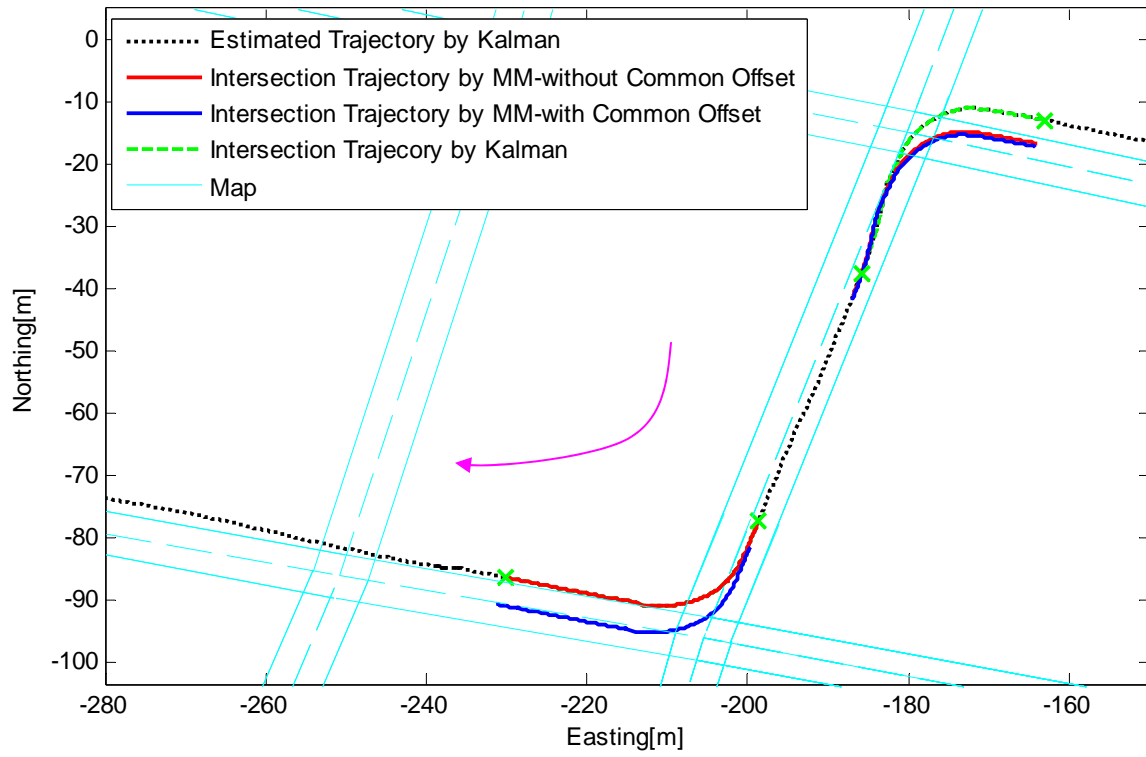


Figure 3-19 Zoom Window 2

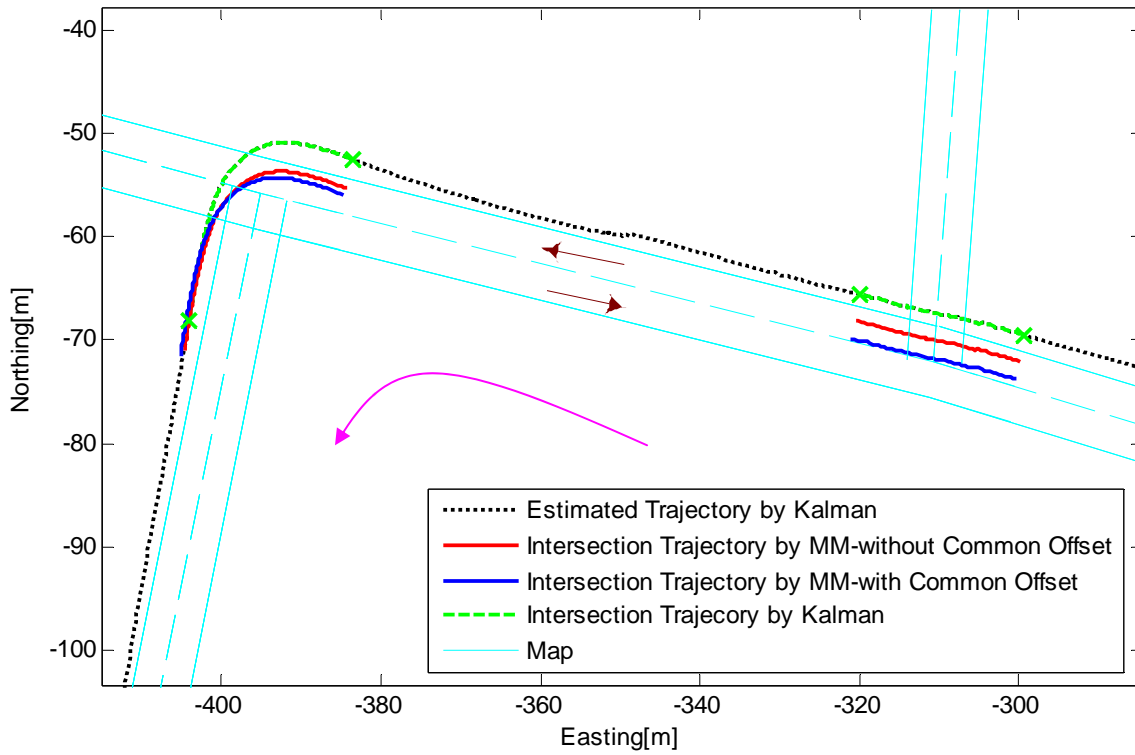


Figure 3-20 Zoom window 3

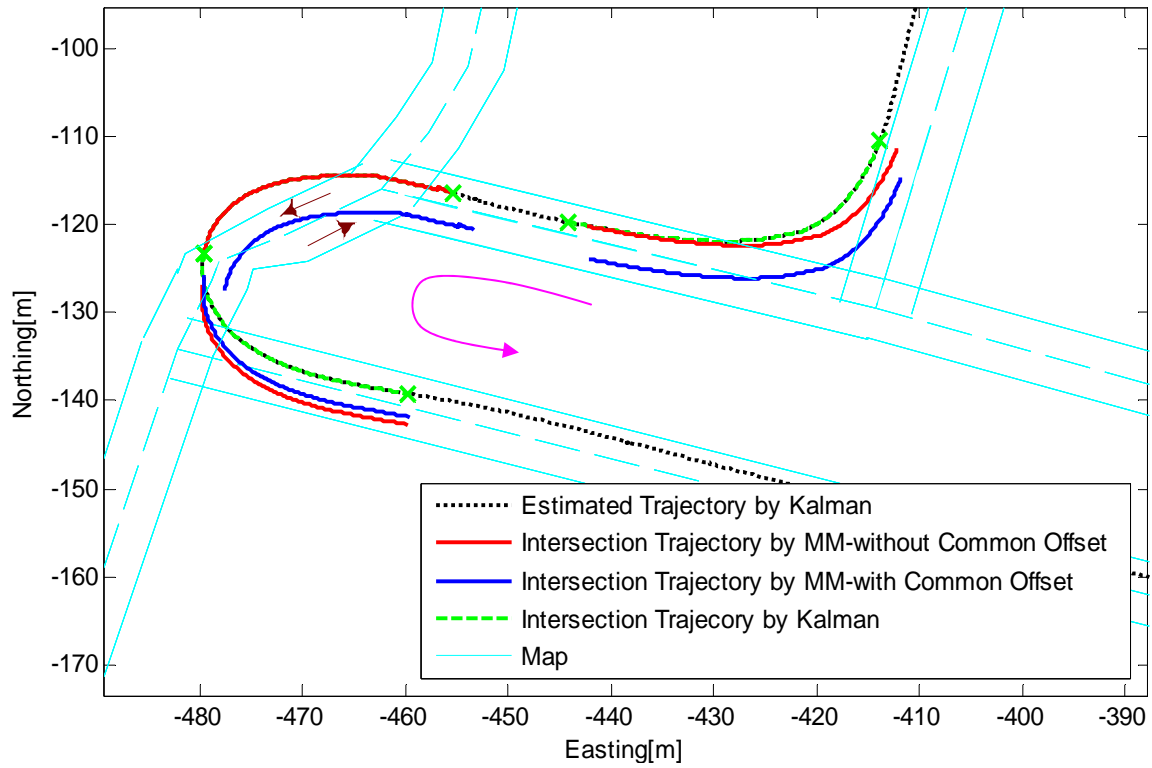


Figure 3-21 Zoom Window 4

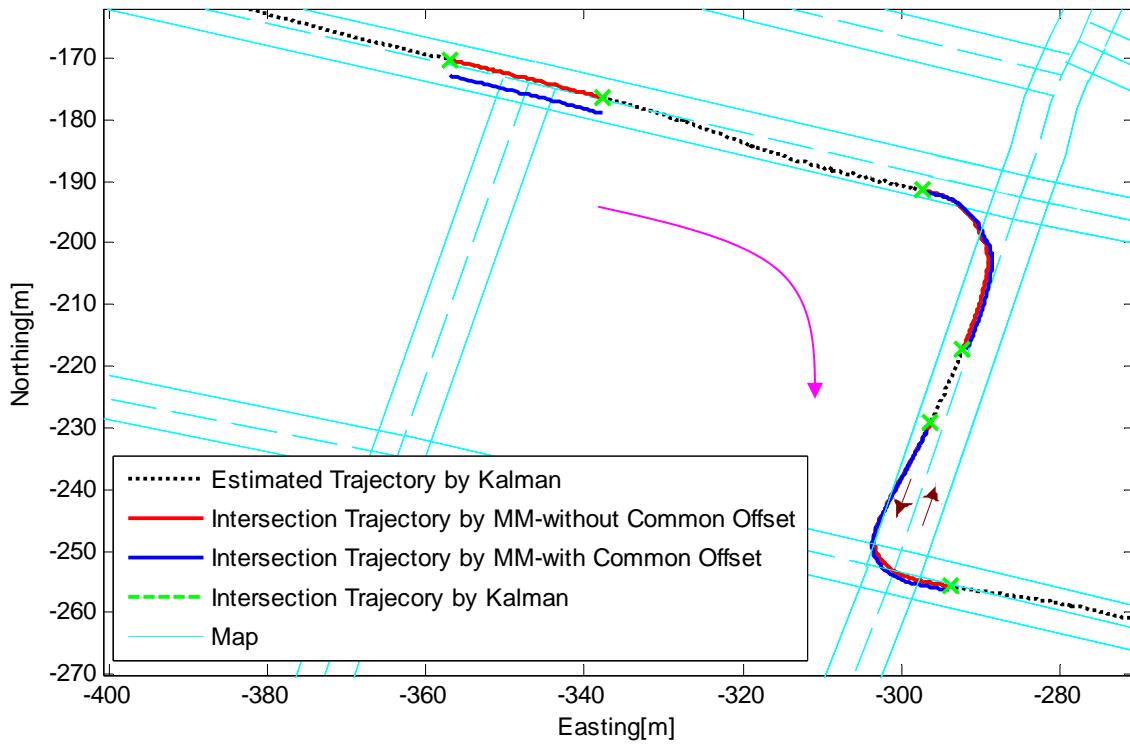


Figure 3-22 Zoom Window 5

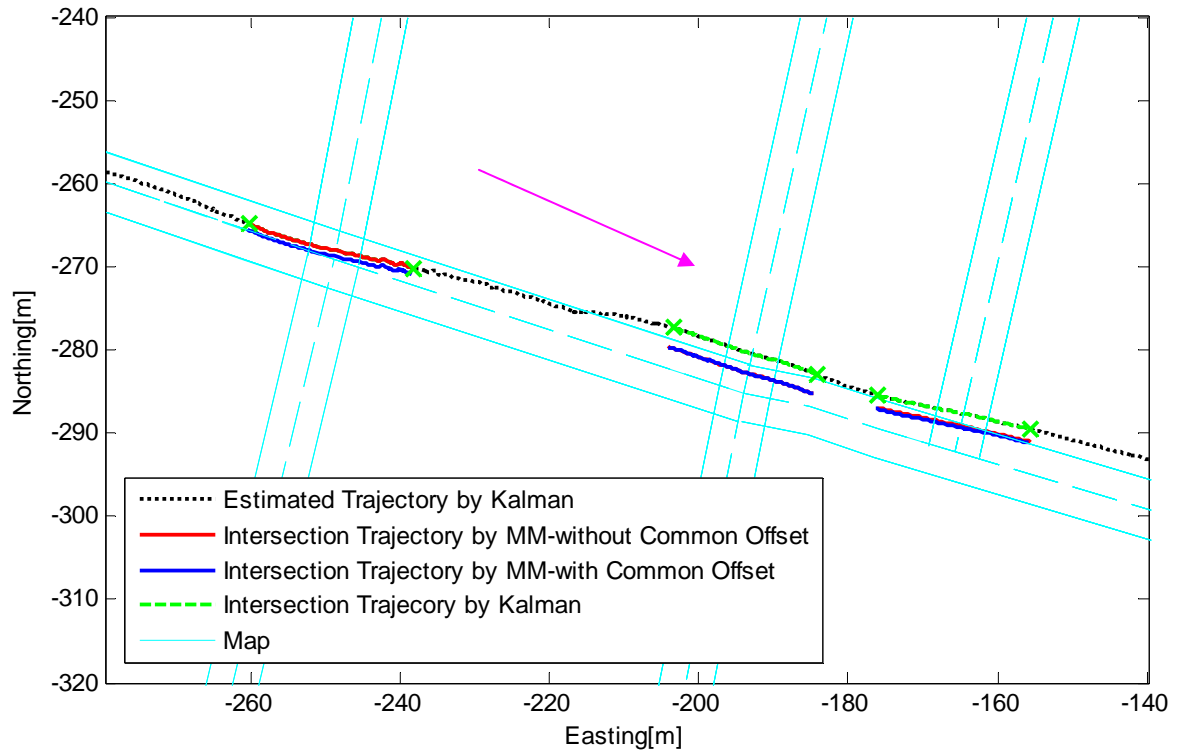


Figure 3-23 Zoom window 6

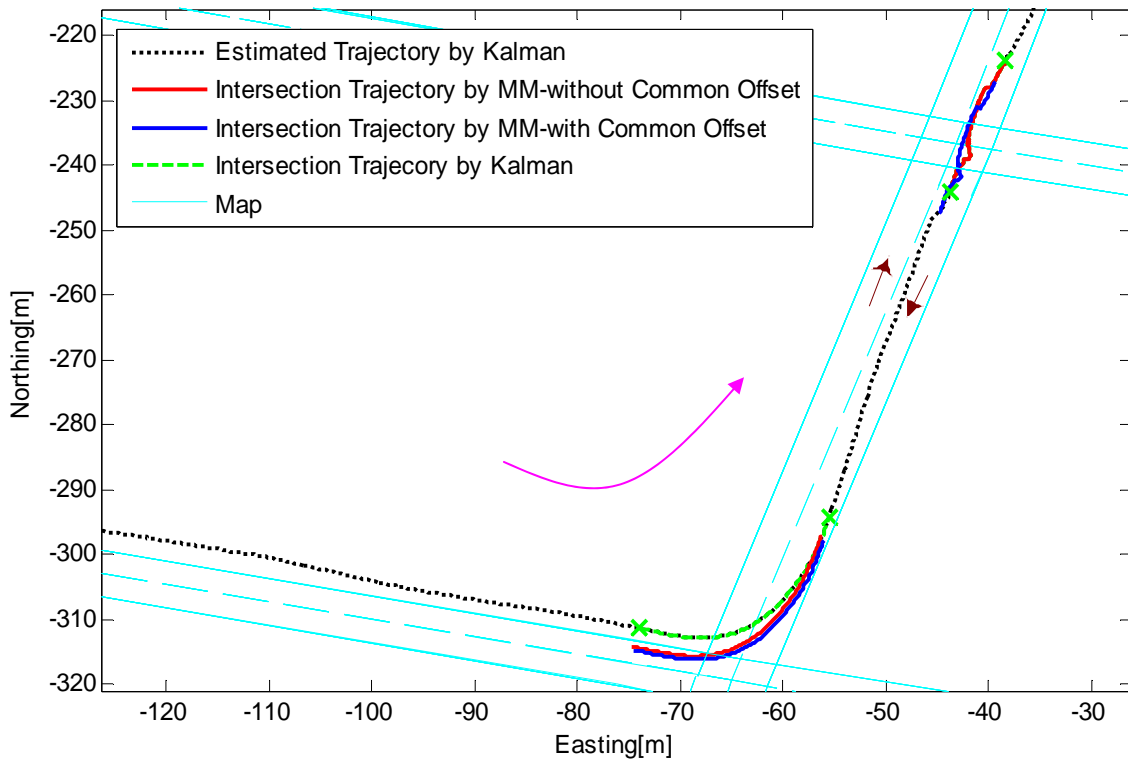


Figure 3-24 Zoom window 7

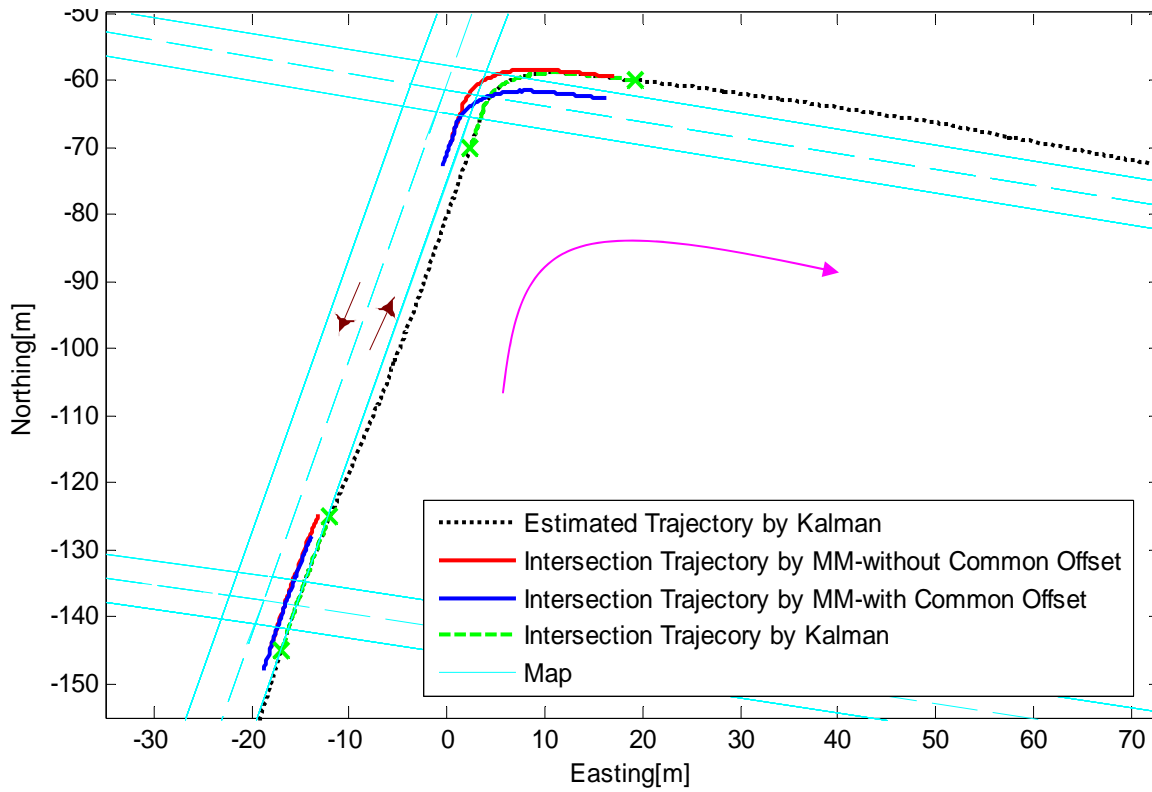


Figure 3-25 Zoom window 8

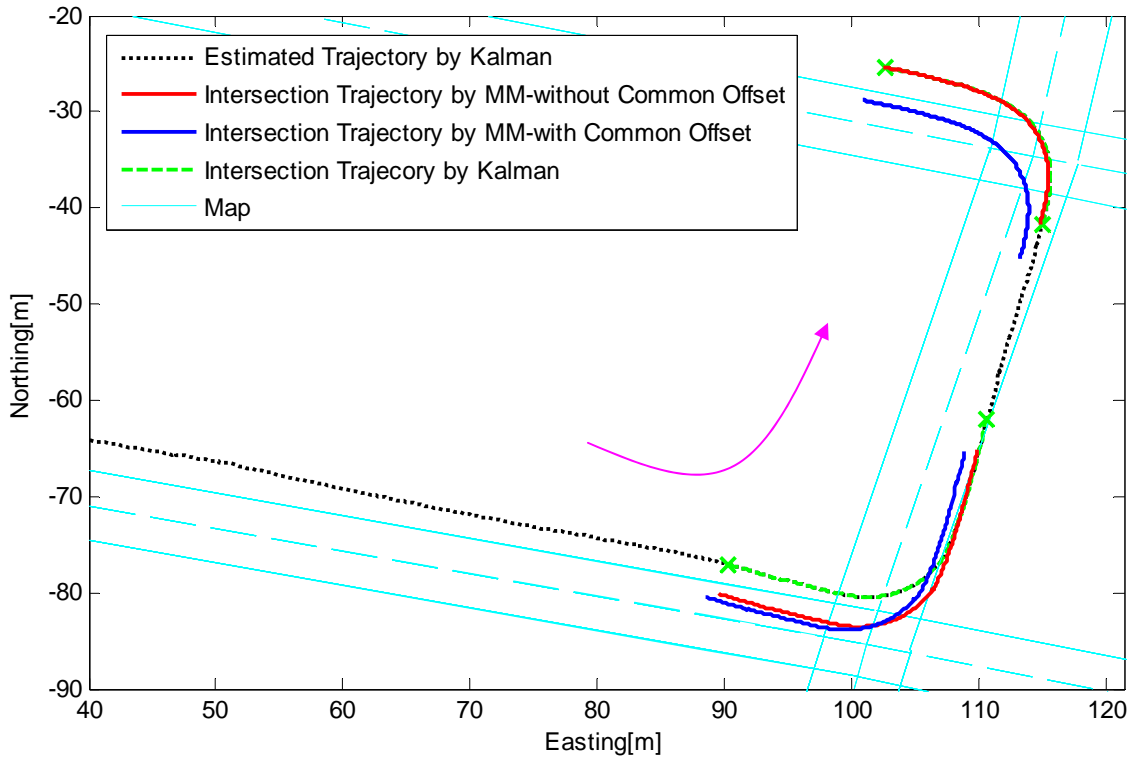


Figure 3-26 Zoom window 9

4. Analysis

In this section an analysis of the fusion results will be presented. It should be noted that the presented positioning result uncertainties in previous section are estimated uncertainties by the Kalman filter and not the real error. The real error calculation and comparison between the achieved results and positioning requirements for an intersection active safety application was not possible due to lack of information about real position of vehicle and intersections. In this section sources of error in positioning results will be analyzed.

4.1. Sources of error in Fusion

Kalman filtering has two steps:

1. Prediction
2. Correction

In the prediction step, a dynamic model is used to predict state of system. In the correction step, sensors' outputs are collected and these measurements are used to correct the prediction in correction step. Errors in estimation can originate from any of these two steps and propagate in fusion output. These sources of error in fusion algorithm will be discussed in following subsections.

4.1.1. Modeling errors

In prediction step a model of the system is used to estimate system state. In this thesis a rigid body dynamic model is used for vehicle trajectory estimation. In this model some assumptions and simplifications are performed that cause errors in the prediction step.

For simplicity, it was assumed in this model that vehicle speed is in local tangent plane or in other words, the up coordinate¹ of vehicle velocity, V_U is zero. This can cause errors when vehicle is climbing an upslope or going down a slope. Effect of slope in vehicle position error can be calculated as follows. (Figure 4-1)

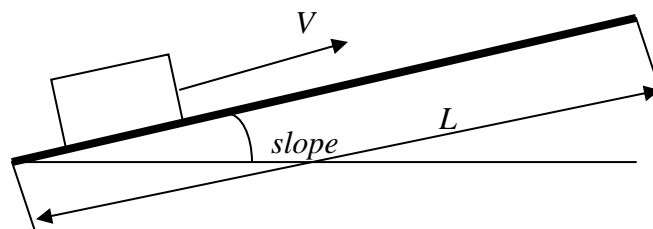


Figure 4-1 effect of slope in positioning

¹ In the ENU (East-North-Up) coordinate

$$\delta L = L - L \cos(\text{slope}) = L(1 - \cos(\text{slope}))$$

where δL is error in longitudinal direction. Table 4-1 presents magnitude of error caused by slope during GPS blockage in two scenarios.

Table 4-1 error caused by slope during GPS blockage

	Scenario 1	Scenario 2
<i>slope</i>	10 degrees	5 degrees
<i>L</i>	100 meters	100 meters
δL	1.51 meters	0.4 meters

It was also assumed that the state variable; heading, is equal to yaw and consequently its rate of change is equal to yaw rate. This is only true at non-slip conditions where direction of vehicle reference point velocity is along the vehicle centerline (Roll axis) and lateral speed is zero.

Vehicle's equations of motion without simplification should be written as follows. (Table 4-2, Figure 4-2)

Table 4-2 Explanation of variables

V_x	Longitudinal Speed
V_y	Lateral Speed
V	Magnitude of speed
V_E	East speed
V_N	North speed
ψ	Heading direction
A_x	Longitudinal acceleration
A_y	Lateral acceleration
Y, \dot{Y}, \ddot{Y}	Yaw and its derivatives
(u, w)	Position vector of accelerometers

$$V_E = V \sin(\psi)$$

$$V_N = V \cos(\psi)$$

$$V = \begin{bmatrix} V_x \\ V_y \end{bmatrix}$$

$$A_x = \frac{dV_x}{dt} - V_y \dot{Y} - w \ddot{Y} - u \dot{Y}^2$$

$$A_y = \frac{dV_y}{dt} + V_x \dot{Y} + u \ddot{Y} - w \dot{Y}^2$$

$$\frac{d}{dt} Y = \dot{Y}$$

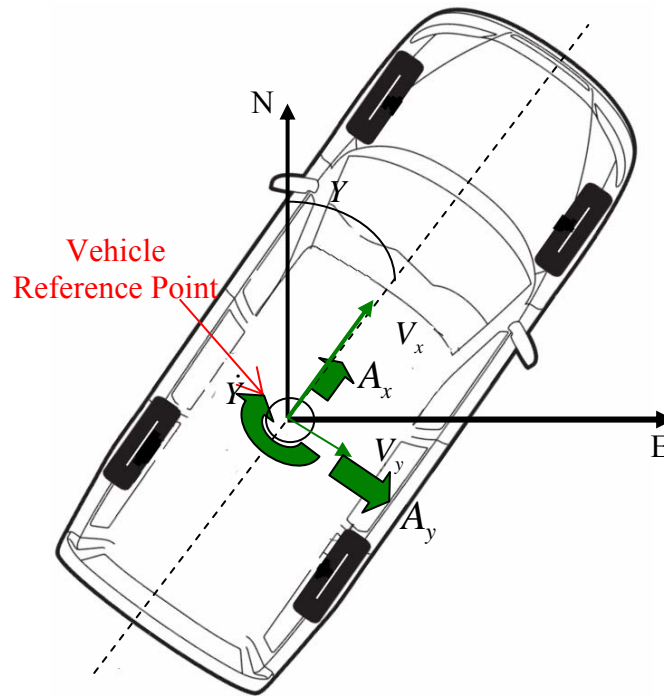


Figure 4-2 State variables with lateral speed and lateral acceleration

To reduce the error caused by this assumption vehicle reference point (GPS antenna location) should be close to vehicle center of rotation. Vehicle center of rotation moves back and forth as vehicle yaw rate, speed and slip condition changes. Therefore the best solution is to put GPS antenna somewhere on vehicle centerline close to vehicle center of rotation in normal driving condition (See Figure 4-5). Another approach to reduce this error is to use two accelerometers in longitudinal and lateral direction in order to calculate heading direction independent of vehicle yaw rate.

The following calculations present an estimate of difference in heading and yaw angle in high speed turns. (See Figure 4-3)

$$\psi - Y \approx \tan^{-1} \left(\frac{L\dot{Y}}{V_f} \right)$$

$$V_f = 10 \text{ m/s}$$

$$\dot{Y} = 0.3 \text{ rad/s}$$

$$L = 1.5 \text{ m}$$

$$\psi - Y = 2.5 \text{ deg}$$

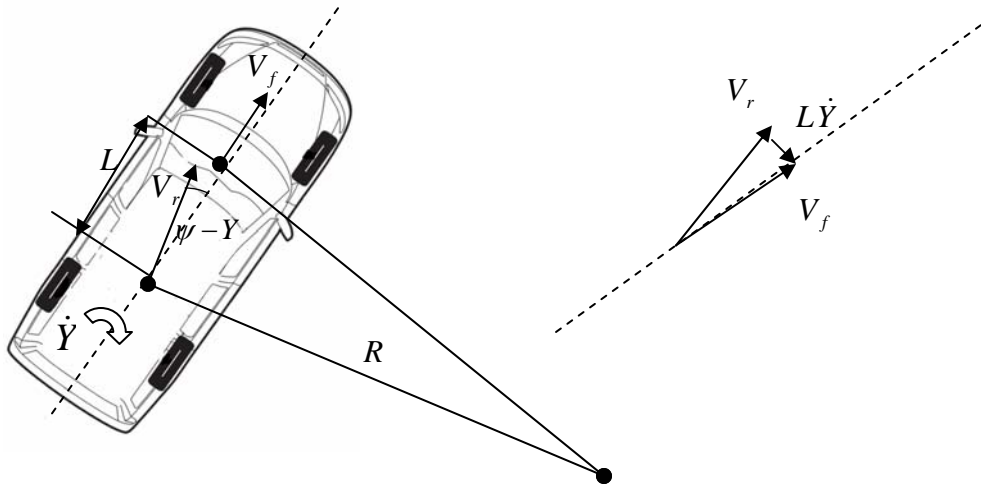


Figure 4-3 A simple model to estimate the difference between heading direction and vehicle yaw in high speed turn

The following calculations present an estimate of difference in heading and yaw angle in low speed turns. (See Figure 4-4)

$$\psi - Y \approx \tan^{-1}\left(\frac{L\dot{Y}}{V_f}\right)$$

$$V_f = 2m/s$$

$$\dot{Y} = 0.3rad/s$$

$$L = 0.7m$$

$$\psi - Y = 6deg$$

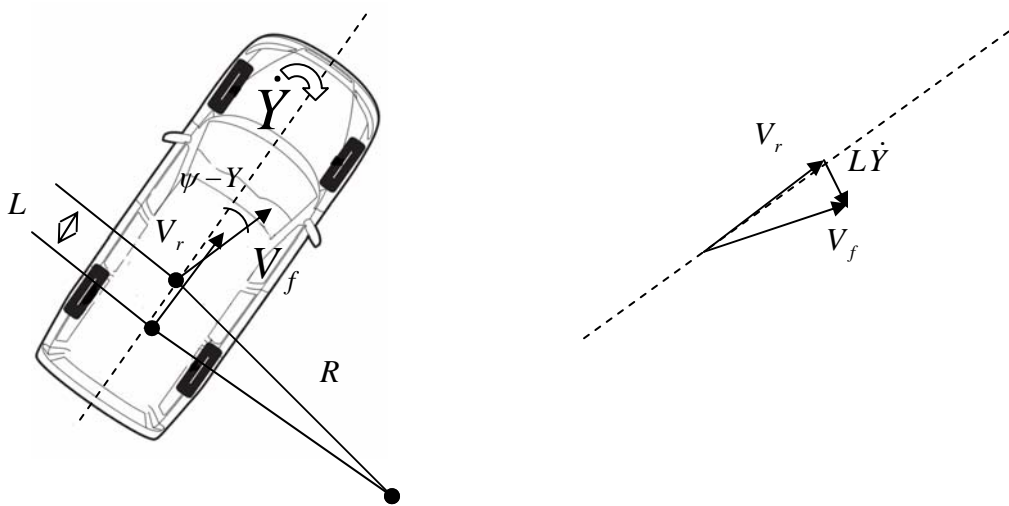


Figure 4-4 A simple model to estimate the difference between heading direction and vehicle yaw in low speed turn

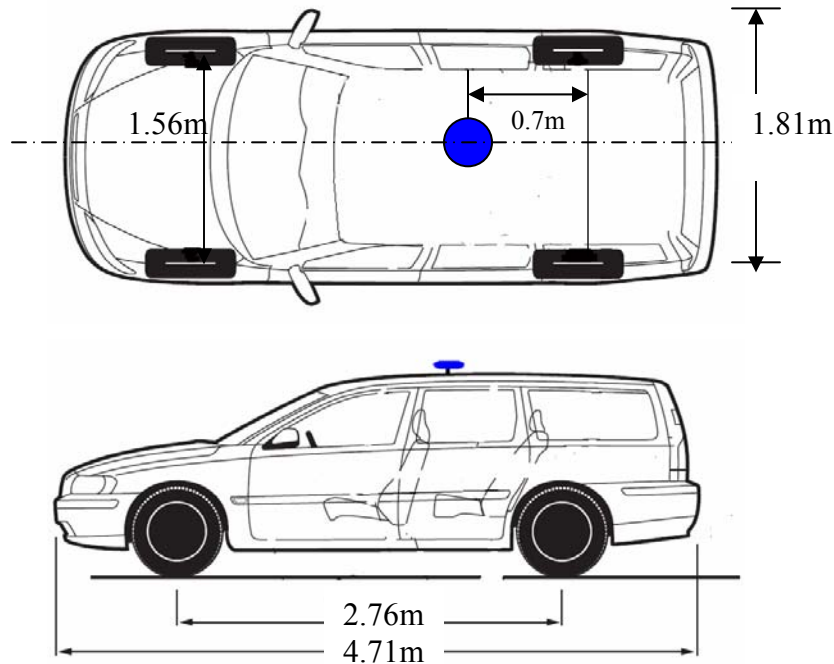


Figure 4-5 Position of GPS antenna (reference point)

One source of error in the positioning system presented in this thesis is due to longitudinal slip. One of the measurements used for estimation of speed is ABS speed which is derived from rotational speed of rear wheels without correction for slip. In the positioning system presented in this thesis a constant slip of 2 percent is assumed which is not always correct. For a better estimation of speed another type of sensor for speed such as accelerometer should be used.

Another source of error which is covered in section 1.5.2 (INS errors) is sensor misalignment. The input axis for a gyroscope defines the component of rotation rate that it senses. Its input axis is a direction fixed with respect to the gyroscope mount. Since the gyroscope is mounted on vehicle body and vehicle body is subjected to roll for example while turning in high speed and pitch for example while going up a slope, output of gyroscope is not rate of change of vehicle body angle with local north axis. For example 5 degree roll angle causes 1.5 percent error in yaw rate and consequently 1 degree error in heading in a 90 degree turn.

4.1.2. Measurement errors

Another source of error in fusion performance is measurement. Sensor noise and resolution contributes in errors in positioning system. Although fusion reduces the effect of noise on positioning system performance, their effect on positioning system can not be completely removed. Sensor noise variance is taken into account in fusion algorithm and propagates in uncertainty estimates. In section 1.5.3 GPS data errors is covered and in sections 1.6.2, 1.7 INS and DR (CAN bus speed) errors are covered respectively.

Another source of error in the sensor fusion algorithm is clock error (time offset). Effect of time offset on positioning system performance is discussed in section 4.2.

4.2. Analysis of effect of clock errors on fusion

In the fusion algorithm data from three sources; Cronos, FOG and GPS receiver, was used. The time at which a measurement from any of these sources is received, is determined by its own clock. Thus time offset between these three clocks can result in error in fusion algorithm which is analyzed in the following subsections.

4.2.1. Effect of delay in Fiber Optic Gyro

An intentional delay of 500ms was applied to FOG source in order to analyze the effect of its clock time offset on fusion performance. The resulting trajectory and trajectory without delay are plotted in Figure 4-6.

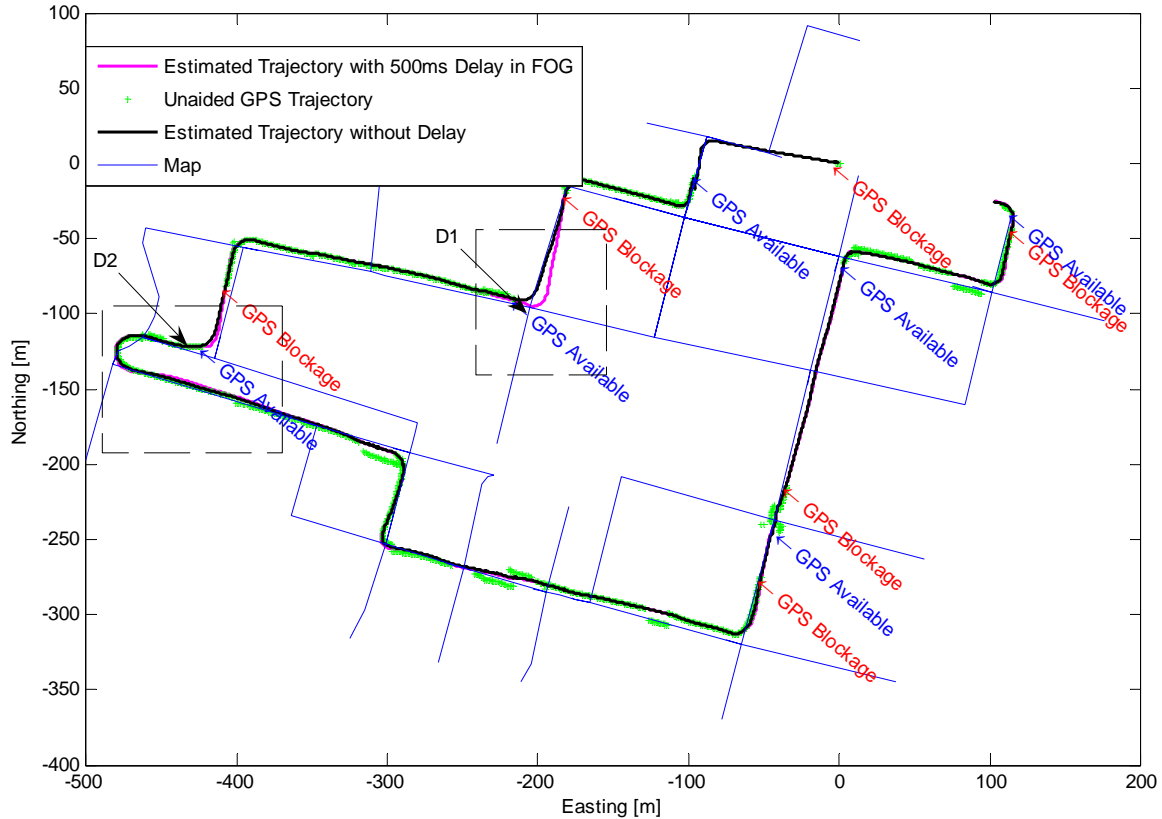


Figure 4-6 Estimated trajectory with an intentional delay of 500ms plotted with original trajectory with no delay

Delay in FOG source causes some deviation in vehicle trajectory especially in turns during which yaw rate has a large magnitude and therefore effect of delay is magnified. Effects of this delay increase when the system relies on inertial navigation as a consequence of GPS blockage.

Figures 4-7 and 4-8 show two zoomed views of vehicle trajectory. In figure 4-7 a lateral deviation about 10 meters after 70 meters of traveling can be observed due to error in heading caused by delay in FOG.

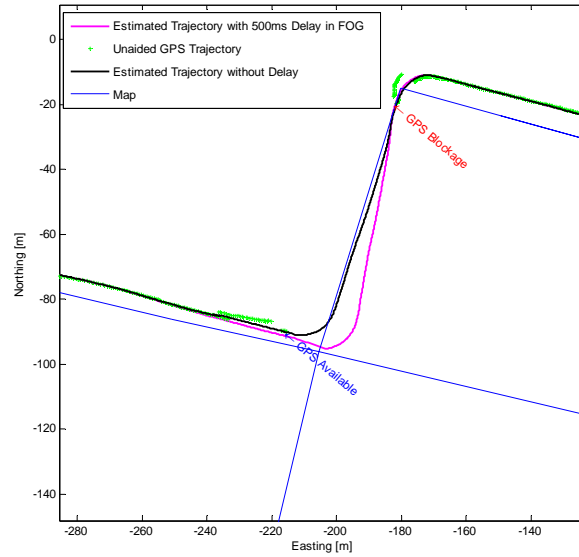


Figure 4-7 zoom window D1 in figure 4-6

In Figure 4-8 zoomed view of two consequent intersections is presented. Deviation increases up to 4 meters after 35 meters traveling without GPS measurement. After the 180 degree turn about 2m deviation from vehicle trajectory without time offset was observed.

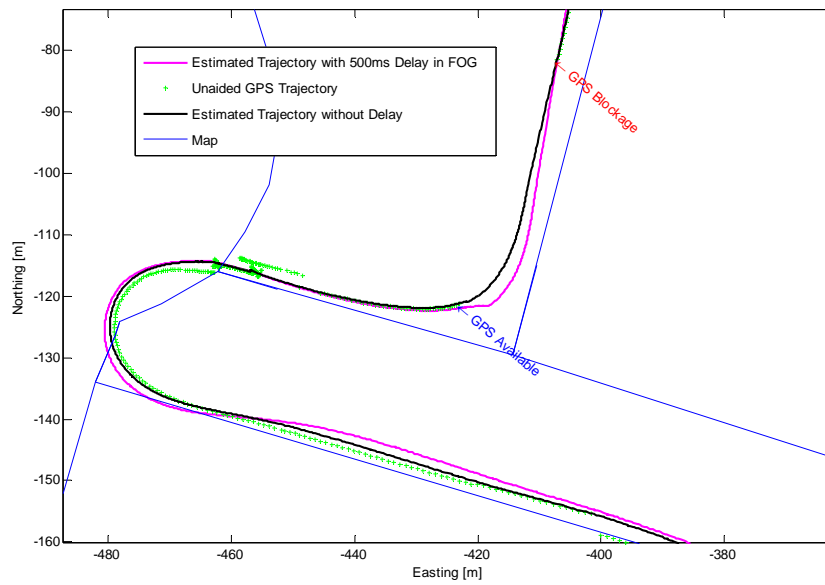


Figure 4-8 zoom window D2 in figure 4-6

In order to investigate the linearity of alteration of position deviation as time delay in FOG changes the following activities was performed:

- Two different intentional time offsets was induced to FOG source by adding delay (100ms and 500ms) to its time vector.
- Deviation of position in two scenarios was calculated for the entire test trajectory.
- Both deviation vectors and their ratio in the entire test trajectory at the same reference time (the fusion time) were plotted in the same figure (see Figure 4-9).

As it can be seen the deviation ratio between the two scenarios is almost linear during most of the trajectory which means deviation of position at 500ms delay is almost 5 times the deviation of position at 100ms delay.

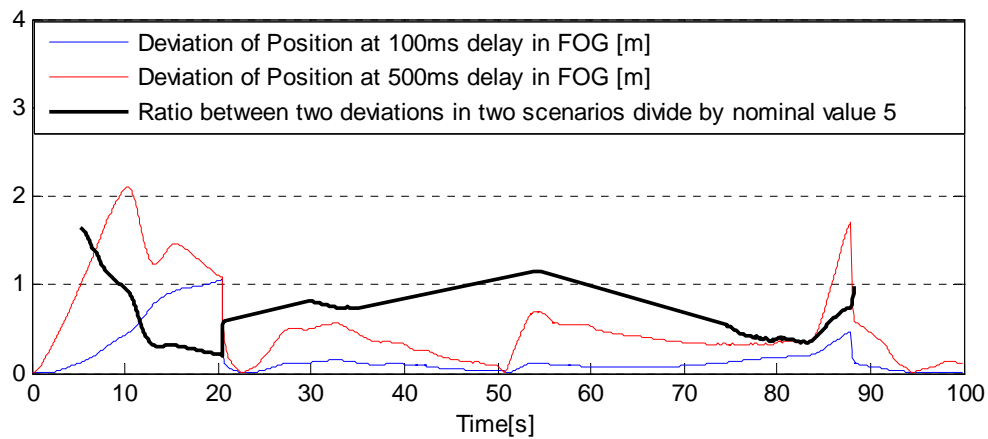


Figure 4-9 Effect of clock error in FOG on positioning for different delays

4.2.2. Effect of delay in Cronos Unit

An intentional delay of 500ms was applied to Cronos source in order to analyze the effect of its clock time offset on fusion performance. Time offset in Cronos unit clock induces delay in ABS speed measurement, longitudinal acceleration measurement and analogue yaw rate sensor. The resulting trajectory and trajectory without delay are plotted in Figure 4-10.

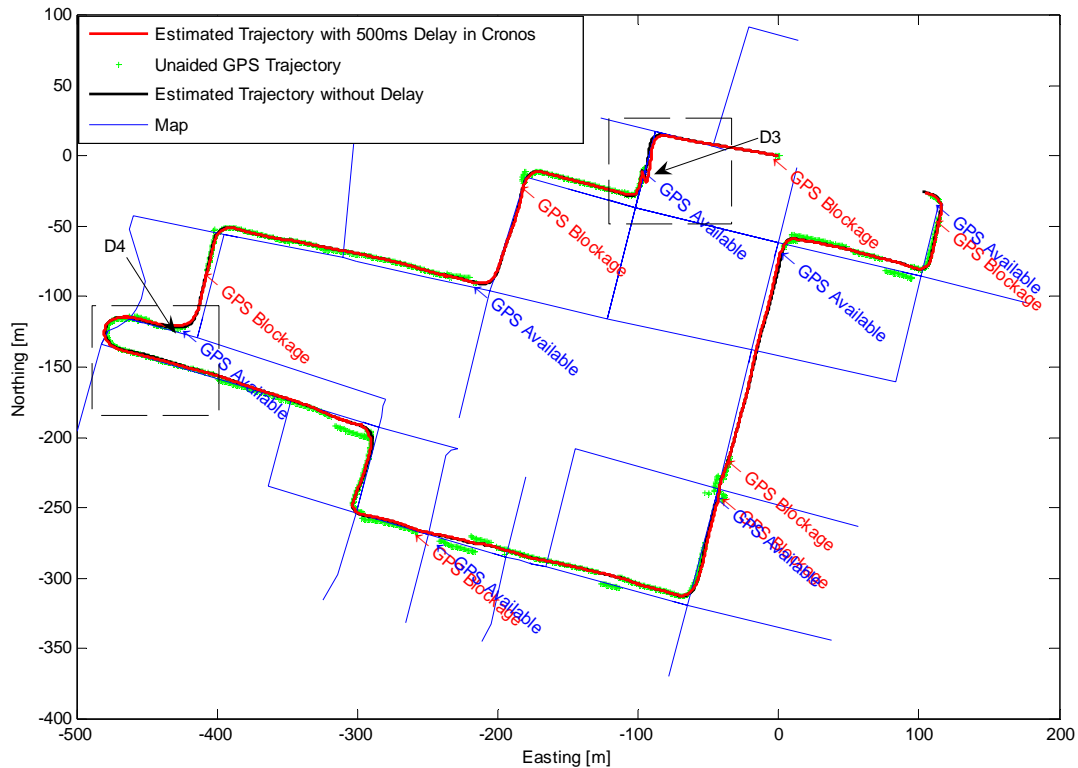


Figure 4-10 Effect of delay in Cronos

Delay in Cronos source causes some deviation in vehicle trajectory especially in longitudinal direction that change to lateral position error after a turn. Effects of this delay increase when the system relies on inertial navigation as a consequence of GPS blockage.

Figures 4-11 and 4-12 show two zoomed views of vehicle trajectory. In figure 4-11 a lateral deviation about 2 meters after 70 meters of traveling can be observed. This error is due to error in longitudinal position caused by delay in ABS speed before turn that has changed to lateral deviation after turn.

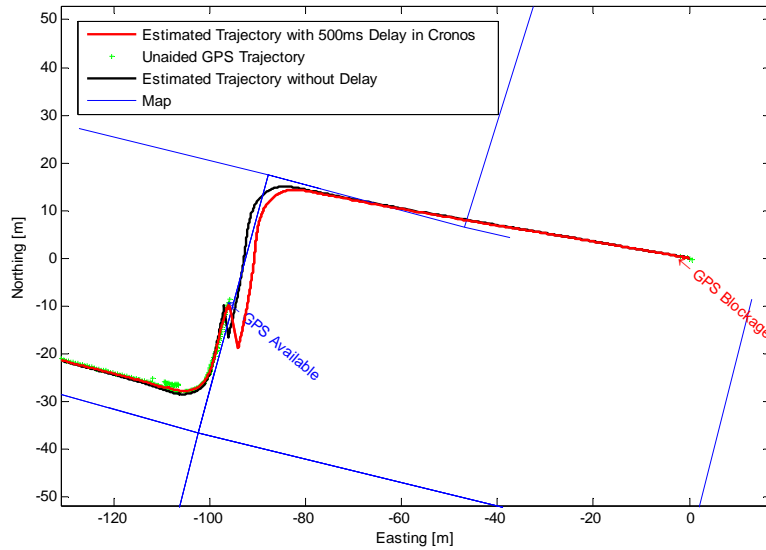


Figure 4-11 Zoom window D3 in figure 4-10

In Figure 4-12 zoomed view of two consequent intersections is presented. Deviation increases up to 2 meters after 35 meters traveling without GPS measurement. After the 180 degree turn about 1m deviation from vehicle trajectory without time offset was observed.

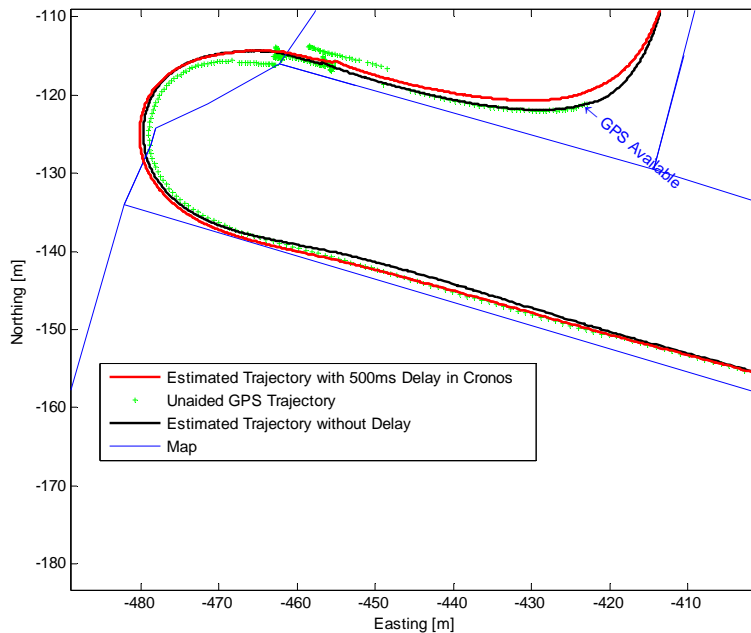


Figure 4-12 Zoom window D4 in figure 4-10

In order to investigate the linearity of alteration of position deviation as time delay in cronos changes the following activities was performed:

- Three different intentional time offsets was induced to Cronos source by adding delay (30ms, 100ms and 500ms) to its time vector.

- Deviation of position in three scenarios was calculated for the entire test trajectory.
- Deviation vectors and their ratio at 500ms delay scenario and at 100ms delay scenario in the entire test trajectory at the same reference time (the fusion time) were plotted in the same figure (see Figure 4-13).
- Deviation vectors and their ratio at 100ms delay scenario and at 30ms delay scenario in the entire test trajectory at the same reference time (the fusion time) were plotted in the same figure (see Figure 4-14).

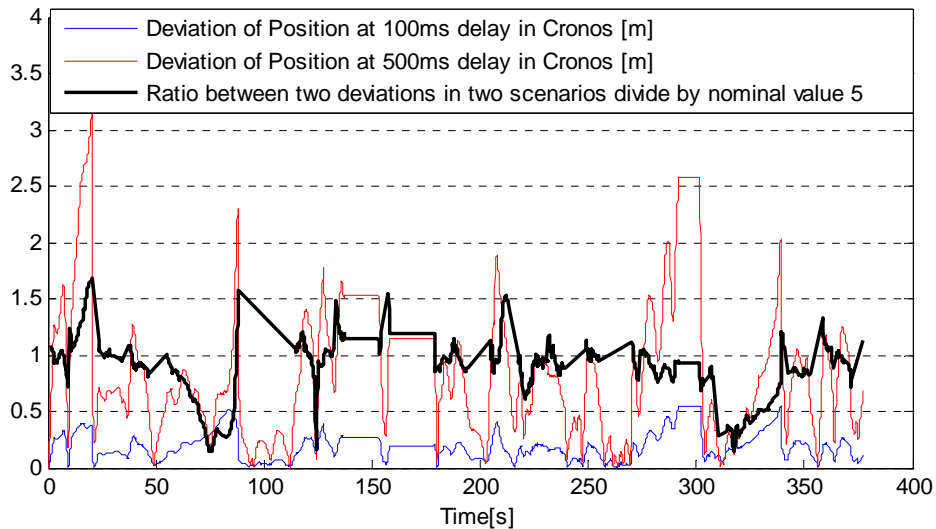


Figure 4-13 Effect of clock error in Cronos on positioning for different delays

As it can be seen the deviation ratio between the two scenarios; 500ms and 100ms delay, is almost linear during most of the trajectory which means deviation of position at 500ms delay is almost 5 times the deviation of position at 100ms delay.

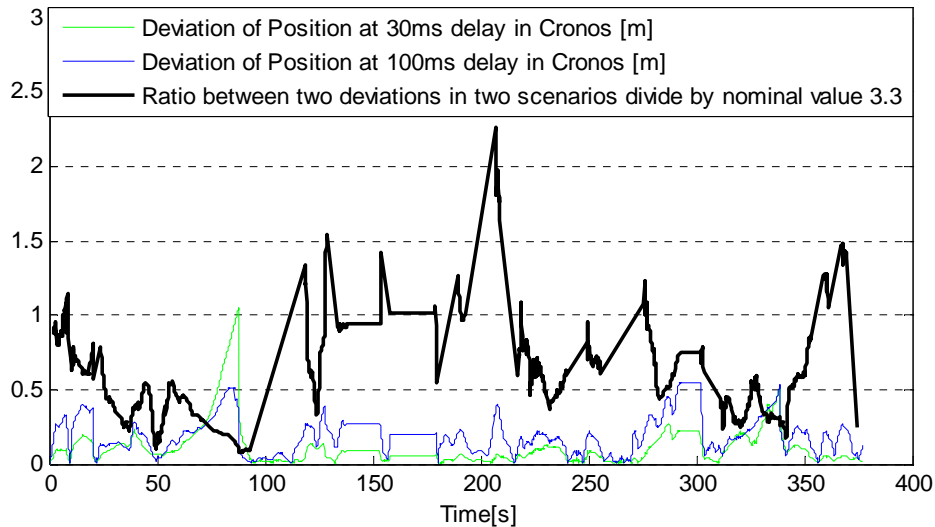


Figure 4-14 Effect of clock error in Cronos on positioning for different delays

Comparison of deviations in two scenarios; 100ms and 30ms, shows that the ratio between two deviations in two scenarios varies considerably from the minimum of 1 to maximum of 7 (Note that the ratio shown in Figure 4-14 is divided by nominal value of 3.3). Therefore to investigate whether the effect of delay in Cronos on deviation of position is proportional to delay more tests should be done in different delays.

4.2.3. Summary of effect of sensors' clock error on fusion

In the proceeding sections investigation of effect of clock error on fusion algorithm was presented. These effects can be summarized as follows:

1. Deviation of position due to delay in measurement units; FOG and Cronos, increases as delay in these sources increases.
2. Deviation of position due to delay in measurement units is nearly proportional to delay in ranges between 100ms and 500ms of delay.
3. Further investigation should be conducted on the deviation of position due to short delays in measurement units; 30ms to 100ms, since the results of the only test in this range did not show a special pattern.

5. Conclusion

A data fusion algorithm based on Kalman filtering and a map matching algorithm for vehicle positioning in intersection active safety applications are presented. The Kalman filter integrates complementary sensors and GPS data to achieve a continuous and precise positioning and map matching algorithm determines location of vehicle on the digital road map with respect to a position fix given by the Kalman filter.

The system was tested on a complex urban roadway where GPS signal occlusion was observed frequently. The GPS was available in only about 70% of the total trajectory length. Furthermore there were trajectory segments with poor GPS performance. The integrated positioning system provided very encouraging results in this test and the project goals: filling the gaps of GPS coverage, giving a continuous and more accurate position and matching the vehicle position to the digital road map were achieved.

Speed estimate was improved slightly in comparison with the given ABS speed by CAN bus, since the accelerometer used in the project was not good for long time applications and had a changing offset which could not improve ABS estimated speed to a more accurate estimation and the Kalman estimated speed was tracking ABS speed.

Heading estimate became more accurate and precise by fusion of Doppler derived heading and yaw rate from Fiber Optic Gyro and analogue yaw rate sensor. Estimated achieved heading accuracy was about 1 degree. The yaw rate sensors used in this thesis were expensive non-automotive grade equipment; however considering the sensor developments, these results can be obtained by automotive grade sensors in near future.

Estimated uncertainty in position both in longitudinal (tangent to vehicle trajectory) and lateral direction was about 0.3 m in average. The given vehicle trajectory in an intersection by the Kalman filter was matched fairly well to the digital map by the developed map matching algorithm, although in a few situations the matched vehicle trajectory was not within the road width completely. This achievement is due to calculation and consideration of a common offset between position fixes and digital map.

The presented positioning result uncertainties are estimated uncertainties by the Kalman filter and not the real error. The real error calculation and comparison between the achieved results and positioning requirements for an intersection active safety application was not possible due to lack of information about real position of vehicle and intersections. But generally it can be said that positioning requirements for warning level was fulfilled and positioning system can probably reach lane level positioning accuracy by adding a local positioning system e.g. Laser Radar information and using Differential GPS and a more accurate digital map with information about road widths.

It should be noted that although the algorithm was tested off-line, it can easily be implemented to work in real-time.

Appendix A

Extended Kalman Filter Equations

In the following general extended Kalman filter equations are presented.

$$\frac{d}{dt} x = f(x, t) + w(t)$$

$$z = h(x) + v(t)$$

x is state vector and $w(t)$ and $v(t)$ are zero mean white noises.

Predicted state vector:

$$\hat{x}_k(-) = \hat{x}_{k-1}(+) + \int_{t_{k-1}}^{t_k} f \cdot dt$$

$$F = \left. \frac{\partial f}{\partial x} \right|_{x=\hat{x}_k}$$

Predicted covariance matrix:

Linearization:

$$\hat{x}_k = \Phi_k \hat{x}_{k-1}$$

$$\dot{\Phi} = F\Phi$$

$$\Phi(t_{k-1}) = I$$

$$E\langle w(t_1)w^T(t_2) \rangle = Q(t_1)\delta(t_2 - t_1)$$

$$E\langle v(t_1)v^T(t_2) \rangle = R(t_1)\delta(t_2 - t_1)$$

$$P(t) = E\langle [x(t) - E\langle x(t) \rangle][x(t) - E\langle x(t) \rangle]^T \rangle$$

where $E\langle x \rangle$ is “expected value” of x .

$$Q_{k-1} = \int_{t_{k-1}}^{t_k} \Phi(t_k, \tau)Q(\tau)\Phi(t_k, \tau)d\tau$$

Error covariance matrix, P :

$$P_k(-) = \Phi_k P_{k-1}(+)\Phi_k^T + Q_{k-1}$$

Kalman gain:

$$\bar{K}_k = P_k(-)H_k^T (H_k P_k(-)H_k^T + R_k)^{-1}$$

$$H_k = \left. \frac{\partial h}{\partial x} \right|_{x=\hat{x}_k}$$

Corrected state estimate:

$$\hat{x}_k(+) = \hat{x}_k(-) + \bar{K}_k [z_k - h(\hat{x}_k(-))]$$

Corrected covariance matrix:

$$P_k(+) = P_k(-) - \bar{K}_k H_k P_k(-)$$

Established Kalman Filter equations

In the following detailed Kalman filter equations for the model used in this thesis is presented. Equations are in the same order as equations presented in previous section for general Kalman filter equations.

State vector is composed of longitude, Latitude altitude, heading, speed, acceleration, yaw rate.

$$x = \begin{matrix} \textit{Longitude} \\ \textit{Latitude} \\ \textit{Altitude} \\ \textit{Heading} \\ \textit{Speed} \\ \textit{Acceleration} \\ \textit{HeadingRate} \end{matrix} \begin{bmatrix} \theta \\ \phi \\ h \\ \psi \\ V \\ A \\ \dot{Y} \end{bmatrix}$$

$$\frac{d}{dt} x = f(x, t) + w(t)$$

$$f = \begin{matrix} \textit{LongitudeRate} \\ \textit{LatitudeRate} \\ \textit{AltitudeRate} \\ \textit{HeadingRate} \\ \textit{SpeedRate} \\ \textit{AccelerationRate} \\ \textit{RateofYawRate} \end{matrix} \begin{bmatrix} V_E / [\cos(\phi)(r_T + h)] \\ V_N / (r_M + h) \\ 0 \\ \dot{Y} \\ A \\ 0 \\ 0 \end{bmatrix}$$

Where

$$r_T = \frac{a}{\sqrt{1 - e^2 \sin^2 \phi}}$$

$$r_M = \frac{a(1 - e^2)}{(1 - e^2 \sin^2 \phi)^{3/2}}$$

a is the semi major axis of reference ellipse and e is the eccentricity.

$$P_0 = \begin{matrix} \textit{Longitude} \\ \textit{Latitude} \\ \textit{Altitude} \\ \textit{Heading} \\ \textit{Speed} \\ \textit{Acceleration} \\ \textit{HeadingRate} \end{matrix} \begin{bmatrix} \hat{\sigma}_\theta^2 & 0 & 0 & 0 & 0 & 0 & 0 \\ 0 & \hat{\sigma}_\phi^2 & 0 & 0 & 0 & 0 & 0 \\ 0 & 0 & \hat{\sigma}_h^2 & 0 & 0 & 0 & 0 \\ 0 & 0 & 0 & \hat{\sigma}_Y^2 & 0 & 0 & 0 \\ 0 & 0 & 0 & 0 & \hat{\sigma}_V^2 & 0 & 0 \\ 0 & 0 & 0 & 0 & 0 & \hat{\sigma}_A^2 & 0 \\ 0 & 0 & 0 & 0 & 0 & 0 & \hat{\sigma}_{\dot{Y}}^2 \end{bmatrix}$$

Where $\hat{\sigma}_x$ is initial estimate of uncertainty on initial value of state variable x .

$$Q = \begin{matrix} \textit{Longitude} \\ \textit{Latitude} \\ \textit{Altitude} \\ \textit{Heading} \\ \textit{Speed} \\ \textit{Acceleration} \\ \textit{HeadingRate} \end{matrix} \begin{bmatrix} 0 & 0 & 0 & 0 & 0 & 0 & 0 \\ 0 & 0 & 0 & 0 & 0 & 0 & 0 \\ 0 & 0 & \sigma_{zh}^2 & 0 & 0 & 0 & 0 \\ 0 & 0 & 0 & 0 & 0 & 0 & 0 \\ 0 & 0 & 0 & 0 & 0 & 0 & 0 \\ 0 & 0 & 0 & 0 & 0 & \sigma_{zA}^2 & 0 \\ 0 & 0 & 0 & 0 & 0 & 0 & \sigma_{z\dot{Y}}^2 \end{bmatrix}$$

Where σ_{zx} is system dynamic noise variance and Q is Disturbance covariance matrix.

GPS measurement equations

$$z_{GPS} = h_{GPS}(x)$$

$$z_{GPS} = \begin{matrix} \text{Longitude} \\ \text{Latitude} \\ \text{Altitude} \\ \text{Heading} \\ \text{Speed} \end{matrix} \begin{bmatrix} \theta_{GPS} \\ \phi_{GPS} \\ h_{GPS} \\ \psi_{GPS} \\ V_{GPS} \end{bmatrix}$$

$$h_{GPS}(x) = \begin{bmatrix} \theta \\ \phi \\ h \\ \psi \\ V \end{bmatrix}$$

$$H_{GPS} = \frac{\partial h_{GPS}}{\partial x} = \begin{bmatrix} 1 & 0 & 0 & 0 & 0 & 0 \\ 0 & 1 & 0 & 0 & 0 & 0 \\ 0 & 0 & 1 & 0 & 0 & 0 \\ 0 & 0 & 0 & 1 & 0 & 0 \\ 0 & 0 & 0 & 0 & 1 & 0 \end{bmatrix}$$

$$R_{GPS} = \begin{matrix} \text{Longitude} \\ \text{Latitude} \\ \text{Altitude} \\ \text{Heading} \\ \text{Speed} \end{matrix} \begin{bmatrix} \sigma_{\theta_{GPS}}^2 & 0 & 0 & 0 & 0 \\ 0 & \sigma_{\phi_{GPS}}^2 & 0 & 0 & 0 \\ 0 & 0 & \sigma_{h_{GPS}}^2 & 0 & 0 \\ 0 & 0 & 0 & \sigma_{\psi_{GPS}}^2 & 0 \\ 0 & 0 & 0 & 0 & \sigma_{V_{GPS}}^2 \end{bmatrix}$$

It should be noted that measurement error covariance used in R_{GPS} are for GPS receiver operation in the stand alone mode and if the GPS receiver is working in DGPS mode these value should be corrected for the error covariance regarding a DGPS measurement.

$\sigma_{V_{GPS}}$ and $\sigma_{\psi_{GPS}}$ has different values in different speeds. $\sigma_{\psi_{GPS}}$ is larger in low speed while $\sigma_{V_{GPS}}$ is larger in high speed.

$\sigma_{\theta_{GPS}}$ and $\sigma_{\phi_{GPS}}$ are related to Horizontal Delusion of Precision (HDOP). The larger HDOP is the larger variances on longitude and latitude will be.

Cronos (CAN) measurement equations

$$z_{CAN} = h_{CAN}(x)$$

$$z_{CAN} = \begin{matrix} \text{Speed} \\ \text{Acceleration} \\ \text{Yaw Rate from CAN} \end{matrix} \begin{bmatrix} V_{CAN} \\ A_{CAN} \\ \dot{Y}_{CAN} \end{bmatrix}$$

$$h_{CAN}(x) = \begin{bmatrix} V \\ A \\ \dot{Y} \end{bmatrix}$$

$$H_{CAN} = \frac{\partial h_{CAN}}{\partial x} = \begin{bmatrix} 0 & 0 & 0 & 0 & 1 & 0 & 0 \\ 0 & 0 & 0 & 0 & 0 & 1 & 0 \\ 0 & 0 & 0 & 0 & 0 & 0 & 1 \end{bmatrix}$$

$$R_{CAN} = \begin{matrix} \text{Speed} \\ \text{Acceleration} \\ \text{Yaw Rate from CAN} \end{matrix} \begin{bmatrix} \sigma_{V_{CAN}}^2 & 0 & 0 \\ 0 & \sigma_{A_{CAN}}^2 & 0 \\ 0 & 0 & \sigma_{\dot{Y}_{CAN}}^2 \end{bmatrix}$$

$$\sigma_{V_{CAN}} = \bar{\sigma}_{V_{CAN}} \cdot (V^2)$$

FOG measurements equations

$$z_{FOG} = h_{FOG}(x)$$

$$z_{FOG} = \text{Yaw Rate from FOG} \quad [\dot{Y}_{FOG}]$$

$$h_{FOG}(x) = [\dot{Y}]$$

$$H_{FOG} = \frac{\partial h_{FOG}}{\partial x} = [0 \quad 0 \quad 0 \quad 0 \quad 0 \quad 0 \quad 1]$$

$$R_{FOG} = \text{Yaw Rate From FOG} \quad [\sigma_{\dot{Y}_{FOG}}^2]$$

Appendix B

GPS Data Errors

Ionospheric Propagation Errors: The ionosphere, which extends from approximately 50 to 1000 km above the surface of the earth, consists of gases that have been ionized by solar radiation. The ionization produces clouds of free electrons that changes GPS signals propagation velocity. The magnitude of measured pseudorange error is directly proportional to the total electron count in a tube of 1 m^2 cross section along the propagation path and this quantity varies spatially due to nonhomogeneity of the ionosphere. A particular location within the ionosphere is alternately illuminated by the sun and shadowed from the sun by the earth in a daily cycle; consequently the characteristics of the ionosphere exhibit a daily variation in which the ionization is usually maximum late in the afternoon and minimum a few hours after midnight. The path delay for a satellite at zenith typically varies from about 1 m at night to 5-15 m during late afternoon. At low elevation angles the propagation path through the ionosphere is much longer, so the corresponding delays can increase to several meters at night and as much as 50 m during the day.

Receivers in nondifferential operation can reduce ionospheric error by using a model of the ionosphere broadcast by the satellites, which reduces the uncompensated ionospheric delay by about 50% on the average. There are also some other models which offer somewhat better performance.

With DGPS ionospheric errors can be nearly eliminated in many applications, because ionospheric errors tend to be highly correlated when the receivers are in sufficiently close proximity.

Tropospheric Propagation Errors: The lower part of the earth atmosphere is composed of dry gases and water vapor, which lengthen the propagation path due to refraction. The magnitude of the resulting signal delay depends on the refractive index of the air along the propagation path and typically varies from about 2.5 m in the zenith direction to 10-15 m at low satellite elevation angles. The refractive index of the troposphere consists of that due to dry gas component and the water vapor component, which respectively contribute about 90% and 10% of the total.

The troposphere errors can also be nearly eliminated by use of DGPS and in nondifferential operation it can be reduced by using a model of the standard atmosphere at the antenna location to within about 0.5 m. Such models use inputs such as the day of the year, and the position of user. Knowledge of the temperature, surface pressure and humidity can improve the estimation of this delay considerably.

The Multipath Problem: Multipath propagation of the GPS signal is a dominant source of error in differential positioning. Objects in the vicinity of a receiver antenna (notably the ground) can easily reflect GPS signals, resulting in one or more secondary

propagation paths. These secondary path signals, which are superimposed on the desired direct-path signal, always have a longer propagation time and can significantly distort the amplitude and phase of the direct-path signal. Errors due to multipath can not be reduced by the use of DGPS, since they depend on local reflection geometry near each receiver antenna. Multipath errors can increase in urban areas due to more severe reflection geometry.

Multipath propagation can be divided into two classes: static and dynamic. For a stationary receiver, the propagation geometry changes slowly as the satellite move across the sky, making the multipath parameters essentially constant for perhaps several minutes. However, in mobile applications there can be rapid fluctuations in fractions of a second. Therefore different multipath mitigation techniques are generally employed for these types of multipath environments.

Ephemeris Data Errors: Small errors in the ephemeris data transmitted by each satellite cause corresponding errors in the computed position of the satellite. Errors in satellite position when calculated from the ephemeris data typically result in range errors less than 1 m. Improvements in satellite tracking will undoubtedly reduce this error further. This error can also be nearly eliminated by use of DGPS.

Onboard Clock Errors: Timing of the signal transmission from each satellite is directly controlled by its own atomic clock without any corrections applied. Although the atomic clocks in the satellites are highly accurate, errors can be large enough to require correction. The onboard clock error is typically less than 1 ms and varies slowly. This permits the correction to be specified by a quadratic polynomial in time whose coefficients are transmitted in the navigation message. The stability of the atomic clocks permits the polynomial correction to be valid over a time interval of 4-6 h. After the correction has been applied, the residual error in GPS time is typically less than a few nanoseconds, or about 1 m in range. This error can also be nearly eliminated by use of DGPS.

Receiver Clock Errors: Because the navigation solution includes a solution for receiver clock error, the requirements for accuracy of receiver clocks is far less severe than for the GPS satellite clocks. In fact, for receiver clocks short-term stability over the pseudorange measurements period is usually more important than absolute frequency accuracy. [Grewal]

Appendix C

Carrier Doppler Measurements

Measurement of the received carrier frequency provides information that can be used to determine the velocity vector of the user. Although this could be done by forming differences of code-based position estimates, frequency measurement is inherently much more accurate and has faster response time in the presence of user dynamics. The equations regarding the measurements of Doppler shift to the user velocity are

$$\begin{aligned}f_{d1} &= \frac{1}{\lambda}(v \cdot u_1 - v_1 \cdot u_1) + f_b \\f_{d2} &= \frac{1}{\lambda}(v \cdot u_2 - v_2 \cdot u_2) + f_b \\&\vdots \\f_{dn} &= \frac{1}{\lambda}(v \cdot u_n - v_n \cdot u_n) + f_b\end{aligned}$$

Where the unknowns are the user velocity vector v and the receiver reference clock frequency error f_b in hertz and the known quantities are the carrier wavelength λ and the measured Doppler shifts f_{di} in hertz, satellite velocity vectors v_i , and unit satellites direction vectors u_i (pointing from the receiver antenna toward the satellite antenna) for each satellite index i . [Grewal]

